行政院國家科學委員會專題研究計畫　成果報告

無線感測網路：基本性質與具環境知覺的資料收集機制

(2/2)

計畫類別：個別型計畫
計畫編號：NSC94-2213-E-216-001-
執行期間：94 年 08 月 01 日至 95 年 07 月 31 日
執行單位：中華大學資訊工程學系

計畫主持人：嚴力行
共同主持人：俞征武
計畫參與人員：鄭仰民、林千惠、楊家政、陳希維、蔡威霆、闕河正

報告類型：完整報告
報告附件：出席國際會議研究心得報告及發表論文
處理方式：本計畫涉及專利或其他智慧財產權，1 年後可公開查詢

中　華　民　國 95 年 10 月 30 日

摘要

無線感測網路 (Wireless Sensor Networks) 乃是由若干數目的感測器透過無線通訊的方式組成。感測器置於目標區域 (Target Region) 內，擁有收集、儲存、及處理環境資訊的能力。無線感測網路的近年來已成為熱門研究的研究主題。本計畫為兩年期，第一年探討無線感測網路的基本性質，第二年為第一部份所得的成果的應用。本報告總結我們這兩年的研究成果。在感測網路基本性質部分，我們成功估算出感測器之間無線連結形成的機率、每個感測器的期望連結數目、考慮邊界效應下個別感測器及整個感測網路的期望偵測面積、感測網路的*k*-coverage期望值、感測網路群聚係數 (Clustering Coefficient)、隱藏終端機數目等等。在成果應用方面，我們為無線感測網路設計出以鏈結構為機礎的資料收集機制，能夠進一步節省資料收集所耗用的電力。我們也設計出不需感測器位置資訊就可以關掉多餘感測器而不減少可偵測面積的協定。最後，我們針對感測網路追蹤移動物件的應用，提出一個可獲得物件在感測器偵測區域間移動頻率的數學分析，此分析不以歷史統計資料為基礎，可用於建立更有效能的資料傳遞樹。上述部分成果已發表三篇學術期刊論文與四篇國際研討會論文，尚有後續研究成果整理中。本計畫亦已支持三位研究生獲得碩士學位。

關鍵詞：無線感測網路, 機率分析, 網路涵蓋, 隱藏終端機, 群聚係數, 鏈結構, 資料收集機制, 省電策略, 物件追蹤.

Abstract

A wireless sensor network consists (WSN) of a number of sensor nodes communicated wirelessly. Sensor nodes deployed in target region are capable of collecting, storing, and processing environmental information. Study of WSNs is becoming a hot research topic. This is a two-year research project. In the first year, we aim to investigate fundamental properties of WSNs. In the second year, we shall apply our research results of the first year to WSN applications. This report summarizes our final results. As to fundamental properties of WSNs, we have successfully estimated the probability of link occurrence, the expected number of links of each sensor, the expected area covered by a sensor or a number of sensors with the consideration of border effects, expected *k*-coverage, clustering coefficient of WSNs, and the number of hidden terminals in a WSN. As to the applications of our fundamental results, we have proposed a chain-based data gathering scheme for WSNs that can minimize energy consumption. We also developed a topology control protocol that turns off redundant sensors while preserving sensory coverage. This scheme needs no location information of sensors. For mobile object tracking in WSNs, we have proposed an analytical work that generates border-crossing rates for target objects without historical statistics. This profiling facilitates tree-based tracking scheme in that it reduces message cost. Our research results have been published partially in three journals as well as in four international conferences.

Key words: Wireless Sensor Networks, Probability Analysis, Network Coverage, Hidden Terminals, Clustering Coefficient, Chain Structure, Data Gathering Scheme, Power Saving Technique, Object Tracking

目錄

報告內容

一.前言

近年來，由於無線通訊及微機電領域技術的突破，使得低成本、低耗電量、體積小但多功能的感測器變得不再是夢想，更讓有計算能力和無線通訊的感測器變得便宜而且更容易獲得 [22]。無線感測網路 (Wireless Sensor Networks) 乃是由若干數目的感測器 (Sensor) 以某種方式建置在目標區域 (Target Region) 內。每個感測器均擁有收集、儲存、及處理環境資訊的能力，並可以無線的方式與其它感測器溝通，共同完成所賦予的偵測任務。

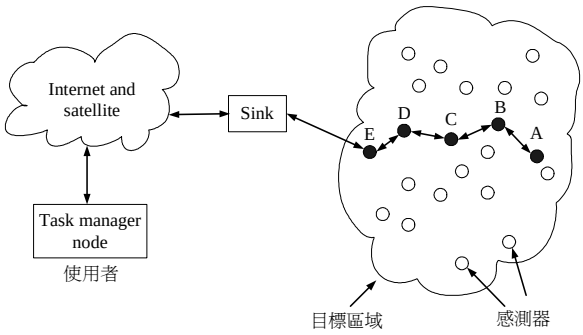

圖一：散佈於感測區域的感測節點 [1]

無線感測網路常見的應用架構如圖一所示。使用者透過 Task Manager 執行應用程式，設定資料匯集點 (Sink Node) 要收集並處理的資料。資料匯集點將要收集的資料請求傳送給感測器。感測器將收集到的感測資料送至資料匯集點彙整，供應用程式應用。感測資料傳輸模式又可分為週期性 (Periodical) 與事件驅動 (Event driven) 兩大類。

由於感測器透過它們的無線傳輸介面可以和其他的感測器做溝通，彼此可以自行組成一隨意感測網路，所以常被視為隨意無線網路 (Ad Hoc Wireless Networks) 的一種。不過無線感測網路與一般學者所考慮的隨意無線網路，還是有不同之處。首先，由於實際應用多要求小型化的感測器，相較一般由筆記型電腦或 PDA 組成之隨意網路，感測網路的感測器擁有較少的資源(電力供應、計算能力、儲存容量等)，導致節點損壞或失去功能的機率較大。另一點不同之處，則是其通訊模式。在一般的隨意網路當中，任何節點都可能成為通訊資料流向的來源或目的端。而在感測網路上的資料，絕大多數都是由感測器傳送到資料匯集點。

網路基本性質

無線感測網路中感測器放置的位置並不一定要事先規劃好 [1]。這是因為感測器的數量可能很龐大[2]；或者是目標區域的某些特性不允許我們這麼做[1]。因為技術上的限制，每個感測器只能偵測某個距離範圍內的事件。這個距離稱為感測器的感測半徑 (Sensing Radius)。同樣地，每個感測器無線電波所能發送的距離也受限於所使用的發射功率。由於較大的發射功率須耗用較多的電力，通常感測器也只能與某個距離範圍內的其他感測器通訊。這個距離稱為感測器的通訊半徑 (Communication Radius)。

「均勻點分佈」模型考慮 n 個感測器均勻分佈 (Uniformly Distributed) 在一個 $l \times m$ 封閉矩形區域內；每個感測器具有通訊半徑 r_c 與感測半徑 r_s。我們如何估計此模型的一些基本性質，如任兩個感測器之間形成無線連結的機率、每個感測器的期望連結數目、整個網路是連結的 (Connected) 的機率或條件、每個感測器及整個感測網路的期望偵測面積等。這一直是個基本卻重要的課題。

許多學者已在隨意無線網路上分析過上述某些基本性質，不過多數學者考慮的是所謂「蒲松點程序」(Poisson Point Process) 的模型。此種模型固定節點分佈

密度λ，而非節點確實數目 [17, 16, 3, 5, 6]。在此種模型下，一個極小的單位面積 *ds* 內是否正好存在一個節點是伯努利分佈 (Binomial Distribution)，機率為 *ds*λ。如果足夠多的節點分佈在足夠大的區域內（但λ維持常數），此網路的連結數目可以用蒲松分佈 (Poisson Distribution) 來趨近，其平均值 (Mean) 為$\lambda\pi r^2$ [5]。許多學者已根據此種模型研究了無線隨意網路的一些基本性質，如整個區域皆被無線電波涵蓋的機率 [17]、產生孤立節點的機率 [5, 3]、以及整個網路是連結的條件 [17, 16, 5, 6]。

然而，由於奠基於蒲松點程序的研究假設系統區域趨近於無限大，它們實際上忽略了「邊界效應」所可能造成的估計誤差。邊界效應指的是位於目標區域邊界的節點，其鄰居節點數目會小於位於目標區域中間位置的節點。這是由於位於邊界的節點其可通訊範圍只有部分會落於目標區域內。此種效應所造成的影響大小，視通訊半徑與系統區域邊長的比值而定。一般而言，邊界效應的影響在合理大小的區域即相當顯著，因此忽略此種效應所得的結果在實際應用時會受到相當的限制。這種模型還有另一個缺點，即節點總數並非可控制的系統變數，而是一個隨機變數 [19]。蒲松點程序只能控制此隨機變數的期望值。

我們認為「均勻點分佈」是較為合理的模型。同時，在分析網路基本性質時，邊界效應是不可以被忽略的。在相關文獻中，我們尚未見到採用均勻點分佈模型且考慮邊界效應的研究。

電力使用問題

電力使用是無線感測網路中最重要的議題之一。因為感測器先天硬體上的限制，所能搭載的電池電量有限，所以我們必須要有效率地使用電力，來延長整個網路運作的時間。在媒體擷取控制 (Medium Access Control; MAC) 機制的設計上，可利用睡眠模式與衝撞預防[37]等技術來達到節省電力的要求。也有學者[38] 提出以分時多重擷取（Time Division Multiple Access; TDMA) 的方式來分配傳送時間，讓不需要傳送的節點得以進入睡眠模式，以節省電力。

有效率的資料傳送方式也是節電設計的重點。因為無線傳輸的電力消耗與傳輸距離的二到四次方成正比，因此一個簡單的節電技巧是感測器不直接傳送資料到資料匯集點，而是透過其它感測器以多次轉送的方式傳送。資料匯整 (Data Aggregation) [39]是另一個節省電力的資料傳送策略。此種策略由某些感測器收集來自於其它感測器的資料，彙整合併後再轉送出去。由於經過彙整、合併、壓縮後資料量便得較少，耗用在資料傳送上的電力消耗也會減少。

雖然也有學者認為，間接多重傳送的方式未必能節省電源，反而有更大的機率面對節點失去功能的問題[40]，不過就現有的文獻資料來看，「間接多重傳送」與「資料彙整」已成為目前國內外學者研究的重點。各式的資料傳送與彙整方式，如邏輯鏈 (Chain) [41–43]、樹 (Tree) [44, 45]、及叢集 (Cluster) [46–51]等，相繼被提出來。

另外一個較新的研究趨勢，是安排多餘的感測器輪流進入休眠模式，以節省電力。有些研究以處於活動 (Active) 模式的鄰居數目多寡，作為感測器判斷自己是否進入休眠模式的條件[52]。有些研究以較精確的方式，安排感測涵蓋面積較小的感

測器進入休眠模式[53, 54, 56]。如此一來整個感測網路的功能可以保持，又能達成省電的效果。一般而言，無論關閉感測器的策略為何，此項作法需滿足一個條件，即任何時刻處於活動模式下的感測器數目及位置，必須維持原有的感測能力，並使網路保持連結狀態。

二.研究目的

本計畫分為兩部分。第一部分(第一年)我們將分析並驗證「均勻點分佈」模型所具有的一些基本性質。這些性質與均勻點分佈模型基本參數 n, l, m, r_c 與 r_s 之間的關係將以明確的數學關係式表達出來。我們想要探討的性質包括下列幾項：

- 任兩個感測器形成無線連結的機率
- 任兩個無線連結的聯合機率(Joint Probability)
- 每個感測器的期望連結數目
- 網路是連結的機率
- 每個感測器的期望涵蓋面積
- 一群感測器的期望涵蓋面積
- 群聚係數(Clustering Coefficient)
- 隱藏終端機(Hidden Terminal)數目的期望值

我們所要探究的網路性質，與無線感測網路的效能有相當密切的關係。無線連結形成的機率與期望值，會影響資料延遲與頻道競爭現象；我們也預期這兩項數值與網路連結的機率相關。個別與整體感測器的期望涵蓋面積，會影響關閉感測器策略的電力節省效能。至於隱藏終端機數目的期望值，與資料衝撞數目直接相關。

本計畫第二部分（第二年）在探討感測網路中的省電策略，包括具電源效率的資料傳送機制與密度控制協定。在資料傳送機制方面，我們計畫以邏輯鏈實現「間接多重傳送」與「資料彙整」的節電策略，並探討如何建立較佳的鍊結構，與最佳的鍊首節點(Header)排程。在密度控制方面，乃是安排多餘的感測器進入休眠模式，以節省電力，但同時維持原有網路的感測能力與連結性。現有的密度控制協定多需要知道所有感測節點的位置資訊。而獲得位置資訊的裝置（如全球定位系統）或機制不是太耗電、體積過大，就是太耗電，以致實用性過低。我們計畫設計出不需位置資訊，僅需要知道訊息傳送與接收節點間距離的協定。其終極目標是儘可能讓多數的感測器進入休眠狀態，以延長感測網路的運作時間。

三. 文獻探討

無線感測網路中，某個連結是否會出現取決於此連結兩端感測器的相對位置關係。當兩個感測器距離小於其通訊半徑時，這兩個感測器方可形成一無線連結(Wireless Link)。理論上，n 個感測器所有可形成的連結數目為 $n(n\text{-}1)/2$ 個。許多學者 [11, 7, 19] 指出，某些連結的出現會影響其它連結出現的機率，所以某特定連結出現事件與其它連結出現事件並非互相獨立的。儘管如此，我們初步的實驗結果支持每個連結出現的機率不互相獨立，但是分佈是相同的 (identical but not independent)。

群聚係數(Clustering Coefficient)是描述複雜動態網路的一個重要性質[28]。以往已有研究學者探討在隨機圖形(Random Graph) [30]或其它圖形中的群聚係數[29]。但迄今尚未有人研究過隨意無線網路的群聚係數。

在感測網路中，如果某塊區域中的所有可能位置，都位於一群感測器中至少一個感測器的偵測範圍內，則我們稱此塊區域被這群感測器所「涵蓋」 (Covered)。我們欲探討無線感測網路中的一個基本性質：給定封閉區域，被一個或一群隨機分佈感測器所涵蓋面積的期望值。這是屬於所謂的「涵蓋問題」 (Coverage Problem)。

現有文獻中，涵蓋問題有數種不同的定義。一個可能的定義是探討如何有效涵蓋一個給定區域。例如，古典的藝廊問題 (Art Gallery Problem) 是決定守衛／攝影機的數目與每個守衛／攝影機的位置，使得一個多邊形的區域（即藝廊）沒有監視上的視覺死角[15]。在 [21] 中，作者探討了 n 個節點以格網 (Grid) 狀放置於正方形區域時，整個區域皆能被涵蓋的充分必要條件。涵蓋問題亦被定義成判斷給定的一群感測器是否能涵蓋整個區域 [10] 或者涵蓋的區域有多少。

有研究學者延伸涵蓋問題的定義，探討所謂 k-coverage 的議題。給定任一封閉區域，其 k-coverage 被定義為至少被 k 個感測器所涵蓋的面積。

於 [14] 中，Meguerdichian 等人定義了最差與最佳涵蓋問題，分別為找出涵蓋度最低與最高的區域。已有學者利用諸如 Voronoi 圖及 Delaunay 三角測量等幾何技巧來解這些問題 [14, 13]。

在上述涵蓋問題的定義中，每個感測器的確實位置不是需要被決定（當作問題的答案）就是需要給定（視為問題的已知條件）。反觀我們所要探討的問題，只將感測器位置的機率分佈而非確切位置視為已知條件。

有兩個因素可能使得我們的問題變得複雜。第一，每個感測器的感測區域可能會互相重疊。第二，位於目標區域邊界的感測器，其感測區域會小於位於目標區域中間位置的感測器。這是由於位於邊界的感測器其可感測區域只有部分會落於目標區域內。這也是邊界效應的影響。

在以往的研究中，Hall [9] 使用所謂環面規則 (Torus Convention) 來避開邊界效應所造成的問題。環面規則是將目標區域視為上下邊界相接且左右邊界相臨。如此一來，原本為二維空間平面的目標區域即成為三維空間的環面 (Torus)，而任何一個感測器的可感測區域均會落於目標區域內，無論其位置為何。因此，這個研究的結果只是漸進成立 (Asymptotically true)。

另一個避開邊界效應的作法是所謂的邊界區域 (Border Zone) 法 [4]。這種方法不考慮落於邊界區域的節點，只統計感測區域全部落於目標區域內的感測器。嚴格來講，這個方法與環面規則都只是“忽略”了邊界效應的影響，並未真正將邊界效應的影響計算在內。

於 [17]，作者研究了隨機分佈的圓幾近涵蓋一個給定區域的條件。此研究所得的結果成立的條件是建立在給定目標區域的面積趨近於無限大。當目標區域的面積趨近於無限大時，邊界效應所造成的影響即變得微不足道。因此，當應用於合理大小的目標區域時，此研究所得結果僅為實際結果之近似值。

涵蓋問題也與其它無線網路的基本性質如網路連結性 (Connectivity) 有關。已有學者指出[12]如果涵蓋問題中的感測半徑視為通訊半徑的一半，則由一群無線節點所聯合涵蓋的通訊面積擁有下列性質：如果此面積是非分割的，則這群節點

必屬同一個連結成分 (Connected Component)。因此在直覺上，如果一塊區域被涵蓋的比例很高，就不大可能有分割的連結成分。最近更有學者[31, 32]進一步指出，當通訊半徑為感測半徑的一倍時，100%的涵蓋率會保證網路一定是連結的。

在隨意無線網路上，已有許多學者研究過網路形成連結的機率問題 [17, 16, 5, 6]，不過他們考慮的是蒲松點程序。Santi 等人 [18–20] 曾經使用均勻點分佈模型，但在稍微予以簡化（假設 $l = m$）的情形下，分析欲使網路連結的機率趨近於 1 時，n^2r 的漸進式極限 (Asymptotic Bounds)。他們結果的正確性乃建立在 l 趨近於無限大時，此時邊界效應變得不明顯。

Xue 和 Kumar [23]以實驗的方式指出，欲讓網路成為連結的，每個節點需與 $\mathbf{O}(\log n)$ 個最近的鄰居有連結存在。

Gupta 和 Kumar [7] 分析了當 n 趨近於無限大時，每個節點的傳輸半徑應為多少，方可使網路維持連結。某些研究探討通訊半徑對網路容量的影響[11,8]。此部分的成果指出要維持一定的傳輸效能，無線網路的綢密度 (Density) 不能太密 [8]（因為太密的網路會有較嚴重的頻道競爭現象）。

部分研究嘗試在不影響連結性的前提下，透過精確控制通訊半徑達成節省電力的效果[12]。少數學者也注意到通訊半徑對資料延遲與頻道競爭現象所造成的效能影響[24]。雖然看似明顯，但尚未有學者詳細研究過通訊半徑與資料衝撞現象間的關係。

隱藏終端機指的是互相偵測不到對方的無線電波、但送訊號給第三者時會互相衝撞的兩部無線主機。對載波偵測多重擷取 (CSMA) 機制而言，隱藏終端機的存在是傳輸效能無法提升的主要原因之一。直覺上，通訊半徑越大，隱藏終端機 數目越少，也就越不容易產生資料衝撞問題。不過我們關心的是通訊半徑與隱藏終端機數目之間明確的數學關係式，這一部份尚未有相關研究成果出現。

當節點有多個鄰居時，鄰居的數目與位置分佈皆會影響該節點感測區域可被鄰居節點感測區域所完全涵蓋的程度。由定義可知，當節點與其鄰居節點間距離 d 小於感測半徑 r_s 時，兩節點感測區域焦點與節點位置構成之中央角θ必介於 2π/3 與 π 之間。因此若要使鄰居節點完全涵蓋節點的感測區域，則鄰居的數量至少要為三個，且節點感測區域邊界皆須完全被鄰居涵蓋。利用此項性質，Tian 等人[53] 所提出選擇休眠節點的方法可達到感測品質無損失。

Augusto 等人[56]使用 Voronoi Diagram 將感測區域劃分為多個小區塊，每一區塊內有一個感測節點。當劃分出來的區塊面積小於某一個值時，就關閉位於此區塊的節點。

上述方法皆須知道感測節點的確實位置。若是沒有了位置相關訊息時，有學者提出使用隨機的方式來決定節點的休息與否[57]。休息的機率值是依照網路節點密度來決定，當節點密度高時則休息機率就高。決定出的機率值可以估算出最感測品質下降程度。利用發出探測訊息[52]來計算收到回應數的方式也不需要知道節點的位置。如果廣播探測訊息的通訊半徑比感測半徑小，當節點收到回應訊息時，可依照收到訊息數的多寡來決定節點是否可以休息。有學者[54]考慮事件被感測到的機率隨與感測器距離增加而下降的模型。在此模型中，某一地點的感測品質被定義為該點被節點感測到的期望值。作者利用某節點休眠後，該節點原先可感測區域的感

測品質下降程度來決定該節點是否可以休息。

四.研究方法

在找出並驗證「均勻點分佈」模型所具有的基本性質這部分，我們以連結機率與連結總數期望值為著手點。

我們直接由均勻分佈的機率密度函數 (Probability Density Function)與連結成立的條件推導出連結機率的值。尚未見到其他學者採取此種直接的估算方式。假設下列「均勻點分佈」模型參數：n 個感測器均勻分佈在一個 $l \times m$ 封閉矩形區域內；每個感測器具有通訊半徑 r_c 與感測半徑 r_s。令任意兩感測器 i 與 j 的位置座標分別為 (X_i, Y_i) 與 (X_j, Y_j)。則 i 與 j 形成通訊連結的機率為

$$\Pr[U + V \le r_c^2] = \int_{u=0}^{r_c^2} \int_{v=0}^{r_c^2 - u} h(u,v)\,dv\,du$$

其中 $U = (X_i - X_j)^2$, $V = (Y_i - Y_j)^2$, 且 $h(u, v)$ 為 U 與 V 的聯合機率密度函數 (Joint Probability Density Function)。因為 U 與 V 互相獨立，上述問題變成求 U 與 V 的機率密度函數。以 U 為例，假設 $F(u)$是 U 的機率分佈函數 (Probability Distributed Function)。我們知道

$$F(u) = \Pr[U \le u] = \Pr[Z^2 \le u] = \Pr[Z \le \sqrt{u}].$$

其中 $Z = |X_i - X_j|$且 $0 \le u \le l^2$。要計算 U 的機率分佈函數，需要一些積分的技巧，但是要特別注意邊界條件。我們相信這是一個可以解決的問題。同理 V 的機率密度函數也可以求得任意連結形成的機率。

連結機率的估算也可以由另一個方向著手。假設我們可以計算出每個感測器無線電波的期望涵蓋面積（已考慮邊界效應)，令其為λ。則兩個感測器形成通訊連結的機率，即為其中一個感測器落入另一個感測器通訊範圍內的機率。這個值因為感測器是均勻分佈的關係，將會是λ / (lm)。這個方法的困難點在於λ的精確值。

上述兩種計算連結機率的方法可互相驗證。另外，也可以透過模擬實驗的方式評量分析的準確度。

另外，我們想出一個方法，可望用來計算一群感測器涵蓋面積的期望值。令 C_n 為 n 個均勻分佈隨機放置的感測器所涵蓋的面積。我們可以將感測器的佈建視為一隨機程序(Stochastic Process)，即以一個接一個的方式隨機放置。假設已有 n - 1 個感測器放置好，當我們放入第 n 個感測器時，這個新放入的感測器將只有部分面積涵蓋原先 n - 1 個感測器未涵蓋處。令δ為此感測器期望感測面積（已考慮邊界效應)，且令ρ為第 n 個感測器期望增加的涵蓋面積占δ的比例。我們可以得到 $\mathrm{E}[C_{n+1}] = \mathrm{E}[C_n] + \rho\delta$。又依據均勻分佈的假設，$\rho$應為放置 n - 1 個感測器後，尚未涵蓋面積佔全部區域面積的比例。因此我們可以得到

$$\rho = \frac{A - \mathrm{E}[C_{n-1}]}{A}.$$

其中 $A = lm$ 代表目標區域的總面積。於是我們可以得到下列的遞迴關係式 (Recurrence Relation)

$$\mathrm{E}[C_n] = \mathrm{E}[C_{n-1}] + \left(1 - \frac{C_{n-1}}{A}\right)\delta.$$

這個問題就可以化簡成解此遞迴關係式與求出δ精確值的問題。同樣地，我們可以透過模擬實驗的方式評量分析的準確度。

五.結果與討論

我們已成功定量分析出下列網路整體性質

與「均勻點分佈」模型基本參數之間的明確數學關係。

- 任兩個感測器形成無線連結的機率
- 任兩個無線連結成立的聯合機率
- 每個感測器的期望連結數目
- 個別感測器的期望涵蓋面積
- 一群感測器的期望涵蓋面積
- 一群感測器的 *k*-coverage 期望值
- 感測網路的群聚係數(Clustering Coefficient)
- 隱藏終端機數目的期望值

令 $A = l \times m$ 為感測節點佈建區域的面積。任兩個感測器形成無線連結的機率，會受到邊界效應的影響。圖二為通訊半徑 400 的感測器在 1000×1000 目標區域內每個 10×10 大小位置的連結出現機率。很明顯可以看出當感測器位於目標區域中央位置時，連結形成的機率較高；當感測器位於邊界周圍時，連結形成的機率較低。可見連結出現機率受到邊界效應的影響。

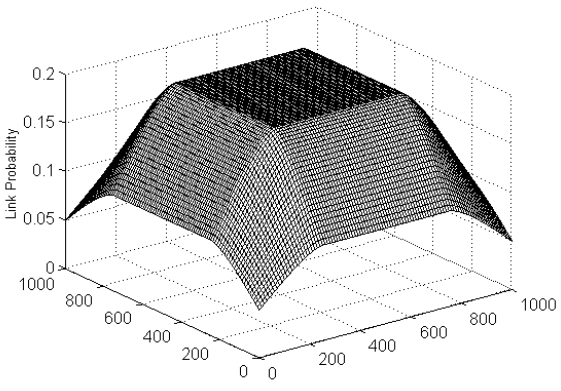

圖二：感測器所在位置與連結形成機率的關係 (r_c = 250)

我們分析出，在不考慮邊界效應時，連結出現的機率為 $p_n = \pi r_c^2/A$。考慮邊界效應時，連結出現機率的期望值為

$$p_b = \frac{\frac{1}{2}r_c^4 - \frac{3}{4}lr_c^3 - \frac{3}{4}mr_c^3 + \pi r_c^2 ml}{m^2 l^2}. \qquad (1)$$

(1)式已經由上節所述述兩種計算連結機率的方法互相驗證過。模擬實驗的結果(如圖三）也證實我們(1)式的正確性。

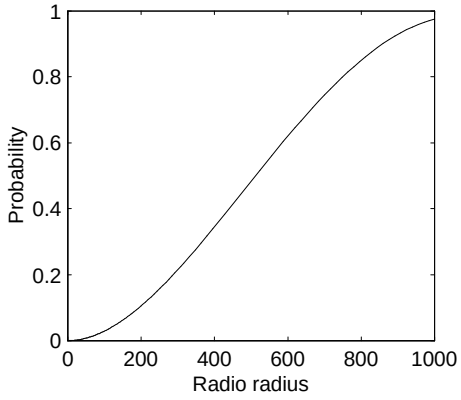

圖三：感測器傳輸半徑與連結形成機率的關係

至於任兩個無線連結同時出現的聯合機率，也受到邊界效應的影響。如果兩個連結沒有共同的連接點，顯然這兩條連結出現與否為互相獨立。當兩個連結有共同的連接點，不考慮邊界效應時，其聯合機率為 p_n^2。這是因為當不考慮邊界效應時，任兩個無線連結成立的事件是互相獨立的。我們已經證明了這一點[25]。

當兩個連結有共同的連接點，且考慮邊界效應時，我們證明了此兩條連結出現與否並不為互相獨立[25]，其理由如下。令 E_{AB} 表感測器 A 與感測器 B 的無線連結，則 E_{AB} 形成的機率與 A 所在的位置有關。當 A 出現在目標區域中央時，E_{AB} 形成的機率會比 A 出現在邊界周圍時 E_{AB} 形成的機率來得大。因此當 E_{AB} 形成時，感測器 A 有較大的機率出現在目標區域中央而非在邊界周圍，導致另一個連結 E_{AC} 形成的機率也會比較大。當初提出本計劃時，我們認為可以推導出考慮邊界效應時，任兩個無線連結成立的聯合機率。經

過我們努力的研究後發現，這項工作並不如想像中容易。

無線感測網路中，每個感測器的期望連結數目為無線連結的形成機率乘以 n-1。因此不考慮邊界效應時其值為 $p_n(n\text{-}1)$；考慮邊界效應時其值為 $p_b(n\text{-}1)$。

在涵蓋面積的計算方面，不考慮邊界效應時，很顯然地個別感測器的涵蓋面積為 πr_s^2。當考慮邊界效應時，令隨機變數 N 為個別感測器的涵蓋面積。則 N 值視感測器所在的位置而異。我們利用簡單機率以及微積分的技巧推導出 N 的期望值為

$$E[N]=\frac{\frac{1}{2}r_s^4-\frac{3}{4}lr_s^3-\frac{3}{4}mr_s^3+\pi r_s^2 ml}{ml}. \qquad (2)$$

於計算一群感測器的涵蓋面積 C_n 時，我們利用上一節所述的方法，將感測器的佈建視為一隨機程序(Stochastic Process)，順利推導出 n 個感測器涵蓋面積的期望值為 [25,27]

$$E[C_n]=\left[1-\left(1-\frac{E[N]}{A}\right)\right]A. \qquad (3)$$

我們在推導過程中，將兩相依事件的聯合機率以個別發生的機率相乘替代，因此(3)式只能算是趨近值。不過我們透過模擬實驗發現(3)式的準確度相當高。圖四顯示在 1000×1000 區域中，依照(3)式所計算出來的感測器覆蓋率與感測器數量和感測半徑間的關係。

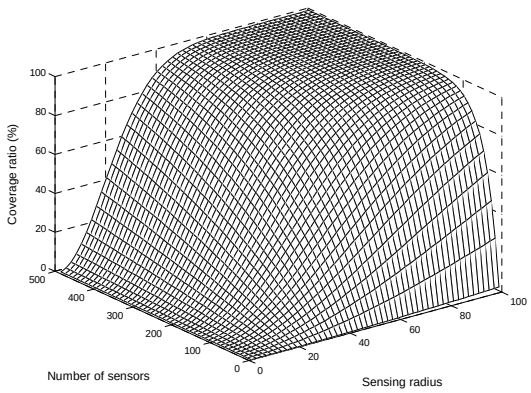

圖四：感測器覆蓋率與感測器數量與感測半徑的關係

至於 k-coverage 的計算與計算 C_n 的觀念類似。令 C_i^j 表示隨機佈置 i 個感測器後被 j-cover 的面積，則對於任何大於等於零且小於等於 i–j 的 d 而言，我們有

$$E[C_i^j]=\sum_{t=0}^{d}\binom{d}{t}p^{d-t}(1-p)^t E[C_{i-d}^{j-d+t}] \qquad (4)$$

其中 p 是連結出現的機率。要計算 n 個感測器的 k-coverage 期望值 $E[C_n^k]$，可根據(4)式再以 Dynamic Programming 的技巧算出 [27]。

這項研究成果的直接應用將是，給定目標區域、感測器的數目及可感測範圍，我們即可明確指出預期會有多少的面積被感測器涵蓋。同樣地，給定感測器的可感測範圍及期望涵蓋面積，我們亦可估計需要多少感測器方能達成。

我們推導出在「均勻點分佈」模型下，不考慮邊界效應時，任何無線隨意網路（包括無線感測網路）的群聚係數 c 是個常數 [26]：

$$c=1-\frac{3\sqrt{3}}{4\pi}. \qquad (5)$$

c 與節點密度或通訊半徑皆無關。我們也順利推導出了在「均勻點分佈」模型下，不考慮邊界效應時隱藏終端機數目的期望值[26]：

$$\eta=\frac{1-c}{2}n(n-1)(n-2)p_n^2. \qquad (6)$$

結果顯示隱藏終端機數目與節點數目的三次方與連結機率的平方乘積成正比。

運用同樣的觀念，我們進一步推導出在無線網路中各種拓樸子結構出現的機率 [36]。

我們的結果顯示，邊界效應是導致許多基本性質在「均勻點分佈」模型中無法精確估算或得到精確結果的原因。我們雖

有一些方法可以對付邊界效應，但得到的結果卻只能為期望值，而非更佳的機率分佈。

在我們的研究過程中也發現，感測器位置隨機放置所造成的影響，可以用隨機程序(Stochastic Process)的模型來分析，如涵蓋面積的計算。這一方面的應用極有潛力。目前我們正嘗試利用隨機程序模型來估測移動物件在感測網路中感測器監視區域間移動的頻率。

在資料傳送機制的成果方面[33,34]，我們分析出以邏輯鏈結構傳送資料的電力耗用來自於兩大部份。第一部分是耗在感測器之間的通訊，主要受到鏈結構的影響。第二部份的電力耗用在 Sink 節點與鏈首節點間的通訊，主要受鏈首排程(Leader Scheduling)的影響。

為了減少第一部分的電力耗用，我們利用了虛擬鏈的概念。傳統鏈結構[41, 42, 43]中的每段邊皆對應成一條直接通訊連結。在虛擬鏈中的每段邊可以不限於直接通訊連結，而可以用間接多重傳送來達成。這樣做除了可以較為省電外，也較具有彈性。當感測器通訊距離有限制時，傳統的鏈建構演算法可能無法順利建立鏈結構。如果以虛擬鏈處理，只要感測網路是連結的，保證可以順利建立鏈結構。

為了建立鏈建構，我們必須計算每一個感測節點到另一個感測節點如使用多重傳送所需耗用的最少電力。此種計算可以使用傳統的 all-pair 最短路徑演算法達成，不過此演算法的計算複雜度較高。我們也可以用另一種方法，在純為直接連結的網路拓樸邏輯上尋找最小連通樹(Minimum Spanning Tree)，再以此樹作為任兩個感測器之間多重傳送所走的路徑藍本。此演算法的計算複雜度較低，但不保證任兩個感測器之間多重傳送所走的路徑是耗用電力最少的。如再加上節點間使用直接傳送所耗用的電力，我們就有三種方法可評估節點間建立鏈連結所需耗用的電力。每一種方法得出的結果都是一個成本圖(Cost Graph)，圖中的節點代表感測器，連結兩個節點的線段標有數字，代表此兩個節點間建立鏈連結所需耗用的電力成本。

我們也提出了一個新的鏈建構演算法。傳統的鏈建構演算法[41, 42, 43]皆使用貪婪的建構策略。差別在於每一次選擇新的節點加入到建立中的鏈時，是附加在鏈的最前端[41, 42]還是可以插入到目前鏈的中間[43]。在此我們的作法是先在 Cost Graph 上尋找最小連通樹，再將此樹全部搜尋(Traverse)一次，以節點搜尋的順序建立鏈。這三種鏈建構演算法與三種 Cost Graph，總共可以組合成九種不同的結果。

在 Sink 節點與鏈首節點間通訊的電力耗用部分，我們順利推導出最佳化鏈首排程問題其實是一個線性規劃(Linear Programming)的問題。我們也以實驗的方式證實，MRPF (Most Residual Power First)此種簡單的鏈首排程策略，效能相當接近最佳排程，而遠勝過簡單的 Round Robin 策略。

在密度控制方面，我們設計出一個分散式密度控制協定[35]，不需要知道所有感測節點的位置資訊，而效能接近有位置資訊的作法。此協定將時間切割為固定長度的 Round。每一 Round 的前半段執行此協定，後半段感測器再根據執行的結果決定是否要進入休眠狀態（如圖五）。

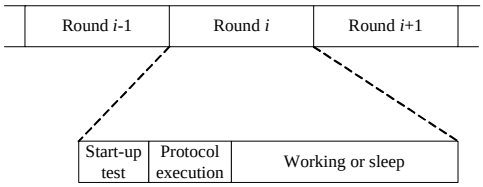

圖五：Round 的結構

我們的方法需要量測訊息傳送與接收節點間的距離。策略是仿照 OGDC[55]的作法，設法在高節點密度的環境中找出如圖六所示的放置模式。此模式中，感測器 S 週遭的鄰居形成一邊長為 $\sqrt{3}$ 倍感測半徑的正六邊形。此時 S 與其鄰居節點可完全覆蓋此一區域而不會產生任何漏洞。

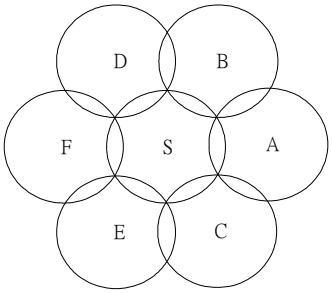

圖六：使用最少感測器數目達到完全覆蓋的感測器放置模式

此種設計要面臨的挑戰如下：

1. 量測誤差：信號傳遞問題如環境干擾及多重路徑衰減都會使得現有的距離量測技術產生誤差。誤差的程度視通訊環境而定。在極度糟糕的通訊環境下，量測誤差有可能高到使任何的距離量測技術皆無法得到有效結果。
2. 工作競爭：當某個感測器徵求與其距離為$\sqrt{3}$倍感測半徑的鄰居節點成為工作夥伴時，可能有超過一個以上的鄰居符合此資格。此種情形下，如何使這些節點不知道對方存在的情況下彼此競爭得到唯一的一個勝出者，是一個設計上的挑戰。
3. 傳輸衝撞：當一個以上鄰近的節點同時送出協定訊息時，會造成傳輸衝撞而使得訊息無法順利收到。

以上第一點並非我們協定要克服的困難。第二點乃是空間上節點的競爭，第三點乃是時間上節點的競爭。我們以複雜的計時器設計來解決最後這兩點問題。圖七是我們設計協定的狀態轉換圖。

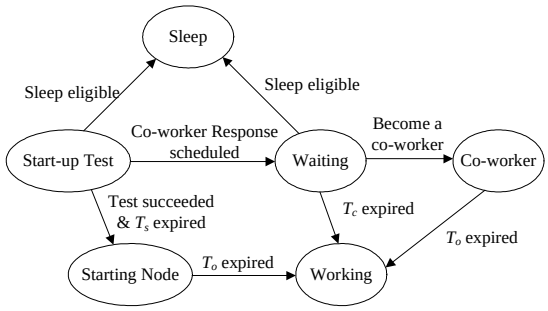

圖七：我們設計出的密度控制協定狀態變換圖

圖八顯示我們設計出來的協定與OGDC[55]與 PEAS[52]這兩個具代表性的密度控制程式，在工作節點數的效能。此結果是使用 ns2 模擬程式得到的結果。可以看出用我們設計出來的協定所得到的工作節點數略多於用 OGDC 所得到的結果，但是少於用 PEAS 所得到的工作節點數。這一點是因為 OGDC 擁有位置資訊，故可以較精確決定所需的工作節點數。我們的協定與 PEAS 皆未使用位置資訊，但我們的協定效能表現又較 PEAS 佳。

在涵蓋率的比較方面，這三種密度控制機制的表現恰好與他們在工作節點數的效能表現相反（如圖九）。PEAS 有較高的覆蓋率，其次為我們設計出來的協定，最差的是 OGDC。可見過分強調使用較少的工作節點，會影響到覆蓋率的表現。

由於我們設計出來的協定乃是模仿 OGDC 的運作。所以我們進一步比較我們的協定與 OGDC 的差異。結果如圖十至圖十一所示。

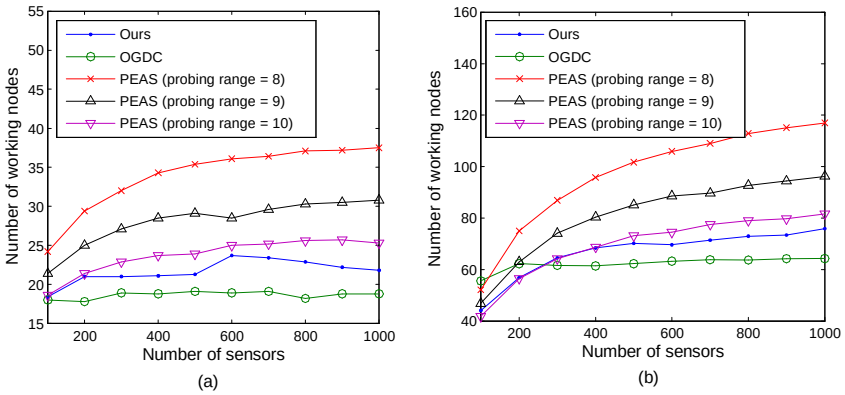

圖八：不同密度控制程式的工作節點數於(a)50×50 網路與(b) 100×100 網路

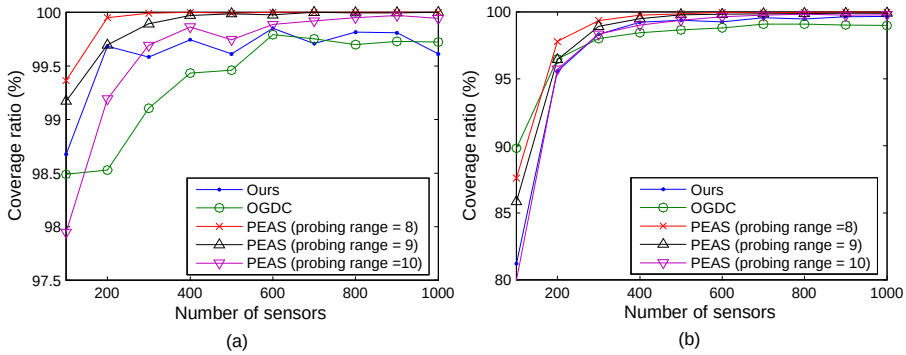

圖九：不同密度控制程式的覆蓋率於(a)50×50 網路與(b) 100×100 網路

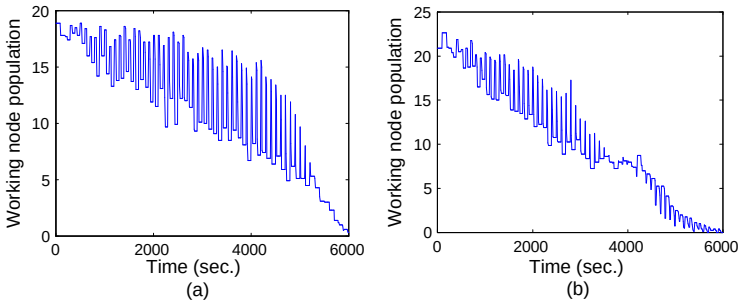

圖十：工作節點數隨網路運作時間變化的情形(a)OGDC 與(b) 我們的協定

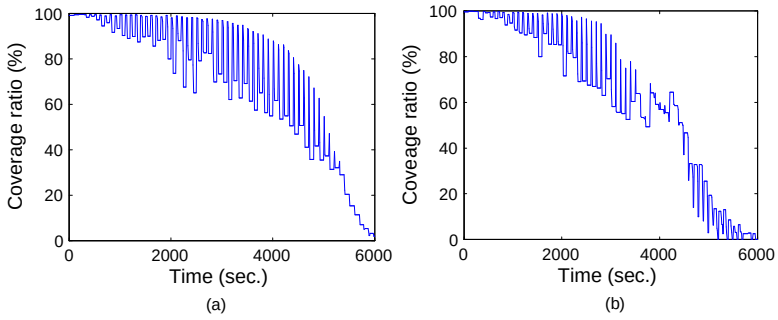

圖十一：覆蓋率隨網路運作時間變化的情形(a)OGDC 與(b) 我們的協定

參考文獻

[1] Ian F. Akyìldìz, Weilian Su, Yogesh Sankarasubramaniam, and Erdal Cayirci, “A survey on sensor networks,” *IEEE Commun. Magazine*, vol. 40, no. 8, pp. 102-114, Aug. 2002.

[2] Nirupama Bulusu, Deborah Estrin, Lewis Girod, and John Heidemann, “Scalable coordination for wireless sensor networks: Self-configuring localization systems,” in *Proc. 6th IEEE Int'l Symp. on Commun. Theory and Application*, Ambleside, U.K., Jul. 2001.

[3] Christian Bettstetter, “On the minimum node degree and connectivity of a wireless multihop network,” in *Proc. of ACM Symp. on Mobile Ad Hoc Netw. and Comp.*, Lausanne, Switerland, Jun. 2002, pp. 80-91.

[4] C. Bettstetter and O. Krause, “On border effects in modeling and simulation of wireless ad hoc networks,” in *Proc. IEEE Int’l Conf. on Mobile and Wireless Commun. Netw.*, Recife, Brazil, Aug. 2001.

[5] C. Bettstetter and J. Zangl, “How to achieve a connected ad hoc network with homogeneous range assignment: an analytical study with consideration of border effects,” in *Proc. of 4th IEEE Int’l Workshop on Mobile and Wireless Commun. Netw.*, 2002, pp. 125-129.

[6] Olivier Dousse, Patrick Thiran, and Martin Hasler, “Connectivity in ad-hoc and hybrid networks,” in *Proc. INFOCOM*, New York, USA, Jun. 2002, pp. 1079-1088.

[7] Piyush Gupta and P. R. Kumar, “Critical power for asymptotic connectivity in wireless networks,” in W.M. McEneaney, G. Yin, and Q. Zhang, editors, *Stochastic Analysis, Control, Optimization and Applications: A Volume in Honor of W.H. Fleming*, Birkhauser, Boston, 1998.

[8] Piyush Gupta and P. R. Kumar, “The capacity of wireless networks,” *IEEE Trans. Inform. Theory*, 46(2): 384-404, 2000.

[9] P. Hall, *Introduction to the Theory of Coverage Processes*, John Wiley and Sons, 1988.

[10] Chi-Fu Huang and Yu-Chee Tseng, “The coverage problem in a wireless sensor network,” in *ACM Int’l Workshop on Wireless Sensor Networks and Applications*, Sep. 2003, pp.115-121

[11] L. Kleinrock and J. Silvester, “Optimum transmission radii for packet radio networks or why six is a magic number,” in *Proc. IEEE 1978 Natl. Telecomm. Conf.*, 1978, pp. 4.3.1-4.3.5.

[12] Kubisch et al., “Distributed algorithms for transmission power control in wireless sensor networks,” in *Proc. IEEE Wireless Commun. and Netw. Conf.* (WCNC), Mar. 2003, pp. 558-563.

[13] Xiang-Yang Li, Peng-Jun Wan, and Ophir Frieder, “Coverage in wireless ad hoc sensor networks,” *IEEE Trans. Comput.*, 52(6): 1-11, Jun. 2003.

[14] S. Meguerdichian, F. Koushanfar, M. Potkonjak, and M.B. Srivastava, “Coverage problems in wireless ad-hoc sensor networks,” in *Proc. IEEE INFOCOM*, Apr. 2001, pp. 1380-1387.

[15] J. O'Rourke, *Art Gallery Theorems and Algorithms*, Oxford University Press, New York, NY, 1987.

[16] P. Piret, “On the connectivity of radio networks,” *IEEE Trans. Inform. Theory*, 37(5): 1490-1492, 1991.

[17] Thomas K. Philips, Shivendra S. Panwar, and Asser N. Tantawi, “Connectivity properties of a packet radio network model,” *IEEE Trans. Inform. Theory*, 35(5): 1044-1047, Sep. 1989.

[18] Paolo Santi and Douglas M. Blough, “An evaluation of connectivity in mobile wireless ad hoc networks,” in *Proc. of IEEE Conf. on Dependable Syst. and Netw.*, 2002, pp. 89-98.

[19] Paolo Santi and Douglas M. Blough, “The critical transmitting range for connectivity in sparse wireless ad hoc networks,” *IEEE Trans. Mobile Computing*, 2(1): 25-39, 2003.

[20] Paolo Santi, Douglas M. Blough, and Feodor Vainstein, “A probabilistic analysis for the range assignment problem in ad hoc networks,” in *Proc. ACM MobiHOC*, CA, USA, Oct. 2001.

[21] Sanjay Shakkottai, R. Srikant, and Ness Shroff, “Unreliable sensor grids: Coverage, connectivity and diameter,” in *Proc. IEEE INFOCOM*, 2003, pp. 1073-1083.

[22] M. Tubaishat and S. Madria, “Sensor networks: an overview,” *IEEE Potentials*, Apr.-May 2003, pp. 20-23.

[23] Feng Xue and P. R. Kumar, “The number of neighbors needed for connectivity of wireless networks,” *Wireless Networks*, April 2002.

[24] Marco Zuniga and Bhaskar Krishnamachari, “Optimal transmission radius for flooding in large scale sensor networks,” in *Proc. IEEE ICDCS Workshops*, May 2003, pp. 697-702.

[25] Li-Hsing Yen and Chang Wu Yu, “Link probability, network coverage, and related properties of wireless ad hoc networks,” *The 1st IEEE Int'l Conf. on Mobile Ad-hoc and Sensor Systems*, Fort Lauderdale, Florida, USA, Oct. 2004, pp. 525-527. (本計畫之論文發表)

[26] Li-Hsing Yen and Yang-Min Cheng, “Clustering coefficient of wireless ad hoc networks and the quantity of hidden terminals,” *IEEE Communications Letters*, Vol. 9, No. 3, pp. 234-236, Mar. 2005. (本計畫之論文發表)

[27] Li-Hsing Yen, Chang Wu Yu, and Yang-Min Cheng, “Expected *k*-Coverage in Wireless Sensor Networks,” *Ad Hoc Networks*, Vol. 5, No. 4, pp. 636-650, Sept. 2006. (本計畫之論文發表)

[28] D. J. Watts and S. H. Strogatz, “Collective dynamics of ‘small-world’ networks,” *Nature*, vol. 393, pp. 440–442, June 1998.

[29] R. Albert and A.-L. Barab´asi, “Statistical mechanics of complex networks,” *Reviews of Modern Physics*, vol. 74, pp. 47–97, Jan. 2002.

[30] B. Bollob´as, *Random Graphs*, 2nd ed. Cambridge University Press, 2001.

[31] G. Xing, X. Wang, Y. Zhang, C. Lu, R. Pless, C. Gill, Integrated coverage and connectivity configuration for energy conservation in sensor networks, *ACM Trans. on Sensor Networks*, to appear.

[32] H. Zhang, J. C. Hou, Maintaining sensing coverage and connectivity in large sensor networks, in *Int’l Workshop on Theoretical and Algorithm Aspects of Sensor, Ad Hoc Wireless and Peer-to-Peer Networks*, 2004.

[33] Li-Hsing Yen, Ming-Zhou Cai, Yang-Min Cheng, and Ping-Yuan Yang, “Energy optimization for chain-based data gathering in wireless sensor networks,” *International Journal of Communication Systems*, in press. (本計畫之論文發表)

[34] Li-Hsing Yen, Ming-Zhou Cai, Yang-Min Cheng, and Ping-Yuan Yang, “Minimizing energy expense for chain-based data gathering in wireless sensor networks,” *The 2nd European Workshop on Wireless Sensor Networks*, Istanbul, Turkey, Jan.-Feb. 2005, pp. 312-320. (本計畫之論文發表)

[35] Yang-Min Cheng and Li-Hsing Yen, “Range-based density control for wireless sensor networks,” *Proc. 4th Annual Communication Networks and Services Research Conference*, Moncton, New Brunswick,

Canada, May 2006, pp. 170-177. (本計畫之論文發表)

[36] C. W. Yu and Li-Hsing Yen, "Computing subgraph probability of random geometric graphs: Quantitative analyses of wireless ad hoc networks," 25th IFIP WG 6.1 Int'l Conf. on Formal Techniques for Networked and Distributed Systems, Oct. 2005, published in *Lecture Notes in Computer Science*, vol. 3731, pp. 458-472. (本計畫之論文發表)

[37] Wei Ye, J. Heidemann, and D. Estrin, "An energy-efficient MAC protocol for wireless sensor networks," in *Proc. IEEE INFOCOM*, Jun. 2002, pp. 1567-1576.

[38] Pei Guangyu and C. Chien, "Low power TDMA in large wireless sensor networks," in *Proc. IEEE MILCOM*, Oct. 2001, vol. 1, pp. 347-351.

[39] L. Krishnamachari, D. Estrin, and S. Wicker, "The impact of data aggregation in wireless sensor networks," in *Proc. IEEE ICDCS Workshops*, Jul. 2002, pp. 575-578.

[40] B. Krishnamachari, Y. Mourtada, and S. Wicker, "The energy-robustness tradeoff for routing in wireless sensor networks," in *Proc. IEEE ICC*, May 2003, pp. 1833-1837.

[41] S. Lindsey and C. S. Raghavendra, "PEGASIS: Power-efficient gathering in sensor information systems," in *Proc. IEEE Aerospace Conf. Proc.*, Mar. 2002, pp. 1125-1130.

[42] S. Lindsey, C. Raghavendra, and K. Sivalingam, "Data gathering algorithms in sensor networks using energy metrics," *IEEE Trans. Parallel and Distr. Syst.*, 13(9): 924-935, Sep. 2002.

[43] Kemei Du, Jie Wu, and D. Zhou, "Chain-based protocols for data broadcasting and gathering in the sensor networks," in *Proc. Int'l Parallel and Distr. Processing Symp.*, Apr. 22-26, 2003, pp. 260 -267.

[44] V. Annamalai, S. K. S. Gupta, L. Schwiebert, "On tree-based convergecasting in wireless sensor networks," in *Proc. IEEE Wireless Commun. and Netw. Conf.*, Mar. 2003, pp. 1942 -1947.

[45] S. Upadhyayula, V. Annamalai, and S. K. S. Gupta, "A low-latency and energy-efficient algorithm for convergecast in wireless sensor networks," in *Proc. IEEE GLOBECOM*, 2003.

[46] W. R. Heinzelman, A. Chandrakasan, and H. Balakrishnan, "Energy-efficient communication protocol for wireless microsensor networks," in *Proc. 33rd Annual Hawaii Int'l Conf. on Syst. Sciences*, Jan. 2000, pp. 3005-3014.

[47] W. Heinzelman, A. Chandrakasan, and H. Balakrishnan, "An application-specific protocol architecture for wireless microsensor networks," *IEEE Trans. Wireless Commun.*, 1(4): 660 -670, Oct. 2002.

[48] Chih-Shun Hsu and Jang-Ping Sheu, "Initialization protocols for IEEE 802.11-based ad hoc networks," in *Proc. 9th Int'l Conf. on Parallel and Distr. Syst., Dec.* 2002, pp. 273-278.

[49] M. A. Youssef, M. F. Younis, and K.A. Arisha, "A constrained shortest-path energy-aware routing algorithm for wireless sensor networks," in *Proc. IEEE WCNC*, Mar. 2002, pp. 794-799.

[50] R. Krishnan and D. Starobinski, "Message-efficient self-organization of wireless sensor networks," in *Proc. IEEE Wireless Commun. and Netw*, Mar. 2003, pp. 1603-1608.

[51] G. Gupta and M. Younis, "Load-balanced clustering of wireless sensor networks," in *Proc. IEEE ICC*, May 2003, pp. 1848-1852.

[52] Fan Ye, G. Zhong, Songwu Lu and Lixia Zhang, "PEAS: a robust energy conserving protocol for long-lived sensor networks," in *Proc. 23rd International Conference on Distributed Computing Systems*,

19-22 May, 2003, pp. 28-37.

[53] Di Tian and N. D. Georganas, "A coverage-preserving node scheduling scheme for large wireless sensor networks," in *Proc. First ACM Int'l Workshop on Wireless Sensor Networks and Applications*, 2002, pp. 32-41.

[54] Jun Lu and Tatsuya Suda, "Coverage-aware self-scheduling in sensor networks," in *Proc. IEEE Annual Workshop on Comput. Commun.*, Oct. 2003, pp. 117-123.

[55] H. Zhang, J. C. Hou, "Maintaining sensing coverage and connectivity in large sensor networks," *Wireless Ad Hoc and Sensor Networks: An International Journal*, vol. 1,no. 1-2, pp. 89-123, 2005.

[56] M.A.M. Viera, L.F.M. Viera, L.B. Ruiz, A.A.F. Loureiro, A.O. Fernandes and J.M.S. Nogueira, "Scheduling nodes in wireless sensor networks: a Voronoi approach," *IEEE International Conference on Local Computer Networks*, Oct. 2003, pp. 423-429.

[57] C.-F. Hsin, M. Liu, "Network coverage using low duty-cycled sensors: Random & coordinated sleep algorithms," in *Int'l Symp. on Information Processing in Sensor Networks*, 2004.

計畫成果自評

本研究計畫成果符合原先預期。計畫成果已有一部份（群聚係數與隱藏終端機數目）發表在 2005 年 3 月份的 *IEEE Communications Letters* 上（見參考文獻[26]），還有一部份（連結機率、期望連結數目、聯合連結機率、與期望涵蓋）發表在 2004 年於美國佛羅里達舉行之 *1st IEEE Int'l Conf. on Mobile Ad-hoc and Sensor Systems* 會議上（見參考文獻[25]）。我們並擴充了期望涵蓋與 *k*-coverage 這部分的內容，發表在 *Ad Hoc Network* 期刊上（參考文獻[27]）。我們推導出的在無線網路中各種拓樸子結構出現的機率，發表在 *25th IFIP WG 6.1 Int'l Conf. on Formal Techniques for Networked and Distributed Systems*（參考文獻[36]）。

在省電的資料傳送機制方面，我們探討的如何建立較佳的鍊結構，與最佳的鍊首節點(Header)排程，成果發表在 *The 2nd European Workshop on Wireless Sensor Networks*（見參考文獻[34]），後續成果並已被 *International Journal of Communication Systems* 期刊接受。密度控制協定方面，我們設計出的不需位置資訊，僅需要知道訊息傳送與接收節點間距離的協定，已發表在 *The 4th Annual Communication Networks and Services Research Conference*（參考文獻[35]）。目前正在修改，準備投稿至國際期刊。

總計此二年期研究計畫已發表三篇國際期刊論文及四篇國際研討會論文，研究成果具有一定之學術價值。但若要增加其應用價值，須將所得結果應用在感測網路的協定設計上，這方面正是我們後續還要努力的目標。在申請專利方面，目前評估並不適合。

Link Probability, Network Coverage, and Related Properties of Wireless Ad Hoc Networks

Li-Hsing Yen and Chang Wu Yu
Dept. of Computer Science and Information Engineering
Chung Hua University
Taiwan 300, Republic of China

***Abstract*— This paper has analyzed link probability, expected node degree, expected number of links, and expected area collectively covered by a finite number of nodes in wireless ad hoc networks. Apart from the formulation of exact mathematical expressions for these properties, we have disclosed two fundamental results: (1) Every possible link has an equal probability of occurrence. (2) It is the border effects that makes two links probabilistically dependent. Simulation results show that our analysis predicts related measure with accuracy.**

I. Introduction

We define an $\langle n, r, l, m\rangle$-network as a wireless ad hoc network (MANET) that possesses the following properties: (1) The network consists of n nodes placed in an $l \times m$ rectangle area. (2) The position of each node is a random variable uniformly distributed over the given area. (3) Each node has a transmission radius of r unit length, where $r \leq \min(l, m)$. (4) Any two nodes that are within the transmission range of each other will have a link connecting them[1]. We are concerned with several fundamental properties in this model.

It was commonly believed that the probability of link occurrence in MANET cannot be identical. However, we found that it is not true. The expected node degree and the expected number of links in a MANET have also been obtained. Previous work on degree estimate [1], [2], [3] does not take into account *border effects* [2], which refers to the circumstance that a node placed near the system border will cover less area (with its radio signal) than nodes placed midway. Border effects makes the conventional estimate inaccurate. In contrast, our results are not subject to border effects.

The next problem to solve is the expected area jointly covered by a finite number of nodes, which is a form of so-called *coverage problem*. Given the expected node coverage, which can be derived from link probability, the problem at hand is still complicated by the fact that region covered by each node may overlap one another in a stochastic way.

We also found that border effects are not only a major obstacle to precise calculations of many network properties, but also the reason behind the probabilistic dependency of two links. This implies that the occurrences of any two links are independent to each other if border effects disappear.

[1]This is a simplified model as only path loss is taken into account. In a practical network, different nodes would experience different shadowing, thus making the transmission radius different for different nodes.

We conducted experiments for a quantitative analysis of the impacts of border effects. The numerical results show that our analysis accurately estimates these network properties.

II. Link Probability and Expected Degree

This section computes analytically the probability that two arbitrary nodes are within the transmission range of each other. Let the position of node i be determined by Cartesian coordinates (X_i, Y_i), where $0 \leq X_i \leq l$ and $0 \leq Y_i \leq m$. Clearly, X_i's are iid random variables with p.d.f. $f(x) = 1/l$ over the range $[0, l]$, while Y_i's are iid with p.d.f. $f(y) = 1/m$ over $[0, m]$.

Lemma 1: For any two distinct nodes i and j in an $\langle n, r, l, m\rangle$-network with positions (X_i, Y_i) and (X_j, Y_j), respectively, let $Z_i = |X_i - X_j|$ and $W_i = |Y_i - Y_j|$. We have $\Pr[Z_i \leq z] = (-z^2 + 2lz)/l^2$, $0 \leq z \leq l$, and $\Pr[W_i \leq w] = (-w^2 + 2mw)/m^2$, $0 \leq w \leq m$.

Proof: We show only the result for $\Pr[Z_i \leq z]$. The result for $\Pr[W_i \leq w]$ can be derived in a similar way. We know that $\Pr[Z_i \leq z] = \Pr[X_i < X_j \leq X_i + z] + \Pr[X_j < X_i \leq X_j + z]$. The value of $\Pr[X_i < X_j \leq X_i + z]$ can be calculated by taking integrals over two non-overlapping intervals and then adding them up. The first interval corresponds to when $X_i + z \leq l$. We have $\Pr[X_i < X_j \leq X_i + z \leq l] = \int_0^{l-z}\int_{x_i}^{x_i+z} f(x_i, x_j)dx_j dx_i$, where $f(x_i, x_j)$ is the joint p.d.f. of X_i and X_j. Since X_i and X_j are independent, $f(x_i, x_j) = f(x_j)f(x_j) = 1/l^2$. So $\Pr[X_i < X_j \leq X_i + z \leq l] = z(1 - z)/l^2$. The second interval corresponds to when $X_i + z > l$. We have $\Pr[l - z < X_i < X_j \leq l] = z^2/2l^2$. Therefore, $\Pr[X_i < X_j \leq X_i + z] = \frac{z}{l^2}(l - z) + \frac{z^2}{2l^2} = \frac{-z^2+2lz}{2l^2}$. Similarly, $\Pr[X_j < X_i \leq X_j + z] = \frac{-z^2+2lz}{2l^2}$. It follows that $\Pr[Z_i \leq z] = \frac{-z^2+2lz}{l^2}$. □

Lemma 2: For any two distinct nodes i and j in an $\langle n, r, l, m\rangle$-network with positions (X_i, Y_i) and (X_j, Y_j), respectively, let $U_i = (X_i - X_j)^2$ and $V_i = (Y_i - Y_j)^2$. The p.d.f. of U_i is $f(u) = (\frac{l}{\sqrt{u}} - 1)/l^2$, $0 \leq u \leq l^2$, and the p.d.f. of V_i is $g(v) = (\frac{m}{\sqrt{v}} - 1)/m^2$, $0 \leq v \leq m^2$.

Proof: Let $F(u)$ be the probability distribution function of U_i. We have $F(u) = \Pr[U_i \leq u] = \Pr[Z_i \leq \sqrt{u}]$, $0 \leq u \leq l^2$, where $Z_i = |X_i - X_j|$. By Lemma 1 we have $\Pr[Z_i \leq \sqrt{u}] = -u + 2l\sqrt{u}/l^2$. Therefore the p.d.f. of U_i is $f(u) = F'(u) = (\frac{l}{\sqrt{u}} - 1)/l^2$, $0 \leq u \leq l^2$. Similarly, the p.d.f. of V_i is $g(v) = (\frac{m}{\sqrt{v}} - 1)/m^2$, $0 \leq v \leq m^2$. □

0-7803-8815-1/04/$20.00 ©2004 IEEE

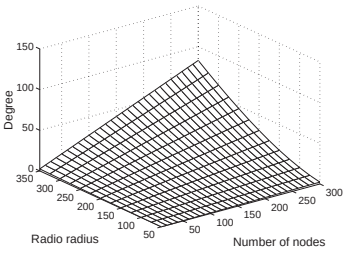

Fig. 1. Expected degree for $n = 10$ to 300 and $r = 50$ to 350 in a 1000×1000 rectangle.

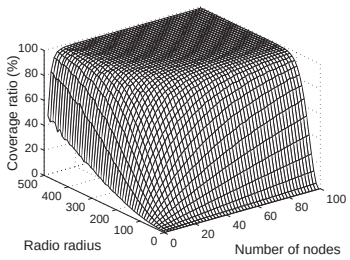

Fig. 2. Ratios of the theoretical network coverage to the whole system area, with n ranging from 1 to 99 and r ranging from 1 to 491.

Theorem 1: In an $\langle n, r, l, m\rangle$-network, the occurrence probability of link $\langle i, j\rangle$ between any two distinct nodes i and j is $(\frac{1}{2}r^4 - \frac{4}{3}lr^3 - \frac{4}{3}mr^3 + \pi r^2 ml)/m^2l^2$.

Proof: Link $\langle i, j\rangle$ forms if and only if the distance between them is not greater than r. Thus the probability of link $\langle i, j\rangle$ is $\Pr[U_i + V_i \leq r^2] = \int_0^{r^2}\int_0^{r^2-u} h(u, v)dvdu$, where $U_i = (X_i - X_j)^2$, $V_i = (Y_i - Y_j)^2$, and $h(u, v)$ is the joint p.d.f. for U_i and V_i. Since U_i and V_i are independent, we have $h(u, v) = f(u)g(v)$, where $f(u)$ and $g(v)$ are as defined in Lemma 2. It follows that $\Pr[U_i + V_i \leq r^2] = (\frac{1}{2}r^4 - \frac{4}{3}lr^3 - \frac{4}{3}mr^3 + \pi r^2 ml)/m^2l^2$. □

Theorem 1 indicates that the probability of link $\langle i, j\rangle$ depends on the values of m, l, and r but not on i, j, or n, and all links have equal probability. The result of identical link probability does not contradict the thought that link occurrences are correlated.

Given n random variables R_i, where $i = 1$ to n, it is known [4] that $E[R_1+R_2+\cdots+R_n] = E[R_1]+E[R_2]+\cdots+E[R_n]$ regardless whether R_i's are independent to each other. Since each node may have $n - 1$ links and there are potentially $n(n-1)/2$ links between n nodes, we have the following two corollaries.

Corollary 1: The average (expected) node degree in an $\langle n, r, l, m\rangle$-network is $(n - 1)(\frac{1}{2}r^4 - \frac{4}{3}lr^3 - \frac{4}{3}mr^3 + \pi r^2 ml)/m^2l^2$.

Corollary 2: The expected number of links in an $\langle n, r, l, m\rangle$-network is $n(n - 1)(\frac{1}{2}r^4 - \frac{4}{3}lr^3 - \frac{4}{3}mr^3 + \pi r^2 ml)/2m^2l^2$.

Fig. 1 shows the expected degree estimated by Corollary 1 for various n and r.

Theorem 2: In an $\langle n, r, l, m\rangle$-network with $r \leq \min(l/2, m/2)$, the expected transmission coverage area of a single node is $\phi = (\frac{1}{2}r^4 - \frac{4}{3}lr^3 - \frac{4}{3}mr^3 + \pi r^2 ml)/ml$.

Proof: It is straightforward since link probability derived in Theorem 1 is equal to ϕ/lm. The result has also been confirmed by geometric computation (for details, refer to [5]). □

III. Expected Network Coverage

Let C_n be the expected area jointly covered by n randomly placed nodes, referred to as *network coverage*. We want to express C_n in terms of expected node coverage ϕ.

The deployment of nodes can be thought of as an iterative process that places nodes one by one. Suppose $n - 1$ nodes have already been placed. When we add the nth node to the $(n - 1)$-node network, the extra coverage area contributed by this newly placed node is a portion of its node coverage. Let ρ_n denote the proportion of this portion to the node coverage. C_n can be expressed as a recurrence relation as $C_n = C_{n-1}+\rho_n\phi$. Since nodes are uniformly distributed, ρ_n is expected to be the proportion of the uncovered area to the whole target area. Thus we have $\rho_n = (A-C_{n-1})/A$, where A denotes the area of the target region. It turns out that $C_n = C_{n-1} + (1 - C_{n-1}/A)\phi$. Since $C_1 = \phi$, solving this recurrence relation yields

$$C_n = [1 - (1 - \phi/A)^n]A. \quad (1)$$

Eq. (1) holds for any shape of target region as well as for any shape of node's coverage. Let us focus on $l \times m$ rectangular where $A = lm$ and, if border effects are not taken into account, $\phi = \pi r^2$. Eq. (1) becomes

$$C_n = [1 - (1 - \pi r^2/lm)^n]lm. \quad (2)$$

This is a rough estimation for expected network coverage. The following theorem gives us a precise estimation considering border effects.

Theorem 3: For an $\langle n, r, l, m\rangle$-network with $l \geq 2r$ and $m \geq 2r$, the expected area collectively covered by all nodes is

$$C_n = \left[1 - \left(\frac{m^2l^2 - \frac{1}{2}r^4 + \frac{4}{3}lr^3 + \frac{4}{3}mr^3 - \pi r^2 ml}{m^2l^2}\right)^n\right] lm$$

.

Proof: We have $A = lm$ for an $l \times m$ rectangle. By Theorem 2 and (1), we obtain the result. □

Fig. 2 shows the ratios of the theoretical network coverage to the whole system area for various n and r.

IV. Link Dependency

Many researchers (e.g., [1]) have pointed out that link occurrences are not independent events. Their arguments are mainly based on a three-link scenario: the event that both link $\langle X, Y\rangle$ and link $\langle X, Z\rangle$ show up is not independent of the event that $\langle Y, Z\rangle$ exists. However, few studies have reported on the dependency of any two links.

Two links that share no common endpoint node are obviously independent to each other. Let X, Y, and Z be three nodes and consider L_{XY}, the event that link $\langle X, Y\rangle$ exists, and

L_{XZ}, the event that link $\langle X, Z\rangle$ exists. When X is located at (x, y), the probability that both Y and Z are located in X's coverage is $[c(x, y)/lm]^2$, where $c(x, y)$ denotes the area that a node located at (x, y) covers. Thus the joint link probability of L_{XY} and L_{XZ} is

$$\Pr[L_{XY}, L_{XZ}] = \frac{1}{lm}\int_0^l\int_0^m \left[\frac{c(x,y)}{lm}\right]^2 dydx. \qquad (3)$$

Theorem 4: If border effects can be removed but system area remains constant (which can be achieved by using, e.g., torus convention [6], [3]), the occurrences of any two links are independent to each other.

Proof: Clearly, $c(x, y) = \pi r^2$ for all x, y if border effects disappear. Thus $\Pr[L_{XY}] = \Pr[L_{XZ}] = \pi r^2/lm$. By (3), we have $\Pr[L_{XY}, L_{XZ}] = \Pr[L_{XY}]\Pr[L_{XZ}]$ for all X, Y, Z. □

Corollary 3: It is the border effects that makes any two links in an $\langle n, r, l, m\rangle$-network dependent.

Note that the three-link argument remains valid regardless of border effects.

V. Simulations and Numerical Results

We conducted additional experiments for a quantitative analysis of the impacts of border effects on network properties. The first property we measured is average degree. Fig. 3(a) shows average degrees estimated with Poisson point process [2] (the rough estimate) while Fig. 3(b) shows the results obtained from the simulation. Fig. 3(c) shows the errors of Corollary 1 in comparison with the simulated results, where the error is defined as $|\text{estimated value} - \text{measured value}|/\text{measured value}$. The mean is 2.56×10^{-4} while the standard deviation is 4.81×10^{-4}. Fig. 3(c) shows the errors of the rough estimate in comparison with the simulated results. Clearly, the errors are in proportional to the radio radius r (the mean is 0.22 and the standard deviation is 0.11). This can be explained as the impacts of border effects become significant as the radio radius becomes large. In contrast, the largest error of our estimate is only 0.6%, occurring on the smallest n and r.

We next measured coverage ratio, the ratio of the network coverage to the whole system area. Fig. 4(a) shows results estimated with Eq. (2). Fig. 4(b) shows the results obtained from the experiments. The errors of Theorem 3 in comparison with the simulated results are shown in Fig. 4(c), with mean $= 0.50 \times 10^{-2}$ and standard deviation $= 0.68 \times 10^{-2}$. Fig. 4(d) shows the errors of the results estimated with (2). The mean is 2.97×10^{-2} and the standard deviation is 5.78×10^{-2}. We conclude that Theorem 3 is more accurate and has smaller variance than (2).

VI. Conclusions

Exact mathematical expressions for link probability, expected node degree, expected number of links, and expected node and network coverage have been formulated. It has been shown that every possible link in a MANET has equal probability of occurrence. It is also proven that two links are probabilistically independent to each other if there is no border effect. Additional experimental results confirm our analysis.

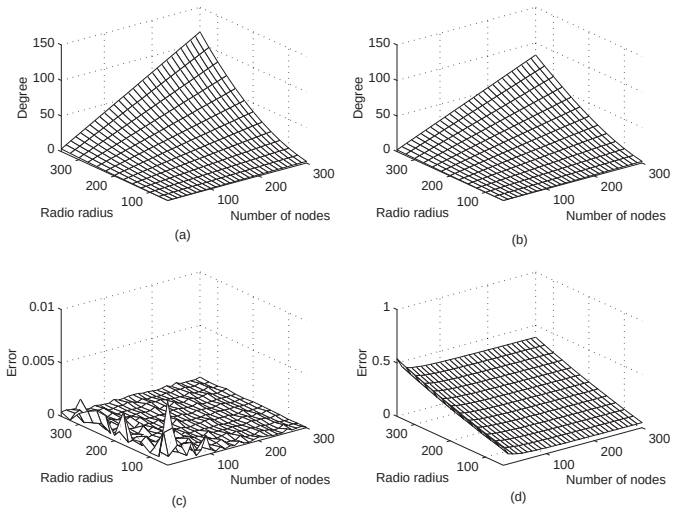

Fig. 3. Average degree in 1000×1000 rectangle. (a) Results of rough estimate. (b) Simulated results. Each value is averaged over 100,000 experiments. (c) Errors of precise estimate. (d) Errors of rough estimate.

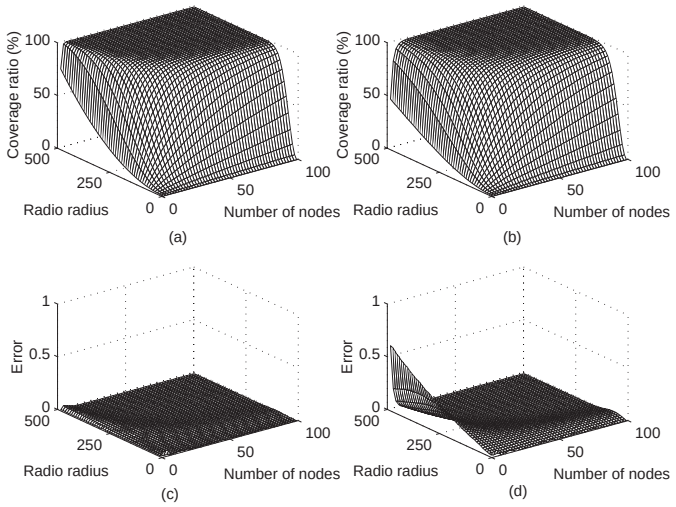

Fig. 4. Network coverage ratio in 1000×1000 rectangle, with the same ranges of n and r as with Fig. 2. (a) Results estimated by Eq. (2). (b) Results obtained from simulations (averaged over 10,000 experiments). (c) Errors with Theorem 3. (d) Errors with Eq. (2).

References

[1] L. Kleinrock and J. Silvester, "Optimum transmission radii for packet radio networks or why six is a magic number," in *Proc. IEEE 1978 Natl. Telecomm. Conf.*, 1978, pp. 4.3.1–4.3.5.

[2] C. Bettstetter and J. Zangl, "How to achieve a connected ad hoc network with homogeneous range assignment: an analytical study with consideration of border effects," in *Proc. 4th IEEE Int'l Workshop on Mobile and Wireless Communications Network*, 2002, pp. 125–129.

[3] C. Bettstetter, "On the minimum node degree and connectivity of a wireless multihop network," in *Proc. of ACM Symp. on Mobile Ad Hoc Netw. and Comp.*, Lausanne, Switerland, June 2002, pp. 80–91.

[4] E. R. Dougherty, *Probability and Statistics for the Engineering, Computing, and Physical Sciences*. Prentice-Hall, Inc., 1990, p. 238.

[5] L.-H. Yen and C. W. Yu, "Link probability, network coverage, and related properties of wireless ad hoc networks," Dept. CSIE, Chung Hua Univ., Taiwan, Tech. Rep. CHU-CSIE-TR-2004-004, May 2004.

[6] P. Hall, *Introduction to the Theory of Coverage Processes*. John Wiley and Sons, 1988.

Clustering Coefficient of Wireless Ad Hoc Networks and the Quantity of Hidden Terminals

Li-Hsing Yen, *Member, IEEE,* and Yang-Min Cheng

***Abstract*— Clustering coefficient has been proposed to characterize complex networks. Hidden terminals may degrade the performance of CSMA (carrier sense multiple access) protocol. This letter computes analytically the clustering coefficient and the quantity of hidden terminals for ad hoc networks. The former turns out to be a constant and the latter is proportional to n^3p^2, where n is the number of nodes and p is the link probability. The connection between them has been established, and simulation results confirm our analytic work.**

***Index Terms*— Hidden terminal, clustering coefficient, ad hoc networks, multihop networks.**

I. Introduction

NETWORKS of complex topology such as social networks and the Internet were traditionally modeled as random graphs [1]. In Watts and Strogatz's pioneer work [2], they recognized that many real systems are better described as 'small-world' networks rather than random graphs. Small-world networks differ from random graphs in the tendency of clustering, or cliqueness, which is the extent to which a node's neighbors are also neighbors to each other. Specifically, for node i having $m_i \geq 2$ neighbors, at most $C(m_i, 2)$ links may exist between these neighbors. Let E_i be the total number of links that exist among i's neighbors. Node i's clustering coefficient, c_i, is defined to be $E_i/C(m_i, 2)$. The clustering coefficient of the whole network is the average of all individual c_i's.

Clustering coefficients of random graph, regular network [2], and small-world network have been well investigated [3]. To the best knowledge of the author, however, the clustering coefficient of mobile ad hoc (multi-hop) networks (MANETs) has not yet been known. In this letter, we have computed analytically the clustering coefficient of MANET under the assumption of uniform location model (Section II).

Hidden terminals refer to a pair of nodes that cannot sense each other but have at least one common neighbor node [4]. Transmission collisions may occur between hidden terminals, which cannot be prevented by carrier sensing. The existence of hidden terminals thus degrades the performance of CSMA (carrier sense multiple access) protocol substantially [5]. There have been extensive schemes proposed to deal with hidden terminal problems (e.g., RTS/CTS-like handshake [6], [7]). However, little research has been done on quantifying hidden terminals for a given MANET. We also have analyzed the number of hidden terminals and found its connection to the clustering coefficient (Section III).

Manuscript received July 20, 2004. The associate editor coordinating the review of this letter and approving it for publication was Dr. Carla-Fabiana Chiasserini. This work has been supported by the National Science Council, ROC, under grant NSC 93-2213-E-216-024.

The authors are with the Department of Computer Science and Information Engineering, Chung Hua University, Hsinchu, Taiwan, ROC (e-mail: lhyen@chu.edu.tw).

Digital Object Identifier 10.1109/LCOMM.2005.03017.

II. Clustering Coefficient of MANET

Definition 1: An $\langle n, r, l, m\rangle$-network is a MANET that possesses the following properties:

- The network consists of n nodes placed in an $l \times m$ rectangle area.
- The position of each node is a random variable uniformly distributed over the given area.
- Each node has a transmission radius of a uniform length r.
- A link exists between two nodes that are within the transmission range of each other[1].

A wireless node is said to cover a region if every point in this region is within the node's radio transmission range. A node placed near system boundary will cover less system area than expected, as part of its coverage region is outside the system. This is referred to as border effects. To avoid clumsy results brought by border effects, we use torus convention [8], which turns the rectangle area into a torus such that the region covered by any node is considered completely within the system. Torus convention leads to the following property.

Lemma 1: The link probability (namely, the probability of occurrence of any link) in an $\langle n, r, l, m\rangle$-network with torus convention is $p = \pi r^2/lm$ when $r \leq \min(l/2, m/2)$.

We must further restrict r's maximum value to $\min(l/3, m/3)$ when torus convention is used. The reason is that two nodes that are not neighbors but have a common neighbor can be distanced up to $2r$ from each other. When torus convention is used and the distance between them is only slightly less than $2r$, they may be incorrectly recognized as neighbors on the opposite direction if $r > \min(l/3, m/3)$, making our analysis imprecise.

The following two lemmas are essential in our derivation.

Lemma 2: [9] Given m random variables R_i, where $i = 1$ to m, $E[R_1 + R_2 + \cdots + R_m] = E[R_1] + E[R_2] + \cdots + E[R_m]$ regardless whether R_i's are independent to each other.

Lemma 3: The expected area jointly covered by two neighboring nodes is

$$r^2\left(\pi - \frac{3\sqrt{3}}{4}\right).$$

Proof: See Appendix. ■

[1]This is a simplified model as only path loss is taken into account.

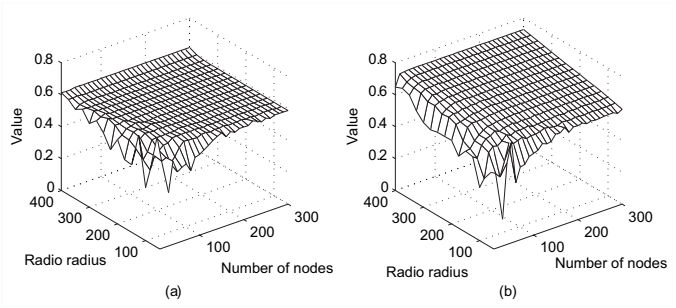

Fig. 1. Measured cluster coefficients in 1000×1000 rectangle (a) with torus convention and (b) without torus convention. Each value is averaged over 100 experiments. Nodes having less than two neighbors are not taken into account.

Given any node A with $m \geq 2$ neighbors, let $N(A) = \{X_1, X_2, \cdots, X_m\}$ be the set of A's neighbors. For any $X_i \in N(A)$, let $N(A)_i = \{X_j | X_j \in N(A) \wedge X_j \in N(X_i)\}$ be the set of nodes that are both neighbors of A and X_i. Note that $|N(A)_i|$ stands for the number of links connecting two neighbors of A such that one end of these links is X_i. The expected number of links connecting any two neighbors of A is

$$\frac{1}{2} E\left[\sum_{i=1}^{m} |N(A)_i|\right].$$

The expected value is divided by two because we count every link twice (at both ends). By Lemma 2 we have

$$\frac{1}{2} E\left[\sum_{i=1}^{m} |N(A)_i|\right] = \frac{1}{2}\sum_{i=1}^{m} E\left[|N(A)_i|\right] = \frac{1}{2}\sum_{i=1}^{m} E_{A,i},$$

where $E_{A,i}$ denotes the expected value of $|N(A)_i|$. By Lemma 3, the ratio of the region jointly covered by A and X_i to A's coverage area is expected to be

$$1 - \frac{3\sqrt{3}}{4\pi}.$$

It follows that

$$E_{A,i} = (m-1)\left(1 - \frac{3\sqrt{3}}{4\pi}\right)$$

for any i. Therefore, the expected number of links connecting any two neighbors of A is

$$\frac{m(m-1)}{2}\left(1 - \frac{3\sqrt{3}}{4\pi}\right).$$

Dividing this value by the maximum number of links (i.e. $m(m-1)/2$) yields the expected clustering coefficient.

Theorem 1: The network clustering coefficient in an $\langle n, r, l, m\rangle$-network is expected to be a constant

$$c = 1 - \frac{3\sqrt{3}}{4\pi}.$$

We conducted simulations to confirm the accuracy of this theorem (See Fig. 1). The measured clustering coefficient data with torus convention have mean 0.5820 (with standard deviation 0.0313), very close to the theoretical value. The clustering coefficient without torus convention is also close to the predicted value but increases slightly with r (mean = 0.6492, standard deviation = 0.0656). Observe the little raise of the measured value with torus convention when $r > \min(l/3, m/3)$.

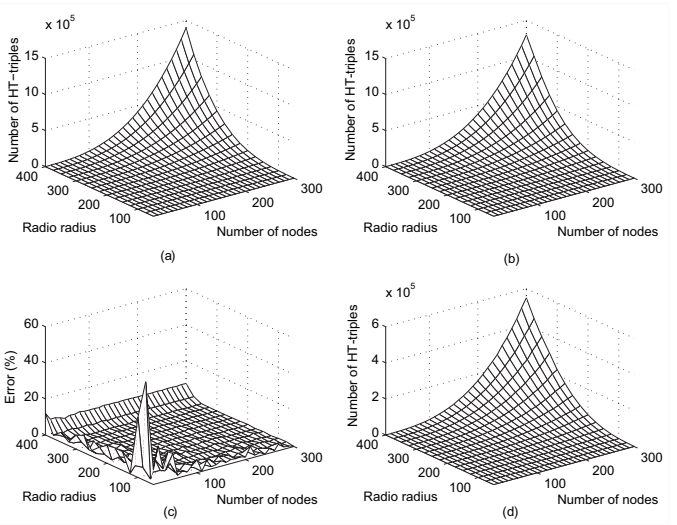

Fig. 2. Number of HT-triples in 1000×1000 rectangle. Each value is averaged over 100 experiments. (a) Theoretical result. (b) Measured result with torus convention. (c) Estimation error of (a) with respect to (b). (d) Measured result without torus convention.

III. Quantity of Hidden Terminals

Definition 2: For any three nodes X, Y, and Z, an HT-triple $\langle X, Y, Z\rangle$ is formed if both X and Z can communicate with Y but they cannot reach each other. Y is said to be the *joint node* of the HT-triple.

$\langle X, Y, Z\rangle$ forms an HT-triple if Y located within X's coverage region and Z located within Y's coverage region but not within X's. By Lemmas 1 and 3, the probability of HT-triple $\langle X, Y, Z\rangle$ is

$$\frac{\pi r^2}{lm} \times \frac{\pi r^2 - r^2\left(\pi - \frac{3\sqrt{3}}{4}\right)}{lm} = (1-c)p^2. \qquad (1)$$

Theorem 2: The total number of HT-triples in an $\langle n, r, l, m\rangle$-network is expected to be

$$\eta = 3\binom{n}{3}(1-c)p^2 = \frac{1-c}{2} n(n-1)(n-2)p^2.$$

Proof: There are $C(n, 3)$ ways to select three nodes from n nodes without order. Any selection may yield three possible HT-triples, each corresponding to a distinct joint node ($\langle X, Y, Z\rangle$ forms an HT-triple whenever $\langle Z, Y, X\rangle$ does and vise versa, so they are treated as one unique HT-triple). Although some of these HT-triples may be correlated, the expected number can still be computed (thanks to Lemma 2). ■

Note that $\eta \propto n^3 p^2$. Fig. 2 compares theoretical result estimated by Theorem 2 with measured values obtained from simulations. Fig. 2(c) shows error of the theoretical estimation, where the error is defined to be

$$\frac{\text{theoretical value} - \text{measured value}}{\text{measured value}}.$$

The error is almost negligible except for the smallest n and r, where the measured value approaches zero. There is also rather

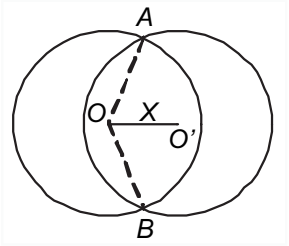

Fig. 3. Two circles intersect each other.

high error when $r > 350$ with torus convention. The measured result obtained by not using torus convention follows the same trend as the theoretical estimation, but with a different scale.

IV. Conclusions

We have formulated the clustering coefficient of MANETs, which turns out to be a constant with torus convention. The number of hidden terminals in a MANET is proportional to n^3p^2, where n is the number of nodes and p is the link probability. Simulation results have confirmed the accuracy of our computation.

References

[1] B. Bollobás, *Random Graphs*, 2nd ed. Cambridge University Press, 2001.

[2] D. J. Watts and S. H. Strogatz, "Collective dynamics of 'small-world' networks," *Nature*, vol. 393, pp. 440–442, June 1998.

[3] R. Albert and A.-L. Barabási, "Statistical mechanics of complex networks," *Reviews of Modern Physics*, vol. 74, pp. 47–97, Jan. 2002.

[4] F. A. Tobagi and L. Kleinrock, "Packet switching in radio channels: Part II - the hidden terminal problem in carrier sense multiple-access modes and the busy-tone solution," *IEEE Trans. Commun.*, vol. 23, pp. 1417–1433, Dec. 1975.

[5] C. L. Fullmer and J. Garcia-Luna-Aceves, "Solutions to hidden terminal problems in wireless networks," in *Proc. SIGCOMM*, Cannes, France, 1997, pp. 39–49.

[6] P. Karn, "MACA: A new channel access method for packet radio," in *Proc. of ARRL/CRRL Amateur Radio 9th Computer Networking Conference*, Sept. 1990, pp. 134–140.

[7] V. Bharghavan, A. Demers, S. Shenker, and L. Zhang, "MACAW: A media access protocol for wireless LAN's," in *Proc. of ACM SIGCOMM'94*, London, England, 1994, pp. 212–225.

[8] P. Hall, *Introduction to the Theory of Coverage Processes*. John Wiley and Sons, 1988.

[9] E. R. Dougherty, *Probability and Statistics for the Engineering, Computing, and Physical Sciences*. Prentice-Hall, Inc., 1990, p. 238.

Appendix

Suppose that two nodes of transmission radius r located at O and O' are neighbors, with the distance between them $X \leq r$ (X is a random variable). We want to calculate the expected area of the lens-shaped region that is jointly covered by these two nodes. Let A and B be two distinct intersecting points of these two circles (refer to Fig. 3). The area of each half of the "lens" is equal to the area of sector OAB minus the area of triangle OAB. Let $\theta = \angle AOB$ be the central angle given X, where $2\pi/3 \leq \theta \leq \pi$. We have

$$X = 2r\cos(\theta/2).$$

The area of triangle OAB is

$$\left[\frac{2r\sin\left(\frac{\theta}{2}\right)\frac{X}{2}}{2}\right] = r^2\sin\left(\frac{\theta}{2}\right)\cos\left(\frac{\theta}{2}\right) = \frac{r^2\sin\theta}{2}.$$

So the area of the lens is

$$2\left[\frac{\pi r^2\theta}{2\pi} - \frac{r^2\sin\theta}{2}\right] = r^2(\theta - \sin\theta).$$

Let $F(x)$ be the probability distribution function (p.d.f.) of X. Since nodes are uniformly distributed, $\Pr[X \leq x]$ is proportional to the area of the circle having radius x and being centered at O. Therefore,

$$F(x) = \Pr[X \leq x] = \frac{\pi x^2}{\pi r^2} = \frac{x^2}{r^2}.$$

Since $\theta = 2\arccos(X/2r)$, the p.d.f. of θ is

$$\begin{aligned} G(y) &= \Pr\left[\frac{2\pi}{3} \leq \theta \leq y\right] \\ &= \Pr\left[2r\cos\frac{y}{2} \leq X \leq r\right] \\ &= F(r) - F\left(2r\cos\frac{y}{2}\right) = -2\cos y - 1. \end{aligned}$$

It follows that the probability density function of θ is $g(y) = G'(y) = 2\sin y$. Therefore, the expected area of the lens-shaped region that is jointly covered by O and O' is

$$\int_{\frac{2\pi}{3}}^{\pi} r^2(\theta - \sin\theta)(2\sin\theta)d\theta = r^2\left(\pi - \frac{3\sqrt{3}}{4}\right).$$

Available online at www.sciencedirect.com
SCIENCE DIRECT®
Ad Hoc Networks 4 (2006) 636–650
Ad Hoc Networks
www.elsevier.com/locate/adhoc

Expected k-coverage in wireless sensor networks

Li-Hsing Yen *, Chang Wu Yu, Yang-Min Cheng

Department of Computer Science and Information Engineering, Chung Hua University, No. 707, Sec. 2, WuFu Road, Hsinchu, Taiwan 300, China

Received 2 December 2004; received in revised form 7 May 2005; accepted 22 July 2005
Available online 24 August 2005

Abstract

We are concerned with wireless sensor networks where n sensors are independently and uniformly distributed at random in a finite plane. Events that are within a fixed distance from some sensor are assumed to be detectable and the sensor is said to cover that point. In this paper, we have formulated an exact mathematical expression for the expected area that can be covered by at least k out of n sensors. Our results are important in predicting the degree of coverage a sensor network may provide and in determining related parameters (sensory range, number of sensors, etc.) for a desired level of coverage. We demonstrate the utility of our results by presenting a node scheduling scheme that conserves energy while retaining network coverage. Additional simulation results have confirmed the accuracy of our analysis.

Keywords: Sensor network; Coverage; Border effect; Node scheduling; Uniform distribution

1. Introduction

Rapid progress in wireless communications and micro-sensing MEMS technology has enabled the deployment of wireless sensor networks. A wireless sensor network consists of a large number of sensor nodes deployed in a region of interest. Each sensor node is capable of collecting, storing, and processing environmental information, and communicating with other sensors. The position of sensor nodes need not be engineered or predetermined [1] for the reason of the enormous number of sensors involved [2] or the need to deploy sensors in inaccessible terrains [1]. Due to technical limitations, each sensor node can detect only events that are within some range from it. A piece of area in the deployment region is said to be *covered* if every point in this area is within the sensory range of some sensor. In this paper, we are concerned with a fundamental property of such

* Corresponding author. Tel.: +886 351 86408; fax: +886 351 86416.
E-mail address: lhyen@chu.edu.tw (L.-H. Yen).

1570-8705/$ - see front matter © 2005 Elsevier B.V. All rights reserved.
doi:10.1016/j.adhoc.2005.07.001

network: the area that can be covered by at least k out of n sensors randomly placed in a bounded region. This is referred to as k-coverage [3,4] and the problem of evaluating k-coverage is a form of so-called *coverage problem*.

In the literature, the coverage problem has been formulated in various ways. A related but different formulation is asking how to effectively cover a given region. For example, the *Art Gallery Problem* is to determine the number of guards/cameras and the position of each guard/camera that are necessary to visually cover a polygonal region (the art gallery) [5]. Shakkottai et al. [6] have considered the necessary and sufficient conditions for covering a sensor network with nodes arranged in a grid over a square region. The coverage problem has also been formulated as to determine whether or how well a given set of sensors covers a region [3]. In [7], Meguerdichian et al. defined worst and best case coverage problems, which are to identify regions of low and high observability, respectively. Geometry techniques such as Voronoi diagram and Delaunay triangulation have been used in solving these problems [7,8]. For other definitions of coverage problem, refer to the survey in [9].

In the aforementioned context, one either needs to determine (as an output) or is given (as an input) the exact position of every sensor. In contrast, it is the distribution of sensor positions rather than exact position of every sensor that is assumed in our problem setting.

The problem of estimating k-coverage is complicated by two factors. First, region covered by each sensor may overlap one another in a stochastic way. Second, a sensor placed near the border of the deployment region will cover less area than sensors placed midway, since not all its disk-shaped sensory region will be within the deployment area. This is referred to as *border effects*. Prior work [10,11] established approximations or asymptotic bounds for 1-coverage problem. In contrast, we have formulated an exact mathematical expression for expected k-coverage in face of border effects. To the best knowledge of the authors, this is the first study that achieves this. A direct application of our result is that given a deployment area and the number of sensors with their sensory range, one can easily point out what level of coverage can be expected. Equivalently, given sensor's sensory range and the expected coverage ratio, one can estimate the number of sensors to be deployed. For a power conserving scheme that allows each sensor to periodically power off its sensory circuitry without coordinations with others, our finding helps in determining the active-to-sleep ratio for a desired network coverage.

The rest of the paper is organized as follows. Problem definition and related work are presented in the next section. Section 3 analyzes the expected network coverage. Section 4 discusses the applications of our finding, including a node scheduling scheme. Simulation model and numerical results are described in Section 5. Section 6 concludes our work.

2. Problem definition and related work

We assume that each sensor can detect events that are within distance r from it, where r is called *sensory range*. The area of the region that is covered by a sensor is defined to be the sensor's *node coverage*. Let N be a random variable denoting a node's coverage. N is πr^2 if the sensor's sensory region is properly contained in the deployment area. However, when a sensor is placed near the border of the deployment region, N is expected to be less than πr^2 due to border effects. A region is said to be k-covered if every location within it is covered by at least k sensors. Define k-coverage to be the size of the k-covered region after a number of sensors have been randomly placed. We want to express the expected value of k-coverage in terms of $E[N]$.

Traditionally, only 1-coverage is of interest. In [11], Philips et al. analyzed the condition that a given area is 1-covered with high probability by randomly located circles. Their analysis was done under the assumption of Poisson point process [11–15], which assumes a fixed density of nodes λ instead of the exact number of nodes n. With this modeling, whether an elemental area ds contains exactly one node is a binomial distribution with probability $ds\lambda$. For a sufficiently large number of nodes deployed within a sufficiently large

system area (but λ remains constant), the node degree can be approximated by a Poisson distribution with mean $\lambda\pi r^2$ [14]. Philips et al. proved that, for any $\epsilon > 0$, if

$$r = \sqrt{\frac{(1+\epsilon)\ln A}{\pi\lambda}},$$

then $\lim_{A\to\infty}\Pr[\text{the deployment region is 1-covered}] = 1$. Since the obtained results hold on the condition that the system area approaches infinity, where border effects become insignificant, the results are only approximations when applied to reasonable-size deployment region. Furthermore, they were sorely concerned with the condition of fully covering a deployment region; their result cannot be used to estimate the coverage degree of an arbitrary given network scenario.

The expected area that n randomly placed circles may cover in a plane (i.e., 1-coverage) has been analyzed by Hall [10]. He avoided border effects by using the so-called torus convention, which models the deployment region as a torus such that a sensor's sensory region is considered completely within the deployment area. Let A denote the area of the deployment region. Hall has shown that when $n/A \to \lambda$, where $0 < \lambda < \infty$, the ratio of uncovered area in the deployment region approaches $\exp(-\lambda\pi r^2)$ as r increases. Here πr^2 is the node coverage with torus convention.

Although Hall's estimate is only an asymptotic result, we found through experiments that it provides good estimates to a certain degree (details will be presented later). In this paper, we take a different approach and obtain a result that improves the precision of Hall's 1-coverage estimate. The improvement is particularly significant when the network is not fully covered.

We analyze k-coverage based on our estimate of 1-coverage. The degree of coverage is considered a measure of quality of service (QoS) that a sensor network provides. High QoS is essential for applications that demands high degree of accuracy or reliability. An example is distributed data fusion [16], which is the process of automatic combining or aggregating sensed data from *multiple* sensors.

Network coverage is central to node scheduling schemes that conserve energy by powering off redundant nodes while retaining network coverage. Node scheduling involves the decisions of when and which node can enter power-saving or sleep mode. Based on how these decisions are made, existing approaches can be classified as coordinated or uncoordinated ones. A coordinated coverage-preserving node scheduling scheme presented in [17] demands that each sensor advertises its location information and listens to advertisements from neighbors. After calculating its coverage and its neighbors', a node can determine if it is eligible to turn off its sensory circuitry without reducing overall network coverage. To avoid potential "uncovered hole" due to simultaneous turning off, a back-off protocol is proposed that requires each off-duty eligible sensor to listen to other sensor's status advertisement and, if necessary, announce its own after a random back-off time period expires. The behaviors of other coordinated schemes [18–20] are similar to [17] in that they all require the exchanges of location information and eligibility status.

Cărbunar et al. [21] transform the problem of detecting redundant sensors to that of computing Voronoi diagrams. Node location information is required in their scheme to compute the Voronoi diagram corresponding to the current node deployment. Xing et al. [4] also exploit Voronoi diagram to ensure k-coverage. They have shown that k-coverage is ensured if every critical point (where two sensor's coverage areas intersect or a sensor's coverage area and border line intersect) is covered by at least k sensors. The protocol they proposed needs location information of every sensor as well.

With location information in hand, coordinated node scheduling [17–21,4] can ensure 100% network coverage. However, the requirement of location information may not be practical if energy-hungry GPS (Global Positioning System) device is assumed for this purpose. Moreover, it is questionable whether the energy gained by turning-off sensors could compensate energy loss due to coordination. PEAS [22] is a coordinated node scheduling scheme that demands no location information. Nodes in PEAS periodically alternate between sleep and working modes. When a node wakes up from sleep mode, it can enter sleep mode again if a "probe" message can be received from

any working neighbor. PEAS does not guarantee 100% network coverage, yet energy has to be consumed on transmitting and receiving probe messages.

A uncoordinated scheme, on the other hand, demands neither positioning nor communications overhead. However, it is intrinsic that 100% network coverage cannot be guaranteed. In this paper, we present a uncoordinated node scheduling scheme that ensures *expected* network coverage.

3. Network coverage estimate

The deployment of n sensors can be modeled as a stochastic process that places sensors one by one according to a uniform distribution over R. For all $1 \leqslant i \leqslant n$, let N_i denote the size of the region that is covered by the ith placed sensor. N_i's are iid random variables with p.d.f. $1/A$ over R, where A is the size of R. Therefore,

$$E[N_i] = E[N] = \frac{1}{A}\int\int_R d(x,y)\mathrm{d}y\,\mathrm{d}x, \tag{1}$$

where $d(x, y)$ denotes the area covered by a node located at location $(x, y) \in R$. When border effects are not taken into account, $d(x, y) = \pi r^2$ for all $(x, y) \in R$ and $E[N] = \pi r^2$. We shall derive $E[N]$ with the consideration of border effects latter in this section.

Let us start with 1-coverage, based on which the estimate of k-coverage can be obtained. When a node is placed, only a portion of its node coverage gives extra 1-coverage. Let X_i denote the extra 1-coverage area contributed by the ith placed sensor and C_i be the random variable denoting the size of the 1-covered region collectively offered by i randomly placed nodes. We have $E[C_1] = E[X_1] = E[N]$ and $C_i = C_{i-1} + X_i$ for all i, $2 \leqslant i \leqslant n$. In the latter case, $E[C_i] = E[C_{i-1} + X_i]$. Although C_{i-1} and X_i are correlated (a larger C_{i-1} often implies a smaller X_i and vise versa), we still have $E[C_i] = E[C_{i-1}] + E[X_i]$ due to the linearity of expected value (which states that, given m random variables R_i, where $i = 1$ to m, $E[R_1 + R_2 + \cdots + R_m] = E[R_1] + E[R_2] + \cdots + E[R_m]$ regardless whether R_i's are independent to each other [23]). Let $F_i = X_i/N_i$ be the proportion of the extra coverage area contributed by the ith placed sensor to its node coverage. It follows that $E[C_i] = E[C_{i-1}] + E[F_iN_i]$.

If border effects are ignored, $E[N_i] = \pi r^2$ by (1), a constant that is independent of F_i, so $E[F_iN_i] = E[F_i] \times E[N_i]$. If border effects must be considered, F_i and N_i are correlated.[1] This can be justified as a smaller N_i implies that the ith node is closer to the boundary, while a larger N_i implies that the node is around the central region. Given C_{i-1}, the value of N_i thus has an effect on the distribution of F_i, though the effect may not be significant. Nevertheless, we propose to approximate $E[F_iN_i]$ by $E[F_i] \times E[N]$, where $E[N]$ is the expected node coverage when border effects are taken into account. Note this does not imply that we assume the independence between F_i and N or, equivalently, ignore border effects.

As sensor nodes are uniformly distributed, F_i is expected to be the proportion of the uncovered area to the whole deployment area. Thus we have

$$E[F_i] = \frac{A - E[C_{n-1}]}{A}.$$

It turns out that

$$E[C_i] = E[C_{i-1}] + \left(1 - \frac{E[C_{i-1}]}{A}\right)E[N]. \tag{2}$$

Since $E[C_1] = E[N]$, solving $E[C_n]$ by (2) yields

$$E[C_n] = \left[1 - \left(1 - \frac{E[N]}{A}\right)^n\right]A. \tag{3}$$

$E[N]/A$ is known to be the probability of link occurrence p if the sensory range is viewed as the range of radio communications [24]. Therefore, (3) can also be expressed as $E[C_n] = [1 - (1 - p)^n]A$.

Eq. (3) holds for any shape of deployment region as well as for any shape of node's coverage region. It is consistent with the intuition that $\lim_{n\to\infty} E[C_n] = A$ and the experimental observation [7] that after deploying some number of sensors, additional sensors do not improve 1-coverage significantly.

[1] In fact, it is border effects that makes F_i and N_i dependent. Border effects are also the cause of the dependency between any two links in MANETs [24].

Now we extend the result to general k-coverage cases. For all $0 \leqslant i \leqslant n$ and $0 \leqslant j \leqslant k$, we define the following random variables:

- C_i^j: the size of the j-covered area after i nodes have been randomly placed. Note that $C_i^0 = A$ and $C_i^1 = C_i$ for all i and $C_i^j = 0$ for all $i < j$.
- X_i^j: the extra area contributed by the ith placed sensor to the size of j-covered region.
- F_i^j: the proportion of X_i^j to N_i.

By definition, $E[C_i^j] = E[C_{i-1}^j] + E[X_i^j]$ for all $i > j$. We also propose to approximate $E[X_i^j]$ by $E[F_i^j] \times E[N]$. F_i^j is expected to be the proportion of the area that is *exactly* covered by $j-1$ out of $i-1$ sensors to the whole deployment area. Thus we have

$$E\left[F_i^j\right] = \frac{E\left[C_{i-1}^{j-1} - C_{i-1}^j\right]}{A} = \frac{E\left[C_{i-1}^{j-1}\right] - E\left[C_{i-1}^j\right]}{A}.$$

It follows that

$$\begin{aligned} E[C_i^j] &= E\left[C_{i-1}^j\right] + \left(\frac{E\left[C_{i-1}^{j-1}\right] - E\left[C_{i-1}^j\right]}{A}\right) E[N] \\ &= (1-p)E\left[C_{i-1}^j\right] + pE\left[C_{i-1}^{j-1}\right], \end{aligned} \tag{4}$$

where $p = E[N]/A$. Expanding the right-hand side recursively, we obtain

$$E[C_i^j] = \sum_{t=0}^{d} \binom{d}{t} p^{d-t}(1-p)^t E\left[C_{i-d}^{j-d+t}\right] \tag{5}$$

for all integer d, $0 \leqslant d \leqslant i-j$. It is not efficient to compute $E[C_n^k]$ by applying (5). In fact, an efficient approach to computing $E[C_n^k]$ is by way of dynamic programming [25], where the computation of $E[C_n^k]$ is carried out as a process of filling a $(n+1) \times (k+1)$ table $c(0,\ldots,n,0,\ldots,k)$. Some entries of the table are already known ($c(i,0) = A$ for all i and $c(i,j) = 0$ for all $i < j$); some can be derived by Eq. (3) ($c(i,1) = C_i$ for all i); and the others can be computed by Eq. (4). The time complexity of this approach is O(nk).

Our estimate of network coverage relies on the estimate of node coverage. Let us focus on $l \times m$ rectangular deployment region and disk-shaped sensory region centered at the sensor with sensory range r. We have $A = lm$ and, if border effects are not considered, $E[N] = \pi r^2$. Eq. (3) becomes

$$E[C_n] = \left[1 - \left(1 - \frac{\pi r^2}{lm}\right)^n\right] lm. \tag{6}$$

This is a rough estimation for expected network coverage. In the following, we shall find the value of $E[N]$ in face of border effects with the restriction that $r \leqslant \min(l,m)/2$. In accordance with the location-dependent nature of coverage, we partition deployment region R into three types of sub-regions, as depicted in Fig. 1.

Let A, B, C represent the events that a sensor node is located in sub-regions A, B, and C, respectively. It follows that

$$E[N] = \Pr[A]\phi_A + \Pr[B]\phi_B + \Pr[C]\phi_C, \tag{7}$$

where ϕ_i denotes the expected coverage when the sensor is located in region i. Since sensor's location is determined at random by uniform distribution, we have

$$\Pr[A] = \frac{(l-2r)(m-2r)}{lm}, \quad \Pr[B] = \frac{2r(l+m-4r)}{lm}, \quad \text{and} \quad \Pr[C] = \frac{4r^2}{lm}. \tag{8}$$

We already know $\phi_A = \pi r^2$. In the following, we are devoted to estimating ϕ_B and ϕ_C.

3.1. Computing ϕ_B

Let u denote the distance from a node located in B to the border of R (see Fig. 2). For a given u the overlapped area of the sensor's sensory region and the deployment region is

$$f_B(u) = u\sqrt{r^2 - u^2} + \left(\pi - \arccos\left(\frac{u}{r}\right)\right) r^2.$$

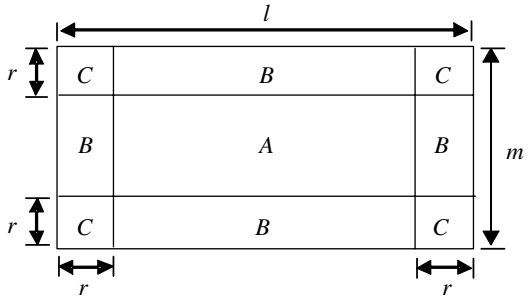

Fig. 1. Regions partitioning an $l \times m$ rectangle R.

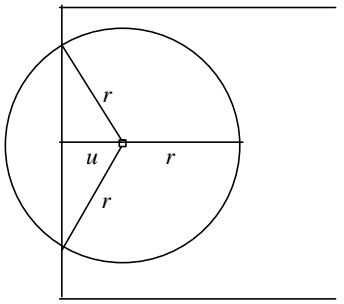

Fig. 2. A sensor node located in region B.

Since $0 \leqslant u \leqslant r$, ϕ_B can be computed as

$$\frac{1}{r}\int_0^r f_B(u)\mathrm{d}u = \frac{1}{r}\left(\int_0^r u\sqrt{r^2-u^2}\,\mathrm{d}u\right) + \pi r\int_0^r \mathrm{d}u - r\int_0^r \arccos\left(\frac{u}{r}\right)\mathrm{d}u.$$

It turns out that

$$\phi_B = \left(\pi - \frac{2}{3}\right)r^2. \tag{9}$$

3.2. Computing ϕ_C

Let the distances from a node located in C to the two borders of the rectangle be u and v, respectively (refer to Fig. 3). Depending on the location of the sensor node, two cases are possible.

1. The distance to the corner is less than r (Fig. 3a).
2. The distance to the corner is larger than or equal to r (Fig. 3b).

Let ϕ_{C1} and ϕ_{C2} denote the expected coverage in Cases 1 and 2, respectively. We have

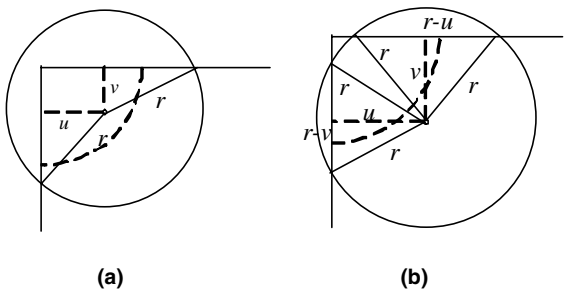

Fig. 3. Two cases of a sensor's location in region C.

$$\phi_C = \Pr[C_1|C]\phi_{C1} + \Pr[C_2|C]\phi_{C2}, \tag{10}$$

where C_1 and C_2 denote the events that the location of the node belongs to Cases 1 and 2, respectively. Due to uniform distribution of node's location, $\Pr[C_1|C]$ and $\Pr[C_2|C]$ account for the proportion of the area where the respect case is concerned. Thus we have

$$\Pr[C_1|C] = \frac{1/4\,\pi r^2}{r^2} = \frac{\pi}{4} \quad \text{and}$$
$$\Pr[C_2|C] = 1 - \frac{\pi}{4}. \tag{11}$$

We then compute ϕ_{C1}. Let $f_{C1}(u,v)$ denote the overlapped area of the node's sensory region and the deployment region in Case 1. By geometry we have (refer to Fig. 3a)

$$f_{C1}(u,v) = uv + \frac{u\sqrt{r^2-u^2}}{2} + \frac{v\sqrt{r^2-v^2}}{2} + \left(1 - \frac{\arccos\left(\frac{u}{r}\right) + \arccos\left(\frac{v}{r}\right) + \frac{\pi}{2}}{2\pi}\right)\pi r^2.$$

The expected area is

$$\phi_{C1} = \frac{1}{\frac{1}{4}\pi r^2}\int_0^r \int_0^{\sqrt{r^2-u^2}} f_{C1}(u,v)\mathrm{d}v\,\mathrm{d}u.$$

Due to space limitation, we omit tedious computation details here and simply show the result (for details, refer to [26])

$$\phi_{C1} = \frac{(\pi^2+1)r^2}{2\pi}. \tag{12}$$

Let $f_{C2}(u,v)$ denote the overlapped area of the node's sensory region and the deployment region in Case 2. We have (refer to Fig. 3b)

$$f_{C2}(u,v) = u\sqrt{r^2-u^2} + v\sqrt{r^2-v^2} + \left(1 - \frac{\arccos\left(\frac{u}{r}\right) + \arccos\left(\frac{v}{r}\right)}{\pi}\right)\pi r^2.$$

Similar technique used in computing ϕ_{C1} can be used here. It turns out that

$$\phi_{C2} = \frac{4r^2\left(\pi - \frac{4}{3} - \frac{\pi^2}{8}\right)}{4-\pi}. \tag{13}$$

By (10)–(13), we have

$$\phi_C = \left(\pi - \frac{29}{24}\right)r^2. \tag{14}$$

We summarize all derived results by the following two theorems.

Theorem 1. *If a sensor node with sensory range r is uniformly distributed at random in an $l \times m$ rectangular region ($r \leqslant \min(l, m)/2$), its expected coverage is*

$$E[N] = \frac{\frac{1}{2}r^4 - \frac{4}{3}lr^3 - \frac{4}{3}mr^3 + \pi r^2 ml}{ml}.$$

Proof. It can be derived by (7)–(9) and (14), and the knowledge that $\phi_A = \pi r^2$. □

Theorem 2. *When n sensor nodes each with sensory range r are uniformly distributed at random in an $l \times m$ rectangle ($r \leqslant \min(l, m)/2$), the expected area collectively covered by these sensors is*

$$E[C_n] = \left[1 - \left(1 - \frac{\frac{1}{2}r^4 - \frac{4}{3}lr^3 - \frac{4}{3}mr^3 + \pi r^2 ml}{m^2 l^2}\right)^n\right] lm.$$

Proof. We have $A = lm$ for an $l \times m$ rectangle. By Theorem 1 and (3), we obtain the result. □

4. Discussions

Our theoretical finding is useful in predicting the degree of coverage a sensor network may provide. For example, if 25 sensor nodes with sensory range 100 are uniformly distributed in 1000×1000 rectangle, 51.8% (55.0% by the rough estimation) of the deployment region is expected to be 1-covered. If we double the number of sensors, the result is increased to 76.8% (79.7% by the rough estimation).

The result can also be used to determine related parameters for a desired network coverage. Define expected network coverage ratio (ENCR) to be $E[C_n^1]/A$. Assuming a fixed sensory range, the following result can be used to determine the minimal number of sensor nodes required for a desired ENCR.

Lemma 3. *Consider a deployment region of size A. Given a fixed sensory range such that the expected node coverage is $E[N]$, the number of sensor nodes needed for* ENCR $\geqslant 1 - \epsilon$, *where* $0 < \epsilon < 1$, *is at least*

$$\frac{\ln \epsilon}{\ln\left(1 - \frac{E[N]}{A}\right)}.$$

Proof. We are given the condition

$$1 - \epsilon \leqslant \left[1 - \left(1 - \frac{E[N]}{A}\right)^n\right] < 1.$$

So we have

$$0 < \left(1 - \frac{E[N]}{A}\right)^n \leqslant \epsilon < 1,$$

which implies

$$n \ln\left(1 - \frac{E[N]}{A}\right) \leqslant \ln \epsilon < 0.$$

Since $\ln(1 - E[N]/A) < 0$, we then have

$$n\left[-\ln\left(1 - \frac{E[N]}{A}\right)\right] \geqslant -\ln \epsilon.$$

It turns out that

$$n \geqslant \frac{-\ln \epsilon}{-\ln\left(1 - \frac{E[N]}{A}\right)} = \frac{\ln \epsilon}{\ln\left(1 - \frac{E[N]}{A}\right)}.$$ □

By Lemma 3, for more than 99% of the deployment region being 1-covered in the previous example, the number of sensors should be increased to 158 or more.

In case when sensory range r is also tunable, we may adjust both n and r to obtain a desired ENCR. The interesting thing is, whatever n and r are set for a particular ENCR, the expected number of communication links per node (i.e., expected link degree) is bounded.

Theorem 4. *If the radio communication range of every node is the same as the sensory range, the expected link degree is upper-bounded by $-\ln \epsilon$ for* ENCR = $1 - \epsilon$, *where* $0 < \epsilon < 1$.

Proof. Yen and Yu [24] have shown that the expected link degree in a n-node network is $f(n) = (n - 1)p$, where p is the probability of link occurrence. Recall that ENCR can be expressed

in terms of p as $1-(1-p)^n$. Letting it be $1-\epsilon$, where $0<\epsilon<1$, we have $p=1-\epsilon^{\frac{1}{n}}$ and the expected link degree is $f(n)=(n-1)(1-\epsilon^{\frac{1}{n}})$. Since $f'(n)=(1-\epsilon^{\frac{1}{n}})+(n-1)(n^{-2}\epsilon^{\frac{1}{n}}\ln\epsilon)>0$ for all $n>1$, $f(n)$ is monotonically increasing when $n>1$. To derive the limit of $f(n)$ when n approaches infinity, let $t=1/n$ and we have

$$\lim_{n\to\infty}(n-1)(1-\epsilon^{\frac{1}{n}})=\lim_{t\to 0}\frac{(1-t)(1-\epsilon^t)}{t}.$$

By L'Hôpital's rule,

$$\lim_{t\to 0}\frac{(1-t)(1-\epsilon^t)}{t}=\lim_{t\to 0}\frac{-(1-\epsilon^t)+(1-t)(-\epsilon^t\ln\epsilon)}{1}=-\ln\epsilon.$$

Therefore, the expected link degree is upper-bounded by $-\ln\epsilon$. □

Higher link degree usually indicates higher degree of channel contentions and thus poor link performance in case of contention-based medium access control (MAC) protocol. Theorem 4 therefore implies that if contention-based MAC protocol (such as CSMA/CA) is used in sensor networks, the degree of channel contentions can be bounded yet a particular ENCR can be ensured.

The result also has theoretical relevance to other fundamental properties such as network connectivity. Let r_t denote the radio communication range of every sensor. It has been pointed out [15] that, given $r_t=2r$, a set of communication units are in the same connected component (connected) if the area jointly 1-covered by these units (with sensory range r) is not partitioned. Intuitively, one would not expect separately covered area with a sufficiently high coverage ratio. In fact, it has been proven recently [20,4] that $r_t=2r$ suffices to ensure network connectedness on the premise of 100% coverage ratio.

The probability of link occurrence becomes $4E[N]/A$ if $r_t=2r$. Accordingly, the expected link degree is upper-bounded by $-4\ln\epsilon$ for ENCR $=1-\epsilon$.

We now demonstrate the utility of our result by presenting a uncoordinated node scheduling scheme. It works as follows:

- Each node independently alternates between active and sleep modes. The decision of switching from active to sleep modes or vise versa is purely stochastic. The time periods of active and sleep modes are exponentially distributed random variables with means λ_a and λ_s, respectively.
- The probability of any node being in active mode initially is $p_a=\lambda_a/(\lambda_a+\lambda_s)$.

Suppose that a node has entered active and sleep modes for m times. The total time that the node stays in active and sleep modes are k-Erlang distributions with means $m\lambda_a$ and $m\lambda_s$, respectively. Therefore, the probability that a node is in active mode at any given time is $m\lambda_a/(m\lambda_a+m\lambda_s)=p_a$. Since the states of nodes are not correlated, the number of active nodes at any given time forms a binomial distribution with mean np_a. Therefore, np_a nodes are expected to be active at any time and the expected network coverage can be estimated by substituting np_a for n in Theorem 2. A merit of this approach is that, though the method is stochastic in nature, it is deterministic to set the values of parameters λ_a and λ_s for a desired network coverage. This is not possible without the help of our theoretical finding.

The above node scheduling scheme is similar to that proposed in [19], where all nodes randomly and independently switch operating modes on a time-slot basis. The assumption of time slots implies that all sensors are clock-synchronized, which incurs additional communications overhead. The authors have analyzed the probability of a point being uncovered under the assumption of Poisson point process. Given that a sensor is in active mode with probability p_a (calculated as a long-term average), the probability that a given point is uncovered in a given time slot has been shown to be $\exp(-p_a\lambda\pi r^2)$. This is consistent with Hall's result on the ratio of uncovered area, as the node scheduling effectively drops node density from λ to $p_a\lambda$.

5. Simulation results

We conducted additional experiments to demonstrate the accuracy of our theoretical findings.

In all experiments, sensor nodes are randomly uniformly distributed over a 1000×1000 rectangle. A Monte Carlo algorithm [27] is used to calculate the size of k-covered region given a particular sensor deployment. It works as follows. We conducted 10,000 random tests for a given deployment. A point in the target area is randomly chosen in each test and the test successes if this point is covered by at least k sensors. Let p be the total number of tests that success. The k-covered area is $1000^2 \times p/10{,}000$.

The simulation design for 1-coverage is as follows. The number of sensors n is varied 1–99 in increments of 2 and sensory range r is varied 1–491 in increments of 10. For each combination of n and r, we repeated 100 experiments and took an average on coverage area.

We measured coverage ratio, the ratio of 1-coverage to the whole system area. Fig. 4(a)–(c) show results estimated by Theorem 2, Eq. (6), and Hall, respectively. Fig. 4(d) shows the results obtained from the experiments. The differences between theoretical estimations and the experimental results are shown in Figs. 5–7, where the difference is defined as value obtained by theoretical estimate minus that of experimental result. Table 1 lists means, standard deviations, maximum values, and minimum values of the differences.

We found that all theoretical predictions overestimate the coverage ratio at most cases. Furthermore, the degree of overestimate is high when the network is not fully covered and approaches zero when 100% coverage ratio is almost ensured. This can be explained as all estimates converge to 100% coverage ratio when the number of nodes or the sensory range goes beyond some value. When numerous sensors are deployed but the sensory range is small enough so that the deployment region is not yet fully covered, the results are similar (Fig. 8). Based on the experimental results, we conclude that Theorem 2 is more accurate and has smaller variance than either Eq. (6) or Hall's estimate, particularly when the network is not completely covered.

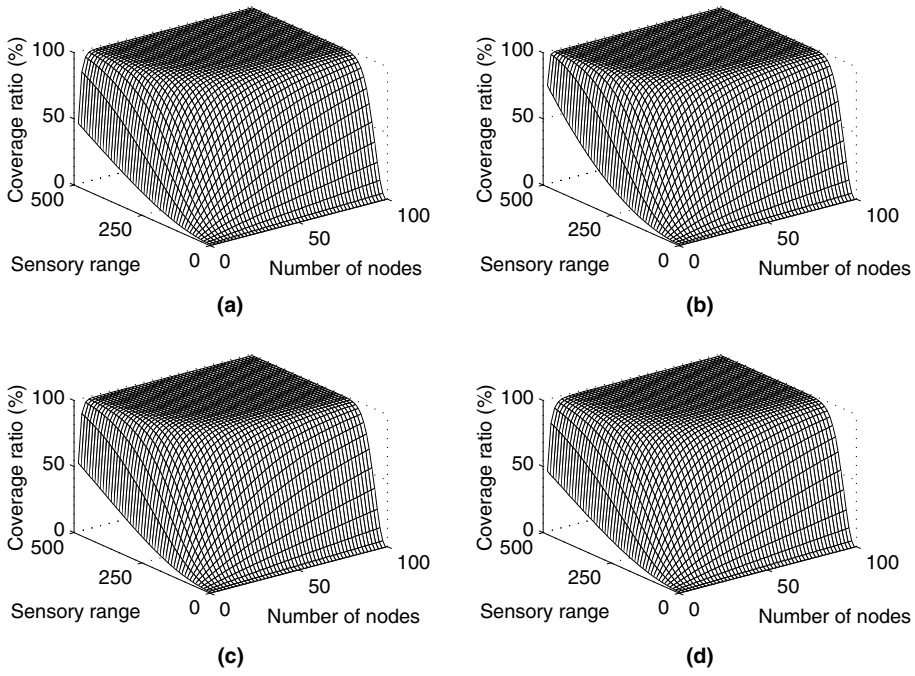

Fig. 4. Network coverage ratios in 1000×1000 rectangle, with n ranging from 1 to 99 and r ranging from 1 to 491. (a) Results estimated by Theorem 2. (b) Results estimated by Eq. (6). (c) Results estimated by Hall [10]. (d) Results obtained from simulations (averaged over 10,000 experiments).

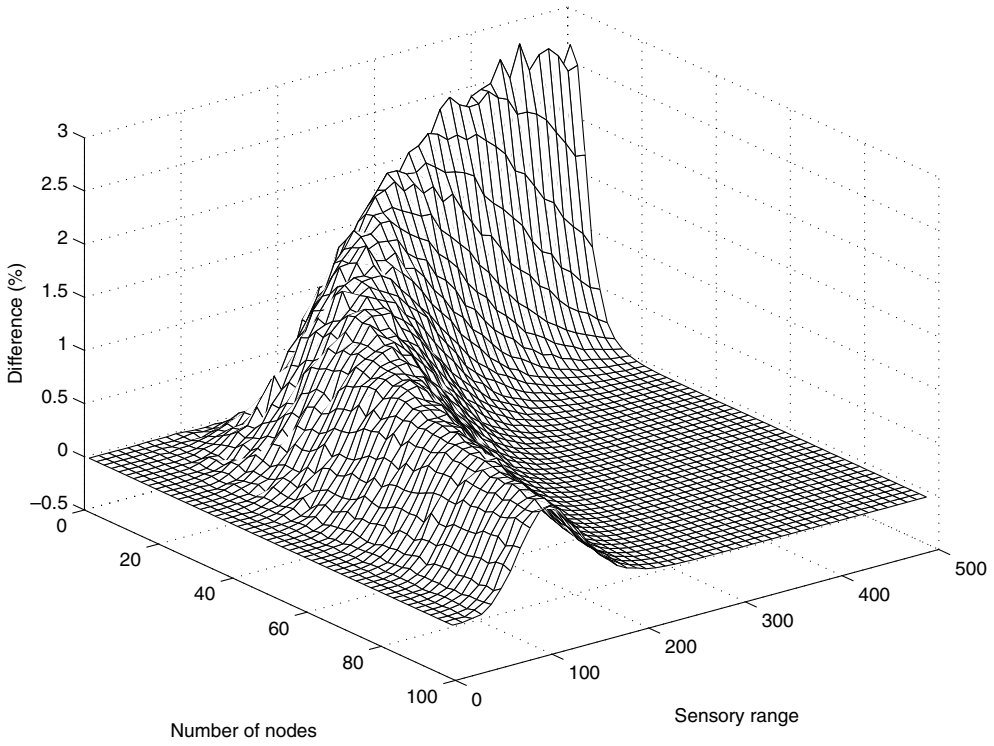

Fig. 5. Differences between Theorem 2's prediction and the experimental results.

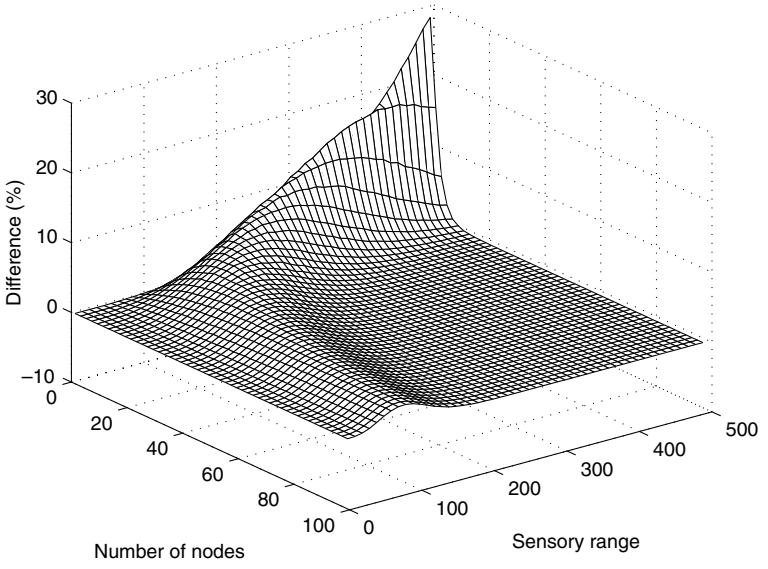

Fig. 6. Differences between Eq. (6)'s prediction and the experimental results.

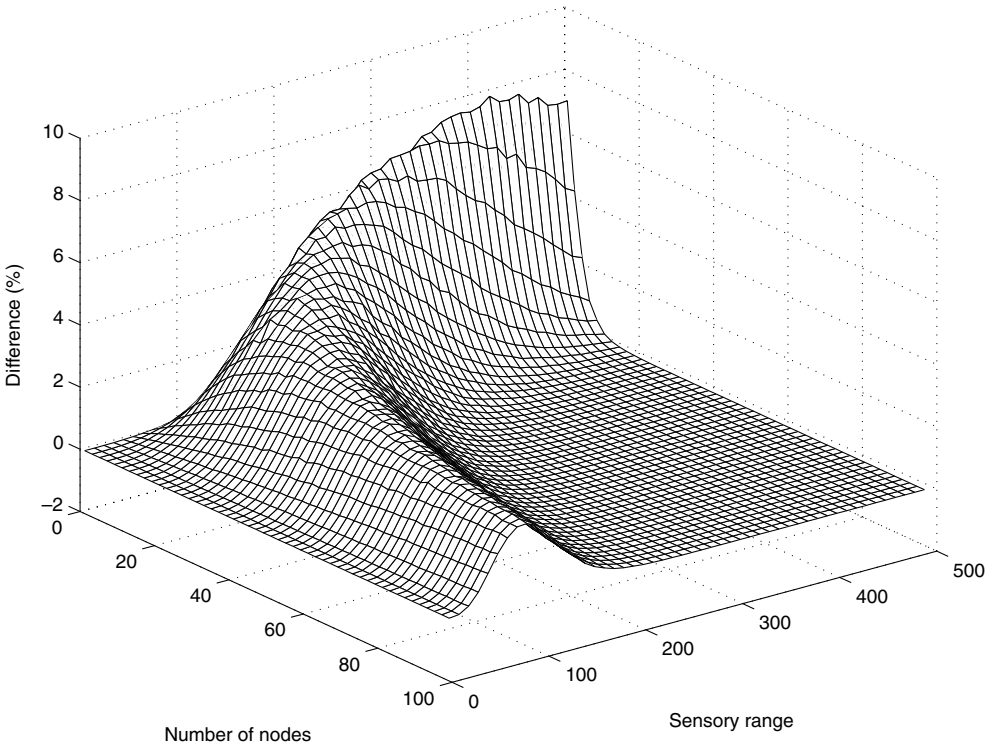

Fig. 7. Differences between Hall's prediction [10] and the experimental results.

Table 1
Differences of various estimations

Estimation	Mean (%)	Standard deviation (%)	Max (%)	Min (%)
Theorem 2	0.3912	0.5747	2.9037	−0.1398
Eq. (6)	1.6590	2.9599	28.6529	−0.0002
Hall's	1.1947	1.6888	8.0457	−0.0002

In k-coverage experiments, we changed the number of sensors n (ranged from 1 to 199) and measured different k's (from 1 to 10). The sensory range r is fixed to 100 and the deployment region is assumed 1000×1000. For each combination of n and k, we repeated 100 experiments and took an average on the ratio of k-coverage to the whole system area.

Fig. 9 shows our estimates, while Fig. 10 shows the results obtained from the experiments. The differences between theoretical estimations and the experimental results are shown in Fig. 11. The

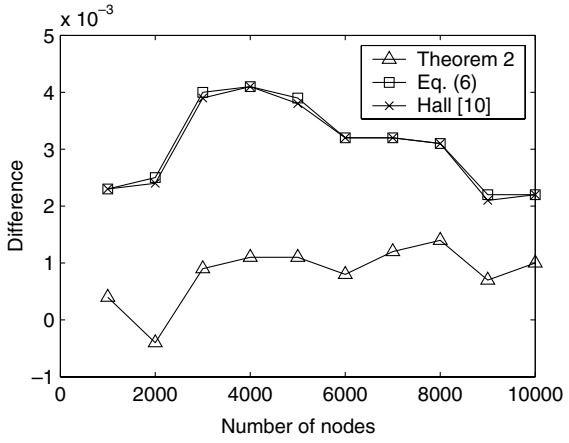

Fig. 8. Differences of all estimates when numerous sensors are deployed. The deployment region is 1000×1000 and the sensory range is 10.

mean, standard deviation, maximum value, and minimum value of the differences are 2.18×10^{-4},

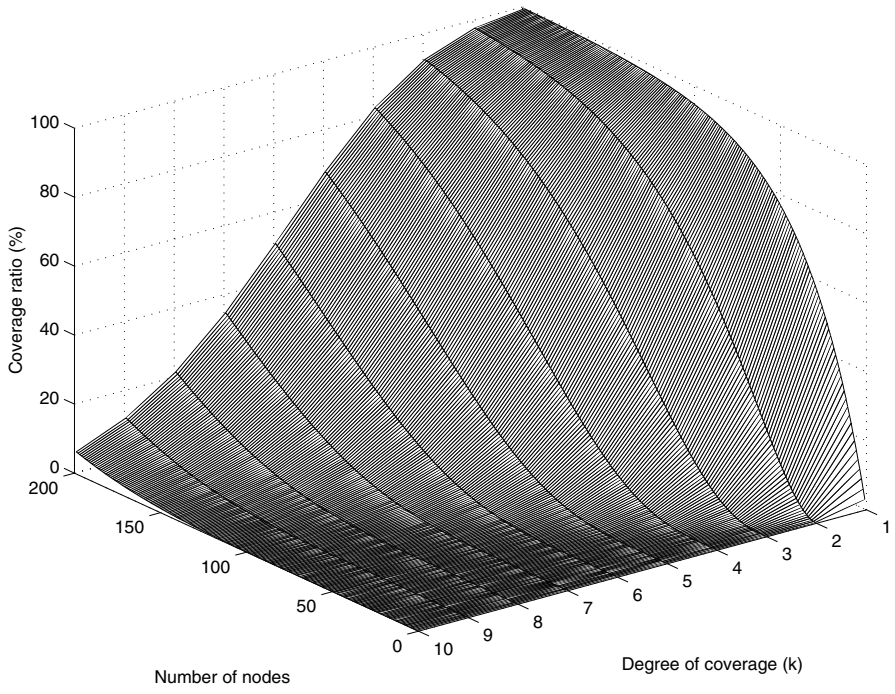

Fig. 9. Estimated k-coverage ratios in 1000×1000 rectangle, with n ranging from 1 to 199 and k ranging from 1 to 10.

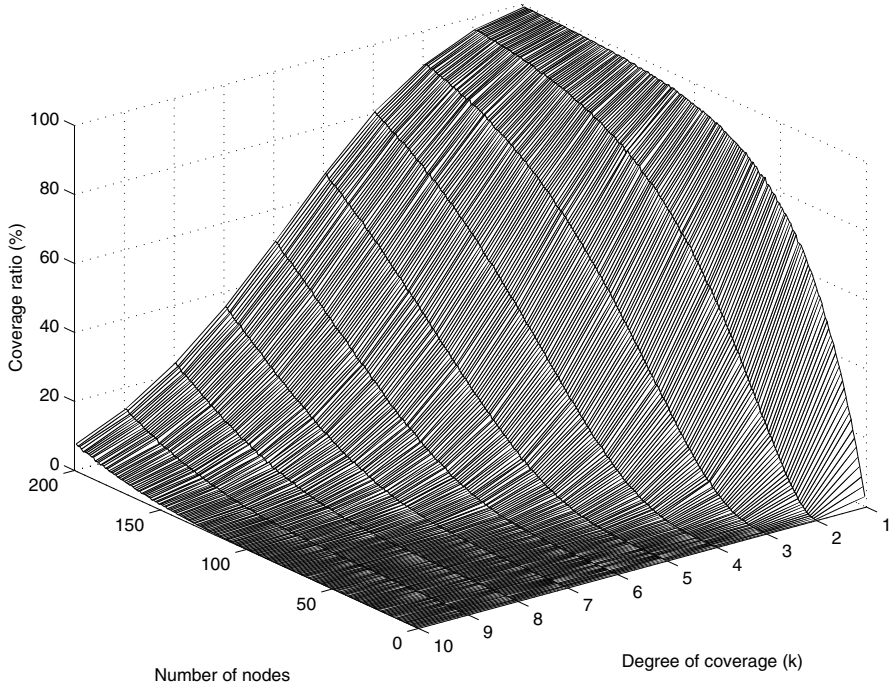

Fig. 10. Measured k-coverage ratios in 1000×1000 rectangle, with n ranging from 1 to 199 and k ranging from 1 to 10.

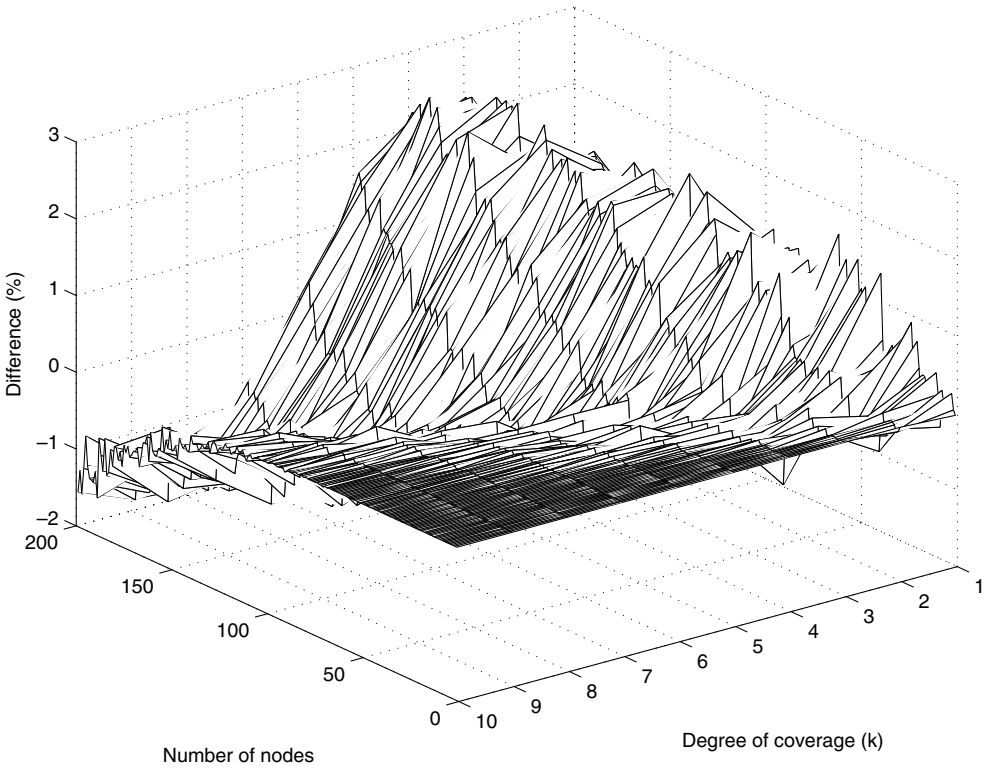

Fig. 11. Differences between theoretical estimations and the measured results.

0.82×10^{-2}, 0.0253, and −0.0190, respectively. The results confirm that our estimate is accurate in general.

6. Conclusions

We have analyzed the expected k-coverage offered by a number of randomly placed sensors with the consideration of border effects. We found that, although many combinations of n (the number of sensors) and r (sensory range) can be set for a particular expected 1-coverage ratio, the expected number of communication links per node has a upper bound that depends only on the desired expected 1-coverage ratio, not on any specific values of n and r. Our results have been exploited to design a stochastic node scheduling algorithm that conserves energy yet preserves network coverage. Additionally, simulation results have demonstrated the accuracy of our theoretical findings. We hope that our finding can be a step stone to the ultimate goal of characterizing other related network properties.

Acknowledgements

This work has been jointly supported by the National Science Council, Taiwan, under contract NSC-93-2213-E-216-024 and by Chung Hua University under grant CHU-93-TR-004.

References

[1] I.F. Akyìldìz, W. Su, Y. Sankarasubramaniam, E. Cayirci, A survey on sensor networks, IEEE Commun. Mag. 40 (8) (2002) 102–114.

[2] N. Bulusu, D. Estrin, L. Girod, J. Heidemann, Scalable coordination for wireless sensor networks: self-configuring

localization systems, in: Proceedings of the 6th IEEE International Symposium on Communication Theory and Application, Ambleside, UK, 2001.
[3] C.-F. Huang, Y.-C. Tseng, The coverage problem in a wireless sensor network, in: ACM International Workshop on Wireless Sensor Networks and Applications, 2003, pp. 115–121.
[4] G. Xing, X. Wang, Y. Zhang, C. Lu, R. Pless, C. Gill, Integrated coverage and connectivity configuration for energy conservation in sensor networks, ACM Trans. Sensor Networks, in press.
[5] J. O'Rourke, Art Gallery Theorems and Algorithms, Oxford University Press, New York, NY, 1987.
[6] S. Shakkottai, R. Srikant, N. Shroff, Unreliable sensor grids: coverage, connectivity and diameter, in: Proceedings of INFOCOM, 2003, pp. 1073–1083.
[7] S. Meguerdichian, F. Koushanfar, M. Potkonjak, M. Srivastava, Coverage problems in wireless ad-hoc sensor networks, in: Proceedings of INFOCOM, 2001, pp. 1380–1387.
[8] X.-Y. Li, P.-J. Wan, O. Frieder, Coverage in wireless ad hoc sensor networks, IEEE Trans. Comput. 52 (6) (2003) 1–11.
[9] M. Cardei, J. Wu, Coverage in wireless sensor networks, in: M. Ilyas, I. Magboub (Eds.), Handbook of Sensor Networks, CRC Press, 2004.
[10] P. Hall, Introduction to the Theory of Coverage Processes, John Wiley and Sons, 1988.
[11] T.K. Philips, S.S. Panwar, A.N. Tantawi, Connectivity properties of a packet radio network model, IEEE Trans. Inform. Theory 35 (5) (1989) 1044–1047.
[12] P. Piret, On the connectivity of radio networks, IEEE Trans. Inform. Theory 37 (5) (1991) 1490–1492.
[13] C. Bettstetter, On the minimum node degree and connectivity of a wireless multihop network, in: Proceedings of ACM Symposium on Mobile Ad Hoc Netw. and Comp., Lausanne, Switzerland, 2002, pp. 80–91.
[14] C. Bettstetter, J. Zangl, How to achieve a connected ad hoc network with homogeneous range assignment: an analytical study with consideration of border effects, in: Proceedings of the 4th IEEE International Workshop on Mobile and Wireless Communications Network, 2002, pp. 125–129.
[15] O. Dousse, P. Thiran, M. Hasler, Connectivity in ad-hoc and hybrid networks, in: Proceedings INFOCOM, New York, USA, 2002, pp. 1079–1088.
[16] P. Varshney, Distributed Detection and Data Fusion, Spinger-Verlag, New York, NY, 1996.
[17] D. Tian, N.D. Georganas, A coverage-preserving node scheduling scheme for large wireless sensor networks, in: First ACM International Workshop on Wireless Sensor Networks and Applications, 2002, pp. 32–41.
[18] J. Lu, T. Suda, Coverage-aware self-scheduling in sensor networks, in: Proceedings IEEE 18th Annual Workshop on Computer Communications, 2003, pp. 117–123.
[19] C.-F. Hsin, M. Liu, Network coverage using low duty-cycled sensors: Random & coordinated sleep algorithms, in: International Symposium on Information Processing in Sensor Networks, 2004, pp. 433–442.
[20] H. Zhang, J.C. Hou, Maintaining sensing coverage and connectivity in large sensor networks, in: International Workshop on Theoretical and Algorithm Aspects of Sensor, Ad Hoc Wireless and Peer-to-Peer Networks, 2004.
[21] B. Cărbunar, A. Grama, J. Vitek, O. Cărbunar, Coverage preserving redundancy elimination in sensor networks, in: 1st IEEE International Conference on Sensor and Ad Hoc Communications and Networks, 2004, pp. 377–386.
[22] F. Ye, G. Zhong, J. Cheng, S. Lu, L. Zhang, PEAS: a robust energy conserving protocol for long-lived sensor networks, in: Proceedings 23rd International Conference on Distributed Computing Systems, 2003, pp. 28–37.
[23] E.R. Dougherty, Probability and Statistics for the Engineering, Computing, and Physical Sciences, Prentice-Hall, Inc., 1990, p. 238.
[24] L.-H. Yen, C.W. Yu, Link probability, network coverage, and related properties of wireless ad hoc networks, in: Proceedings 1st IEEE International Conference on Mobile Ad-hoc and Sensor Systems, 2004, pp. 525–527.
[25] T.H. Cormen, C.E. Leiserson, R.L. Rivest, Introduction to Algorithms, MIT Press, 1990.
[26] C.W. Yu, L.-H. Yen, Estimating the number of links in ad hoc mobile networks with applications, Tech. Rep. CHU-CSIE-TR-2003-002, Dept. CSIE, Chung Hua Univ., Taiwan. Available from: <http://www.csie.chu.edu.tw/tech/tech_file/tech143630.pdf>, July 2003.
[27] E. Horowitz, S. Sahni, S. Rajasekaran, Computer Algorithms/C++, Computer Science Press, 1996.

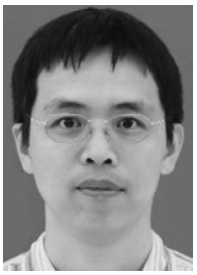

Li-Hsing Yen was born in Taiwan, ROC, in 1967. He received his B.S. (1989), M.S. (1991), and Ph.D. (1997) degrees in computer science, all from National Chiao Tung University, Taiwan. From 1997 to 1998, he worked for the Communications Research Laboratories (CCL), Industrial Technology Research Institute (ITRI), Taiwan, as an engineer. He was an Assistant Professor (1998–2003) and has been an Associate Processor since 2003 at the Department of Computer Science and Information Engineering, Chung Hua University, Taiwan. His current research interests include mobile computing, wireless networking, and distributed algorithms.

Chang Wu Yu was born in Taoyuan, Taiwan, ROC in 1964. He received the B.S. degree from Soochow University in 1985, M.S. degree from National Tsing Hua University in 1989, and Ph.D. degree from National Taiwan University in 1993, all in computer science. From 1995 to 1998, he was an Associate Professor at the Department of Information Management, Ming Hsin Institute of Technology. In 1999, he joined the Department of Computer Science & Information Engineering, Chung Hua University. His current research interests include algorithm design, distributed computing, and wireless networks.

Yang-Min Cheng received his B.S. and M.S. degrees in computer science from Chung Hua University, Hsinchu, Taiwan, ROC, in 2003 and 2005, respectively. His research interests include wireless communications and mobile computing.

Computing Subgraph Probability of Random Geometric Graphs: Quantitative Analyses of Wireless Ad Hoc Networks

Chang Wu Yu and Li-Hsing Yen

Department of Computer Science and Information Engineering,
Chung Hua University, Taiwan, R. O. C
{cwyu, lhyen}@chu.edu.tw

Abstract. This paper undergoes quantitative analyses on fundamental properties of ad hoc networks including estimating the number of hidden-terminal pairs and the number of exposed-terminal sets. To obtain these results, we propose a paradigm to systematically derive exact formulas for a great deal of subgraph probabilities of random geometric graphs. In contrast to previous work, which established asymptotic bounds or approximation, we obtain closed-form formulas that are fairly accurate and of practical value.

Keywords: Ad hoc networks, sensor networks, analytical method, random geometric graphs, performance evaluation, hidden terminal, exposed terminal, quantitative analysis.

1 Introduction

Ad hoc networks (MANETs), which are wireless networks with no fixed infrastructure, have received extensive attentions [1, 5, 8, 12, 38-41, 46, 49-52]. Each mobile node in the network functions as a router that discovers and maintains routes for other nodes. These nodes may move arbitrarily, and therefore network topology changes frequently and unpredictably. Other limitations of ad hoc networks include high power consumption, scare bandwidth, and high error rates. Applications of ad hoc networks are emergency search-and-rescue operations, meetings or conventions in which persons wish to quickly share information, data acquisition operations in inhospitable terrain, and automated battlefield [38]. Bluetooth networks [53] and sensor networks [35, 42] are commercial products of ad hoc networks.

A *geometric graph* $G=(V, r)$ consists of nodes placed in 2-dimension space R^2 and edge set $E=\{(i,j) \mid d(i,j)\le r$, where $i,j\in V$ and $d(i,j)$ denotes the Euclidian distance between node i and node $j\}$. Let $X_n=\{x_1, x_2, \ldots, x_n\}$ be a set of independently and uniformly distributed random points. We use $\Psi(X_n, r, A)$ to denote the *random geometric graph* (RGG) [29] of n nodes on X_n with radius r and placed in an area A. RGGs consider geometric graphs on random point configurations. Applications of RGGs include communications networks, classification, spatial statistics, epidemiology, astrophysics, and neural networks [29].

A RGG $\Psi(X_n, r, A)$ is suitable to model an ad hoc network $N=(n, r, A)$ consisting of n mobile devices with transmission radius r unit length that are independently and uniformly

F. Wang (Ed.): FORTE 2005, LNCS 3731, pp. 458 – 472, 2005.

distributed at random in an area A. When each vertex in $\Psi(X_n, r, A)$ represents a mobile device, each edge connecting two vertices represents a possible communication link as they are within the transmission range of each other. A random geometric graph and its representing network are shown in Figure 1. In the example, area A is a rectangle that is used to model the deployed area such as a meeting room. Area A, however, can be a circle, or any other shape, and even infinite space.

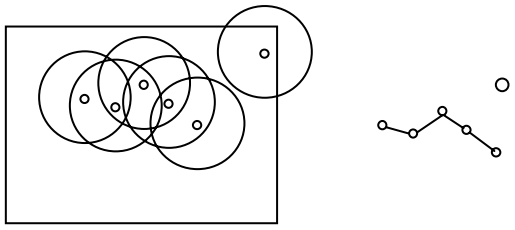

(a) (b)

Fig. 1. (a) An ad hoc network $N=(6, r, A)$, where A is a rectangle. (b) Its associated random geometric graph $\Psi(X_6, r, A)$.

RGGs are different from well-known *random graphs* [3, 13, 28]. One kind of random graph can be characterized by two parameters n and p, where n represents the number of nodes and p represents the probability of the existence of each possible edge. Edge occurrences in the random graph are independent to each other, which is not the case in MANETs. Therefore the fruitful results of random graphs cannot be directly applied to MANETs. Other graph models proposed for MANETs are interval graphs [16], unit disk graph [7, 17], proximity graphs [29], and indifference graphs [37].

Many fundamental properties of ad hoc networks are related to subgraphs in RGGs. For example, the IEEE 802.11 CSMA/CA protocol suffers from the hidden and the exposed terminal problem [41, 45]. The hidden terminal problem is caused by concurrent transmissions of two nodes that cannot sense each other but transmit to the same destination. We call such two terminals a *hidden-terminal pair*. The existence of hidden-terminal pairs in an environment seriously results in garbled messages and increases communication delay, thus degrading system performance [24, 25, 45].

A hidden-terminal pair can be represented by a pair of edges (x, y) and (x, z) of $G=(V, E)$ such that $(x, y)\in E$ and $(x, z)\in E$, but $(y, z)\notin E$. In graph terms, such a pair of edges is an induced subgraph p_2 that is a path of length two (See Figure 2). Counting the occurrences of p_2 in a given RGG helps counting the number of hidden-terminal pairs in the network.

The exposed terminal problem is due to prohibiting concurrent transmissions of two nodes that sense each other but can transmit to different receivers without conflicts [41]. The problem results in unnecessary reduction in channel utilization and throughput. We name these nodes an *exposed-terminal set*. Similarly, the problem can be modeled as a subgraph H of $G=(V, E)$ with four vertices $\{x, y, z, w\}\subseteq V$ such that $\{(x, y), (y, z), (z, w)\}\subseteq E$, but $(x, z)\notin E$ and $(y, w)\notin E$ (See Figure 2).

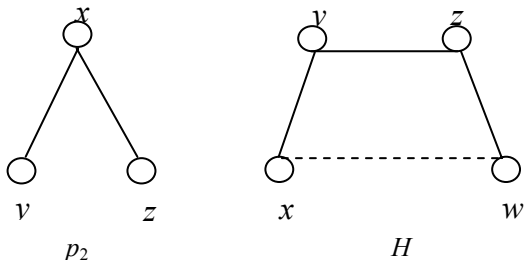

Fig. 2. The subgraphs of hidden-terminal pair p_2 and exposed-terminal set H

Quantitative analyses on specific subgraphs of a given RGG are of importance for understanding and evaluating the fundamental properties of MANETs. There is extensive literature on the subgraph probability of RGGs [29]. Penrose had shown that, for arbitrary feasible connected subgraph Γ with k vertices, the number of induced subgraphs isomorphic to Γ satisfies a Poisson limit theorem and a normal limit theorem [29]. To the best of our knowledge, previous related results are all asymptotic or approximate.

In the paper, we make the first attempt to propose a paradigm to systematically derive the exact formulas for a great deal of subgraph probabilities in RGGs. In contrast to previous asymptotic bounds or approximation, the closed-form formulas we derived are fairly accurate and of practical value. With the paradigm, we undergoes quantitative analyses on fundamental properties of ad hoc networks including the number of hidden-terminal pairs and the number of exposed-terminal sets.

Computing the probability of occurrence of RGG subgraphs is complicated by the assumption of finite plane. For example, one device in Figure 1 is deployed nearby the boundary of rectangle A so its radio coverage region (often modeled by a circle) is not properly contained in A. This is due to *border effects*, which complicate the derivation of closed formulas. Previous discussions usually circumvent the border effects by using *torus convection* [1, 20]. Torus convention models the network topology in a way that nodes nearby the border are considered as being close to nodes at the opposite border and they are allowed to establish links. Most of the time, we adopt *torus convention* to deal with border effects in the paper. However, we also obtain an exact formula for the single edge probability of RGGs when confronting the border effects.

Our definition of random geometric graphs $\Psi(X_n, r, A)$ is different from those of Poisson point process [1, 12], which assume that the distribution of n points (vertices) on a possibly infinite plane follows a Poisson distribution with parameter λ (the given density). In Poisson point process, the number of vertices can only be a random number rather than a tunable parameter. In practice, however, some MANET modeling requires a fixed input n or a finite deployed area.

The rest of the paper is organized as follows. In Section 2, some definitions and notations are introduced. In Section 3, we briefly survey related results on RGGs. A paradigm for computing the subgraph probability of RGGs with torus convention is presented in Section 4. Section 5 presents those derivations when confronting border effects. In Section 6, quantitative analyses on ad hoc networks are discussed. Finally, Section 7 concludes the paper.

2 Definitions and Notations

A *graph* $G=(V, E)$ consists of a finite nonempty vertex set V and edge set E of unordered pairs of distinct vertices of V. A graph $G=(V, E)$ is labeled when the $|V|$ vertices are distinguished from one another by names such as $v_1, v_2, \ldots, v_{|V|}$. Two labeled graphs $G=(V_G, E_G)$ and $H=(V_H, E_H)$ are identical, denoted by $G=H$ if $V_G= V_H$ and $E_G=E_H$. A graph $H=(V_H, E_H)$ is a *subgraph* of $G=(V_G, E_G)$ if $V_H \subseteq V_G$ and $E_H \subseteq E_G$. Suppose that V' is a nonempty subset of V. The subgraph of $G=(V, E)$ whose vertex set is V' and whose edge set is the set of those edges of G that have both ends in V' is called the subgraph of G *induced* by V', denoted by $G_{V'}$. The *size* of any set S is denoted by $|S|$. The *degree* of a vertex v in graph G is the number of edge incident with v. The notation $\binom{n}{m}$ denotes the number of ways to select m from n distinct objects.

The *subgraph probability* of RGGs is defined as follows. Let $\Omega=\{G_1, G_2, \ldots, G_k\}$ represent every possible labeled graphs of $\Psi(X_n, r, A)$, where $k=2^{\binom{n}{2}}$. When G_x is a labeled subgraph in Ω, we use $\Pr(G_x)$ to denote the probability of the occurrence of G_x. Suppose $S \subseteq V$ and $T \subseteq V$, we define $\Pr(G_s)= \sum_{\forall G_w \in \Omega \text{ and } G_s \subseteq G_w} \Pr(G_w)$, when $1 \le w \le k$.

A *walk* in $G=(V, E)$ is a finite non-null sequence $W=v_0e_1v_1e_2\ldots e_kv_k$, where $v_i \in V$ and $e_j \in E$ for $0 \le i \le k$ and $1 \le j \le k$. The integer k is the *length* of the walk. When $v_o, v_1, \ldots, v_k$ are distinct, W is called a *path*. A path is *a cycle* if its origin and terminus are the same. An induced subgraph that is a path of length i is denoted by p_i. Similarly, an induced subgraph that is a cycle of length i is denoted by c_i; c_3 is often called a *triangle*. A set of vertices is *independent* if no two of them are adjacent. An induced subgraph which is an independent set of size i is denoted by I_i. The notational conventions used in the paper can be found in [4].

3 Related Work in RGG

A book written by Penrose [29] provides and explains the theory of random geometric graphs. Graph problems considered in the book include subgraph and component counts, vertex degrees, cliques and colorings, minimum degree, the largest component, partitioning problems, and connectivity and the number of components.

For n points uniformly randomly distributed on a unit cube in $d \ge 2$ dimensions, Penrose [32] showed that the resulting geometric random graph G is k-connected and G has minimum degree k at the same time when $n \to \infty$. In [9, 10], Díaz *et al.* discussed many layout problems including minimum linear arrangement, cutwidth, sum cut, vertex separation, edge bisection, and vertex bisection in random geometric graphs. In [11], Díaz *et al.* considered the clique or chromatic number of random geometric graphs and their connectivity.

Some results of RGGs can be applied to the connectivity problem of ad hoc networks. In [39], Santi and Blough discussed the connectivity problem of random geometric graphs $\Psi(X_n, r, A)$, where A is a d-dimensional region with the same length size. In [1], Bettstetter investigated two fundamental characteristics of wireless networks: its minimum node degree

and its k-connectivity. In [12], Dousse *et al.* obtained analytical expressions of the probability of connectivity in the one dimension case. In [18], Gupta and Kumar have shown that if $r=\sqrt{\frac{\log n + c(n)}{\pi n}}$, then the resulting network is connected with high probability if and only if $c(n)\to\infty$. In [47], Xue and Kumar have shown that each node should be connected to $\Theta(\log n)$ nearest neighbors in order that the overall network is connected.

Recently, Yen and Yu have analyzed link probability, expected node degree, and expected coverage of MANETs [49]. In [48], Yang has obtained the limits of the number of subgraphs of a specified type which appear in a random graph.

4 A Paradigm for Computing Subgraph Probability

In the section, we develop a paradigm for computing subgraph probability of RGGS. First of all, we are to prove that the occurrences of arbitrary two distinct edges in RGGs are independent in the next subsection. The property of edge independence greatly simplifies our further calculations. For simplicity, we always assume that A is sufficiently large to properly contain a circle with radius r in a $\Psi(X_n, r, A)$ throughout the paper; that implies $\pi r^2 \le |A|$. In the paper, notation E_i (E_i') denotes the event of the occurrence (absence) of edge e_i.

Since we adopt torus convention to avoid border effects in the section, single-edge probability in RGG is obtained trivially and listed below.

Theorem 1: We have $\Pr(E_j)=\pi r^2/|A|$, for an arbitrary edge $e_j=(u, v)$ and $u\neq v$, in a $\Psi(X_n, r, A)$.

4.1 Edge Independence in RGGs

The next theorem will indicate that the occurrences of arbitrary two distinct edges in RGGs are independent. The result is somewhat difficult to be accepted as facts at first glance for some scholars. The following theorem shows that the occurrences of arbitrary two distinct edges in RGGs are independent even if they share one end vertex.

Theorem 2 [49]: For arbitrary two distinct edges $e_i=(u, v)$ and $e_j=(w, x)$ in a $\Psi(X_n, r, A)$, we have $\Pr(E_iE_j)=\Pr(E_i)\Pr(E_j)$.

Note that Theorem 2 does not imply that the occurrences of more than two edges in RGGs are also independent. In fact, we will show their dependence later.

By Theorem 1 and 2, we obtain the probability of two-edge subgraphs immediately.

Corollary 3: For arbitrary two distinct edges $e_i=(u, v)$ and $e_j=(w, x)$ in a $\Psi(X_n, r, A)$, we have $\Pr(E_iE_j)=(\pi r^2/|A|)^2$.

4.2 Base Subgraphs

In this subsection, we consider eight labeled subgraphs with three vertices as *base subgraphs*, the probabilities of which will be used to compute the probability of larger subgraphs later. Based on the number of edges included, subgraphs of three vertices can be classified into four groups: a triangle (c_3), an induced path of length two (p_2), an edge with an isolated vertex (p_1+I_1), and three isolated vertices (I_3) (See Figure 3).

To compute the probability of c_3, we need the following lemma. Two equal-sized circles are *properly intersecting* if one circle contains the center of the other. Due to page limit, we omit the proofs of Lemma 4-5 and Theorem 6- 9 intentionally.

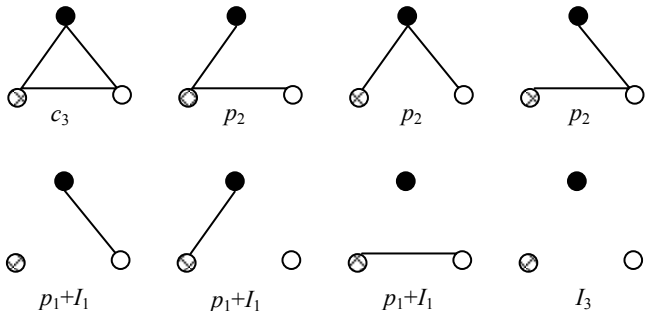

Fig. 3. Eight base subgraphs

Lemma 4: The expected overlapped area of two properly intersecting circles with the same radius r is $\left(\pi - \frac{3\sqrt{3}}{4}\right) r^2$ in a $\Psi(X_n, r, A)$.

The following conditional probability is a consequence of Lemma 4.

Lemma 5: For three distinct edges $e_i=(u, v)$, $e_j=(u, w)$, and $e_k=(v, w)$ in a $\Psi(X_n, r, A)$, we have $\Pr(E_iE_j \mid E_k)=\left(\pi - \frac{3\sqrt{3}}{4}\right) r^2/|A|$, where $u\neq v\neq w$.

The probability of the first base subgraph c_3 (triangle) can then be obtained.

Theorem 6: For three distinct edges $e_i=(u, v)$, $e_j=(u, w)$, and $e_k=(v, w)$ in a $\Psi(X_n, r, A)$, we have $\Pr(E_iE_jE_k)=\left(\pi - \frac{3\sqrt{3}}{4}\right) \pi r^4/|A|^2$, where $u\neq v\neq w$.

Next, we consider the subgraph of an edge with an isolated vertex (p_1+I_1).

Theorem 7: For three distinct edges $e_i=(u, v)$, $e_j=(u, w)$, and $e_k=(v, w)$ in a $\Psi(X_n, r, A)$, we have $P(E_iE_j'E_k')=\frac{\pi r^2}{|A|}\left(1-\frac{\pi r^2}{|A|}-\frac{3\sqrt{3}}{4|A|} r^2\right)$, where $u\neq v\neq w$.

We have shown that the occurrences of two distinct edges in a $\Psi(X_n, r, A)$ are independent (Theorem 2). The next theorem, however, shows that edge independence does not exist for subgraphs with three or more edges.

Theorem 8: The occurrences of arbitrary three distinct edges in a $\Psi(X_n, r, A)$ are dependent.

The next base subgraph we considered is an induced path p_2, which will be used to model a hidden-terminal pair.

Theorem 9: For arbitrary three distinct edges $e_i=(u, v)$, $e_j=(u, w)$, and $e_k=(v, w)$ in a $\Psi(X_n, r, A)$, we have $\Pr(E_iE_jE_k')=\left(\frac{3\sqrt{3}}{4}\right) \pi r^4/|A|^2$, where $u\neq v\neq w$.

The last base subgraph we considered is I_3.

Theorem 10: For arbitrary three distinct edges $e_i=(u, v)$, $e_j=(u, w)$, and $e_k=(v, w)$ in a $\Psi(X_n, r, A)$, we have $\Pr(E_i'E_j'E_k')=1-\frac{\pi r^4}{|A|}-\frac{\frac{3\sqrt{3}}{4}}{|A|^2}\pi r^4$, where $u\neq v\neq w$.

Proof: (Omitted.) ■

4.3 A Paradigm for Computing Subgraph Probability of RGGs

To simplify calculation, we adopt the following graph drawings. A solid line denotes an edge of G; a broken line denotes a possible edge between them; two vertices without a line denote a non-edge of G. Note that such graph drawing represent a class of graphs $G=(V, E_S, E_B)$, where $E_S(E_B)$ denotes solid-line edge (broken-line edge) set. For example, the following graph denotes eight base graphs depicted in Figure 3.

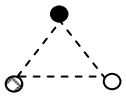

We list some subgraphs discussed in Section 4.1 or 4.2 with their notations, drawings, and probabilities in Table 1.

Table 1. Probabilities of subgraphs with three vertices or less in a RGG

Notation	p_1	E^2	c_3	p_2	E^1+I_1	I_3
G		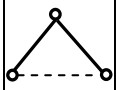	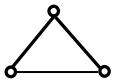	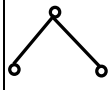	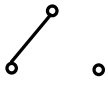	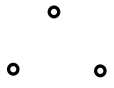
$\Pr(G)$	$\pi r^2/\lvert A\rvert$	$(\pi r^2/\lvert A\rvert)^2$	$\left(\pi-\frac{3\sqrt{3}}{4}\right)\pi^4/\lvert A\rvert^2$	$\left(\frac{3\sqrt{3}}{4}\right)\pi^4/\lvert A\rvert^2$	$\frac{\pi r^2}{\lvert A\rvert}\left(1-\frac{\pi r^2}{\lvert A\rvert}-\frac{\frac{3\sqrt{3}}{4}r^2}{\lvert A\rvert}\right)$	$1-\frac{\pi r^4}{\lvert A\rvert}-\frac{\frac{3\sqrt{3}}{4}}{\lvert A\rvert^2}\pi r^4.$

Note that we have $\Pr(E^2)=\Pr(c_3)+\Pr(p_2)$ in Table 1. This equation can be derived by the following two types of derivation rules.

Type I Type II

In fact, type I (type II) graph derivation rule can be applied on any broken-line edge (non-edge) of any graph. That is, for any $e\in E_B$, we have $G(V, E_S, E_B)=G_1(V, E_S\cup\{e\}, E_B-\{e\})+G_2(V, E_S, E_B-\{e\})$. Similarly, for any $e\notin E_S\cup E_B$, we have $G(V, E_S, E_B)=G_1(V, E_S, E_B\cup\{e\})-G_2(V, E_S\cup\{e\}, E_B)$ equivalently. We will show how these derivation rules can be used to systematically compute subgraph probability of RGGs.

Given a subgraph of a RGG, we try to obtain its probability by following three basic steps in the paradigm:

(1) Decompose the graph into a linear combination of base graphs by recursively applying the derivation rules.
(2) Compute the probabilities of base graphs.

(3) Compute the probability of the graph by manipulating the probabilities of base graphs.

We have established probability formulas for essential components (*i.e.* base graphs) in Section 4.2. The following example demonstrates the great convenience of this paradigm. A graph H (representing the exposed-terminal set) is decomposed into a set of subgraphs according to the derivation rules.

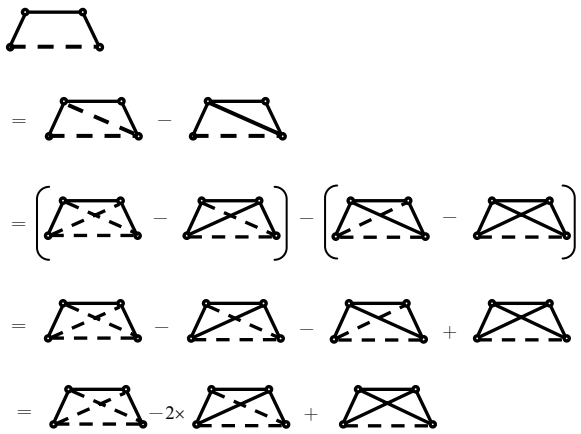

Graph H turns out to be a linear combination of three graphs. Although these subgraphs are not base graphs, we can obtain their probabilities with the help of base graphs. The first graph (denoted by E^3) consists of three solid edges (which form a path of length three) and three other broken edges; therefore we can obtain its probability by applying Theorem 1 three times; that is, we have $\Pr(E^3)=(\pi r^2/|A|)^3$. The second graph (denoted by E^1+c_3) consists of a triangle and a solid edge; then its probability can be obtained by applying Theorem 6 and Theorem 1 once; that is, we have $\Pr(E^1+c_3)=\left(\pi-\frac{3\sqrt{3}}{4}\right)\frac{\pi r^4}{|A|^2}\times\frac{\pi r^2}{|A|}$. The last graph (denoted by c_3^2) consists of two triangles with a common edge; we can also obtain its probability by applying Theorem 1 once and Lemma 5 twice; that is, we have $\Pr(c_3^2)=\left(\left(\pi-\frac{3\sqrt{3}}{4}\right)\frac{r^2}{|A|}\right)^2\times\frac{\pi r^2}{|A|}$. According to above discussion, we have

$$\Pr(H)=\Pr(E^3)-2\times\Pr(E^1+c_3)+\Pr(c_3^2)=(\pi r^2/A)^3-2\times\left(\pi-\frac{3\sqrt{3}}{4}\right)\frac{\pi^2 r^6}{|A|^3}+\left(\pi-\frac{3\sqrt{3}}{4}\right)^2\frac{\pi r^6}{|A|^3}=\frac{27}{16}\frac{\pi r^6}{|A|^3}.$$

In summary, we have the following theorem.

Theorem 11: For arbitrary four distinct nodes x, y, z, and w in a $\Psi(X_n, r, A)$, we have $\Pr(G_S=H)=\frac{27}{16}\frac{\pi r^6}{|A|^3}$, where $S=\{x, y, z, w\}$ and $H=(V_H, E_H)$ with $V_H=S$ and $\{(x, y), (y, z), (z, w)\}\subseteq E_H$, but $(x, z)\notin E_H$ and $(y, w)\notin E_H$.

Table 2 lists subgraphs and associated probabilities mentioned above.

Table 2. Probabilities of some subgraphs with four vertices in a RGG

Notation	E^3	E^1+c_3	c_3^2	H
G	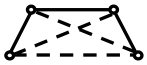	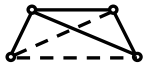		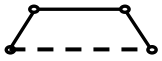
Pr(G)	$(\pi r^2/\lvert A\rvert)^3$	$\left(\pi-\frac{3\sqrt{3}}{4}\right)\frac{\pi^2 r^6}{\lvert A\rvert^3}$	$\left(\pi-\frac{3\sqrt{3}}{4}\right)^2\frac{\pi r^6}{\lvert A\rvert^3}$	$\frac{27}{16}\frac{\pi r^6}{\lvert A\rvert^3}$

Following our paradigm, the probability formulas of a great deal of subgraphs (in RGGs) can be obtained systematically. In Section 6, we will demonstrate that such specific subgraphs with their properties have considerable merit in quantitative analyses of wireless ad hoc networks.

5 Computing Subgraph Probability in the Face of Border Effects

In the section, we restrict the deployed area A to an $l\times m$ rectangle. We make an attempt to face border effects and obtain a closed-form formula of computing the single edge probability of RGGs. The results derived in the section can be used to measure the extent of coverage and connectivity of ad hoc networks [23].

Due to page limit, the main result and its corollaries are listed only.

Theorem 12 [49]: Given a $\Psi(X_n, r, A)$ and an $l\times m$ rectangle A, the single edge probability considering border effects is $\frac{\frac{1}{2}r^4-\frac{4}{3}lr^3-\frac{4}{3}mr^3+\pi r^2 ml}{m^2 l^2}$.

Corollary 13: The average (expected) degree of a vertex in a $\Psi(X_n, r, A)$ considering border effects is $(n\text{-}1)\times(\frac{\frac{1}{2}r^4-\frac{4}{3}lr^3-\frac{4}{3}mr^3+\pi r^2 ml}{m^2 l^2})$, where A is an $l\times m$ rectangle.

Corollary 14: The expected edge number of a $\Psi(X_n, r, A)$ considering border effects is $(\frac{n(n-1)}{2})\times(\frac{\frac{1}{2}r^4-\frac{4}{3}lr^3-\frac{4}{3}mr^3+\pi r^2 ml}{m^2 l^2})$, where A is an $l\times m$ rectangle.

To obtain these results, we first derive some necessary lemmas. Let $X_n=\{x_1, x_2, \ldots, x_n\}$ be a set of independently and uniformly distributed random points in a given $\Psi(X_n, r, A)$, where $x_i=(X_i, Y_i)$ and $0\le X_i\le l$ and $0\le Y_i\le m$, for $1\le i\le n$. Clearly, X_i's (and Y_i's) are independent, identically distributed random variables with probability density function (p.d.f.) $f(x)=1/l$ ($g(y)=1/m$) over the range $[0, l]$ ($[0, m]$).

Lemma 15 [49]: Given a $\Psi(X_n, r, A)$ and any two distinct nodes $x_i=(X_i, Y_i)$ and $x_j=(X_j, Y_j)$, we have $\Pr[|X_i\text{-}X_j|\le z]=\frac{-z^2+2lz}{l^2}$ and $\Pr[|Y_i\text{-}Y_j|\le w]=\frac{-w^2+2mw}{m^2}$ where $0\le z\le l$ and $0\le w\le m$.

Lemma 16 [49]: Given a $\Psi(X_n, r, A)$ and any two distinct nodes $x_i=(X_i, Y_i)$ and $x_j=(X_j, Y_j)$, we have that: (1) the p.d.f. of $(X_i-X_j)^2$ is $f(u)=\frac{lu^{-\frac{1}{2}}-1}{l^2}$ where $0\le u\le l^2$, and (2) the p.d.f. of $(Y_i-Y_j)^2$ is $g(v)=\frac{mv^{-\frac{1}{2}}-1}{m^2}$, where $0\le v\le m^2$.

Lemma 17 [43]: $\int u^{-\frac{1}{2}}\sqrt{a^2-u}du=u^{\frac{1}{2}}\sqrt{a^2-u}+a^2\sin^{-1}\frac{\sqrt{u}}{a}+c$, where c is a constant.

We conclude that border effect does affect the value of the single edge probability of $\Psi(X_n, r, A)$. If A is an $l\times m$ rectangle, the difference between the single edge probabilities with and without avoiding border effects (by adopting torus convention) is $\frac{\frac{4}{3}mr^3+\frac{4}{3}lr^3-\frac{1}{2}r^4}{m^2l^2}$.

6 Quantitative Analyses of Wireless ad Hoc Networks

In the section, we make use of the derived results to develop quantitative analyses of ad hoc (sensor) networks including the number of hidden-terminal pairs and the number of exposed-terminal sets.

6.1 The Number of Hidden-Terminal Pairs

First, we compute the expected number of hidden-terminal pairs in any RGG. The performance of media access control (MAC) scheme is in close relation to the number of hidden-terminal pair of a given wireless network [24, 25, 45]. In literature, a hidden-terminal pair can be modeled by Hearing graph [45]; RTS/CTS mechanism and other methods have been designed for alleviate the hidden terminal problems [2, 14].

Since each hidden-terminal pair consists of three distinct labeled vertices, we set S to be the selected three-vertex set. There are $\binom{n}{3}$ different combinations for selecting three from n vertices, and three different settings for labeling one from three as the center of the hidden-terminal pair (*i.e.* the internal node of the induced path with length 2). Therefore, we have the number of hidden-terminal pairs $\binom{n}{3}\times 3\times \Pr(G_S=p_2) = 3\binom{n}{3}\left(\frac{3\sqrt{3}}{4}\right)\pi r^4/|A|^2$ by Theorem 9.

Theorem 18: The expected number of hidden-terminal pairs in a $\Psi(X_n, r, A)$ is $3\binom{n}{3}\left(\frac{3\sqrt{3}}{4}\right)\pi r^4/|A|^2$.

Since $3\binom{n}{3}\left(\frac{3\sqrt{3}}{4}\right)\pi r^4/|A|^2=3\times\left(\frac{n\times(n-1)\times(n-2)}{1\times 2\times 3}\right)\times\left(\frac{3\sqrt{3}}{4}\right)\pi r^4/|A|^2$ $=(n^3-3n^2+2n)\left(\frac{3\sqrt{3}}{8}\right)\pi r^4/|A|^2$, we conclude that the hidden terminal pairs grow as like $O(n^3r^4)$, where n is the number of mobile nodes and r is the range of power.

In [24], Khurana *et al*. have shown that if the number of hidden terminal pairs is small and when collisions are unlikely, the RTS/CTS exchange is a waste of bandwidth. On the other hand, if the number of hidden terminal pairs is large, RTS/CTS mechanism helps avoid collision. Moreover, the optimal value for the RTS_Threshold in IEEE 802.11 [24] depends on the number of hidden terminals.

In [25], Khurana *et al.* have shown that hidden terminals can have a detrimental effect on the performance (including throughput, packet delay, and blocking probability) of the IEEE 802.11 MAC protocol. Specifically, they have showed that throughput is acceptable when the number of hidden-terminal pairs is less than 10%, beyond which throughput can fall sharply [25]. When determining a network-level simulation of a mobile ad hoc network or designing a wireless network, we can (with Theorem 18) precisely control the quantity of hidden terminal pairs by adjusting the number of mobile nodes or the power range.

6.2 The Number of Exposed Terminal Sets

To derive a tight bound of the number of exposed-terminal sets in a given RGG, we need to compute first the subgraph probability of c_4 (a cycle of length four). The paradigm proposed in Section 5 can be applied to tackle a great deal of subgraphs, but not some types of subgraphs such as cycles. We try to obtain tight bounds for $\Pr(c_4)$ in a different way.

Theorem 19: For arbitrary four distinct nodes u, v, w, and x in a $\Psi(X_n, r, A)$, we have $\Pr(G_S=c_4)\le\left(\frac{3\sqrt{3}}{4}\right)\frac{\pi r^6}{|A|^3}$, where $S=\{u, v, w, x\}$.

Proof: Consider the geometric graph c_4 and its circle model (See Figure 4(a) and Figure 4(b)). These four nodes need to be placed properly near to each other in order to form the cycle of length four. Since the longest distance between every two neighboring centers is r, the four centers in the circle model must be placed in a convex quadrilateral with the same size length r (See Figure 4(c)).

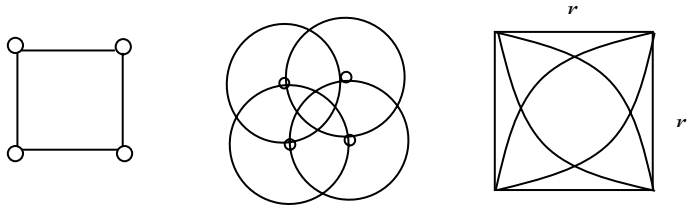

Fig. 4. (a) A cycle of length four. (b) Its circle model. (c) The convex quadrilateral in the circle model.

Since the subgraph c_4 consists of a induced path p_2 and another nearby vertex, we have $\Pr(G_S=c_4)\le\Pr(G_S=p_2)\times\Pr$(the remaining vertex is near p_2 properly). Because Pr(the remain vertex is near p_2 properly) is the probability of putting the center of the remaining node in the convex quadrilateral, we have Pr(the remaining vertex is near p_2 properly)$\le(r^2/|A|)$. In a sequel, we have $\Pr(G_S=c_4)\le\frac{r^2}{|A|}\times\left(\frac{3\sqrt{3}}{4}\right)\frac{\pi r^4}{|A|^2}=\left(\frac{3\sqrt{3}}{4}\right)\frac{\pi r^6}{|A|^3}$ by Theorem 9. ■

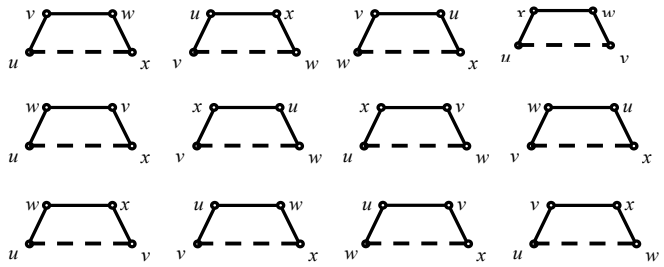

Fig. 5. Twelve different ways of labeling H graph

Counting the number of exposed-terminal sets is equivalent to counting the number of labeled subgraph H (See Table 2). There are $\binom{n}{4}$ ways to select four from n elements. Each has $\binom{4}{2}\times 2$ =12 ways in forming the subgraph H (Figure 5).

Note that every graph in the same row contains the same subgraph (cycle of length four). Therefore the number of exposed-terminal sets is equal to the number of labeled H graphs minus the number of the duplicated cycles (=3(duplicated counting)×3(rows)):

$$\binom{4}{2}\times 2\times\binom{n}{4}\times\Pr(G_S=H)\text{-}3\times 3\times\binom{n}{4}\times\Pr(G_S=c_4)$$

$$=\frac{3^4}{4}\binom{n}{4}\frac{\pi r^6}{|A|^3}\text{ -}9\times\binom{n}{4}\times\Pr(G_S=c_4) \qquad \text{(by Theorem 11)}$$

$$\geq\frac{3^4}{4}\binom{n}{4}\frac{\pi r^6}{|A|^3}\text{ -}9\times\binom{n}{4}\times\left(\frac{3\sqrt{3}}{4}\right)\frac{\pi r^6}{|A|^3} \qquad \text{(by Theorem 19)}$$

$$\geq\left(\frac{3^4-27\sqrt{3}}{4}\right)\binom{n}{4}\frac{\pi r^6}{|A|^3}.$$

Theorem 20: The expected number of exposed-terminal sets in a $\Psi(X_n, r, A)$ is no less than $\left(\frac{3^4-27\sqrt{3}}{4}\right)\binom{n}{4}\frac{\pi r^6}{|A|^3}$.

Similarly, we conclude that the exposed-terminal sets grow as like $O(n^4r^6)$, where n is the number of mobile nodes and r is the range of power. In [41], Shukla *et al.* have mitigated the exposed terminal problem by identifying exposed terminal sets and scheduling concurrent transmissions whenever possible. Combing with Theorem 20, we can estimate the extent of performance degradation due to the exposed-terminal problem, and adopt similar techniques used in [41] to improve system performance.

7 Conclusions

We have proposed a paradigm for computing the subgraph probabilities of RGGs, and have shown its applications in finding fundamental properties of wireless networks. We are surprised at finding some interesting properties:

1. The occurrences of two distinct edges in RGG are independent.
2. The occurrences of three or more distinct edges in RGG are dependent.
3. Probabilities of some specific subgraphs in RGG can be estimated accurately.

Many interesting subgraph probabilities and their applications in MANETs are still uncovered. For example, we are now interested in accurately estimating the diameter of RGGs. We also believe that the techniques developed in the paper can be exploited to conduct quantitative analysis on other fundamental properties of wireless ad hoc networks.

Acknowledgements

We would like to thank Dr. Jau-Ling Shih for her invaluable help.

References

1. Christian Bettstetter, "On the minimum node degree and connectivity of a wireless multi-hop network," *MobiHoc*, 2002, pp. 80-91.
2. V. Bharghavan, A. Demers, S. Shenker, and L. Zhang, "MACAW: a media access protocol for wireless LANs," *ACM SIGCOMM*, 1994, pp. 212-215.
3. B. Bollobas, *Random Graphs*, London: Academic Press, 1985.
4. J. A. Bondy and U. S. R. Murty, *Graph Theory with Applications*, Macmillan Press, 1976.
5. Josh Broth, David A. Maltz, David B. Johnson, Yih-Chun Hu, and Jorjeta Jetcheva, "A performance comparison of multi-hop wireless ad hoc network routing protocols," *Mobicom*, 1998, pp. 85-97.
6. C.-L. Chang and R. C. T. Lee, *Symbolic Logic and Mechanical Theorem Proving*, Academic Press, New York, 1973.
7. B. N. Clark, C. J. Colbourn, and D. S. Johnson, "Unit disk graphs," *Discrete Mathematics*, vol. 86, pp. 165-177, 1990.
8. Bevan Das and Vaduvur Bharghavan, "Routing in ad-hoc networks using minimum connected dominating sets," *IEEE International Conference on Communications*, 1997, pp. 376-380.
9. J. Díaz, M. D. Penrose, J. Petit, and M. Serna, "Convergence theorems for some layout measures on random lattice and random geometric graphs," *Combinatorics, Probability, and Computin*g, No. 6, pp. 489-511, 2000.
10. J. Díaz, M. D. Penrose, J. Petit, and M. Serna, "Approximating layout problems on random geometric graphs," *Journal of Algorithms*, vol. 39, pp. 78-116, 2001.
11. J. Díaz, J. Petit, and M. Serna, "Random geometric problems on [0, 1]2, "*Lecture Notes in Computer Science*, vol. 1518, Springer-Verlag, New York/ Berlin, 1998.
12. O. Dousse, P. Thiran, and M. Hasler, "Connectivity in ad-hoc and hybrid networks," *Infocom*, 2002.
13. P. Erdös and A. Rényе, "On Random Graphs I," *Publ. Math. Debrecen*, vol. 6, pp. 290-297, 1959.
14. C. Fullmer and J. Garcia-Luna-Aceves, "Solutions to hidden terminal problems in wireless networks," *ACM SIGCOMM*, 1997, pp. 39-49.
15. E.N. Gilbert, "Random Graphs," *Ann. Math. Stat.*, vol. 30, pp. 1141-1144, 1959.
16. M. C. Golumbic, *Algorithmic Graph Theory and Perfect Graph*s, Academic Press, New York, 1980.
17. A. Gräf, M. Stumpt, and G. Wei β enfels, "On coloring unit disk graphs," *Algorithmica*, vol. 20, pp. 277-293, 1998.

18. P. Gupta and P. R. Kumar, "Critical power for asymptotic connectivity in wireless networks," *Stochastic Analysis, Control, Optimization and Applications*, pp. 547-566, 1998.
19. P. Gupta and P. R. Kumar, "The capacity of wireless networks," *IEEE Transactions on Information Theory*, vol. 46, no. 2, pp. 388-404, 2000.
20. Peter Hall, *Introduction to the Theory of Coverage Process*, John Wiley and Sons, New York, 1988.
21. Paul G. Hoel, Sidney C. Port, and Charles J. Stone, *Introduction to Probability Theory*, Houghton Mifflin Company, Boston, Mass., 1971.
22. T. Hou and V. Li, "Transmission range control in multihop packet radio networks, "*IEEE Transaction on Communications*, vol. 34, pp. 38-44, 1986.
23. C.-F. Hsin and M. Liu, "Network coverage using low duty-cycled sensors: Random and coordinated sleep algorithm," *International Symposium on Information Processing in Sensor Networks*, 2004.
24. S. Khurana, A. Kahol, S. K. S. Gupta, and P. K. Srimani, "Performance evaluation of distributed co-ordination function for IEEE 802.11 wireless LAN protocol in presence of mobile and hidden terminals," *International Symposium on Modeling, Analysis and Simulation of Computer and Telecommunication Systems*, 1999, pp. 40-47.
25. S. Khurana, A. Kahol, and A. Jayasumana, "Effect of hidden terminals on the performance of the IEEE 802.11 MAC protocol," Proceedings of Local Computer Networks Conference, 1998.
26. L. Kleinrock and J. Silvester, "Optimum transmission radii for packet radio networks or why six is a magic number," *Proc. IEEE National Telecom. Conf.*, 1978, pp. 4.3.1-4.3.5.
27. S.-J. Lee and M. Gerla, "AODV-BR: Backup routing in Ad hoc Networks," *IEEE Wireless Communications and Networking Conference*, 2000, vol. 3, pp. 1311-1316.
28. Edgar M. Palmer, *Graphical Evolution: An Introduction to the Theory of Random Graphs*, New York: John Wiley and Sons, 1985.
29. Mathew D. Penrose, *Random Geometric Graphs*, Oxford University Press, 2003.
30. M. D. Penrose, "A strong low for the longest edge of the minimal spanning tree," *The Annals of Probability*, vol. 27, no. 1, pp. 246-260, 1999.
31. M. D. Penrose, "The longest edge of the random minimal spanning tree," *The Annals of Applied Probability*, vol. 7, no. 2, pp. 340-361, 1997.
32. M. D. Penrose, "On *k*-connectivity for a geometric random graph," *Random structures and Algorithms*, vol. 15, no. 2, pp. 145-164, 1999.
33. T. K. Philips, S. S. Panwar, and A. N. Tantawi, "Connectivity properties of a packet radio network model," *IEEE Transactions on Information Theory*, pp. 1044-1047, 1989.
34. P. Piret, "On the connectivity of radio networks," *IEEE Transactions on Information Theory*, pp. 1490-1492, 1991.
35. G. J. Pottie and W. J. Kaiser, "Wireless integrated network sensors," *Commun. ACM*, vol. 43, no. 5, pp. 51–58, May 2000.
36. V. Ravelomanana, "Extremal Properties of three-dimensional sensor networks with applications," *IEEE Transactions on Mobile Computing*, vol. 3, no. 3, pp. 246-257, 2004.
37. F. S. Roberts, "Indifference graphs," in *Proof Techniques in Graph Theory*, F. Harary (editor), Academic Press, New York, pp. 139-146, 1969.
38. E.M. Royer and C-K Toh, "A Review of Current Routing Protocols for Ad Hoc Mobile Wireless Networks," *IEEE Personal Communication*, pp. 46-55, 1999.
39. Paolo Santi and Douglas M. Blough, "The critical transmitting range for connectivity in sparse wireless ad hoc networks," *IEEE Transactions on Mobile Computing*, vol. 2, no. 1, pp. 25-39, 2003.
40. Paolo Santi and Doulas M. Blough,"A probabilistic analysis for the radio range assignment problem in ad hoc networks," *MobiHoc*, 2001, pp. 212-220.

41. D. Shukla, L. Chandran-Wadia, and S. Iyer, "Mitigating the exposed node problem in IEEE 802.11 ad hoc networks," *International Conference on Computer Communications and Networks*, 2003, pp. 157-162.
42. K. Sohrabi, J. Gao, V. Ailawadhi, and G. J. Pottie, "Protocols for self-organization of a wireless sensor network, " *IEEE Personal Commun.*, vol. 7, no. 5, pp. 16–27, Oct. 2000.
43. J. Stewart, *Calculus*, 4th ed., Gary W. Ostedt, 1999.
44. H. Takagi and L. Kleinrock, "Optimal transmission ranges for randomly distributed packet radio terminals," *IEEE Transaction on Communications*, vol. 32, pp. 246-257, 1984.
45. F. Tobagi and L. Kleinrock, "Packet switching in radio channels, Part II-The hidden terminal problem in carrier sense multiple access and the busy tone solution," *IEEE Trans. Commun.*, vol. COM-23, no. 12, pp. 1417-1433, 1975.
46. J. Wu and H. Li, "Domination and its application in ad hoc wireless networks with unidirectional links," *International Conference on Parallel Processing*, 2000, pp. 189 – 197.
47. F. Xue and P. R. Kumar, "The number of neighbors needed for connectivity of wireless networks," *Wireless Networks*, vol. 10, pp. 169-181, 2004.
48. K. J. Yang, *On the Number of Subgraphs of a Random Graph in [0, 1]d*, Unpublished D.Phil. thesis, Department of Statistics and Actuarial Science, University of Iowa, 1995.
49. L.-H. Yen and C. W. Yu, "Link probability, network coverage, and related properties of wireless ad hoc networks," *The 1st IEEE International Conference on Mobile Ad-hoc and Sensor Systems*, 2004, pp. 525-527.
50. C. W. Yu, L.-H. Yen, and Yang-Min Cheng, "Computing subgraph probability of random geometric graphs with applications in wireless ad hoc networks," Tech. Rep., CHU-CSIE-TR-2004-005, Chung Hua University, R.O.C.
51. Chang Wu Yu, Li-Hsing Yen, Kun-Ming Yu, and Zhi Pin Lee, "An Ad Hoc Routing Protocol Providing Short Backup Routes," *Eighth IEEE Internation Conference on Communication Systems*, 2002, Singapore, pp.1052-1056.
52. Kun-Ming V. Yu, Shi-Feng Yand, and Chang Wu Yu, "An Ad Hoc Routing Protocol with Multiple Backup Routes," *Proceedings of the IASTED International Conference Networks, Parallel and Distributed Processing, and Applications*, 2002, pp. 75-80.
53. The Bluetooth Interest group," http://www.bluetooth.com."

INTERNATIONAL JOURNAL OF COMMUNICATION SYSTEMS
Int. J. Commun. Syst. (in press)
Published online in Wiley InterScience (www.interscience.wiley.com). DOI: 10.1002/dac.848

Energy optimization for chain-based data gathering in wireless sensor networks

Li-Hsing Yen[1,*,†], Ming-Zhou Cai[2], Yang-Min Cheng[2] and Ping-Yuan Yang[2]

[1] *Department of Computer Science and Information Engineering, National University of Kaohsiung, Taiwan 811, ROC*
[2] *Department of Computer Science and Information Engineering, Chung Hua University, Hsinchu, Taiwan 300, ROC*

SUMMARY

This paper aims to minimize energy expense for chain-based data gathering schemes, which is essential to prolong the operation lifetime of wireless sensor networks. Energy expense in chain-based data gathering schemes consists of two parts. One corresponds to inter-sensor communications and depends on chain structure. The other corresponds to leader-BS (base station) communications and depends on leader scheduling policy. To optimize inter-sensor communications, the notion of virtual chain is utilized, where an edge may correspond to a multi-hop data propagation path to conserve power. In contrast, an edge in previous work can only be a costly direct communication link. To optimize leader-BS communications, a leader scheduling rule is presented, where the node with the maximum residual power will be selected to be the leader of the chain. In contrast, nodes in previous work act as leaders by turns, resulting in non-uniform energy consumption among sensors. Simulation results show that our strategies are nearly optimal in terms of power conservation. Copyright © 2006 John Wiley & Sons, Ltd.

Received 30 December 2005; Revised 7 June 2006; Accepted 30 June 2006

KEY WORDS: wireless sensor networks; energy consumption; data gathering; logical chain

1. INTRODUCTION

Rapid progress in wireless communication and micro-sensing MEMS technology has enabled the deployment of wireless sensor networks. A wireless sensor network consists of a large number of sensor nodes deployed in a region of interest. Each sensor node is capable of collecting, storing, and processing environmental information, and communicating with other sensors.

*Correspondence to: Li-Hsing Yen, Department of Computer Science and Information Engineering, National University of Kaohsiung, Kaohsiung, Taiwan 811, ROC.
† E-mail: lhyen@nuk.edu.tw

Contract/grant sponsor: National Science Council, Taiwan; contract/grant number: NSC-93-2213-E-216-024
Contract/grant sponsor: Chung Hua University; contract/grant number: CHU-93-TR-004

Data gathering refers to the process of collecting sensed data from every sensor to a remote base station (BS), where end users can access the data [1]. Since sensor nodes are usually battery powered, power-conserving techniques are essential to prolong the operation lifetime of a sensor network. One such technique is in-node processing, a process of automatically combining or aggregating sensed data before sending out the data. Another technique is multi-hop transmission, which replaces the otherwise direct transmission between every sensor and the BS. Multi-path transmission consumes less power than corresponding direct transmission does, since radio signal attenuation varies non-linearly with distance [1].

To facilitate in-node processing and multi-hop transmission, existing data gathering approaches organize nodes into clusters [1, 2], a tree [3, 4], or a chain [5, 6]. Cluster-based approaches are inherently distributed, but they may not effectively minimize power dissipation [5]. Both tree-based and chain-based approaches have reported less energy consumption when compared with cluster-based counterparts. Tree-based approaches allow simultaneous data transmissions so the data-collection latency is expected to be low. However, simultaneous transmission requires involved slot/code scheduling to prevent potential transmission interference or collision [3, 4]. In a pure chain-based scheme [7], simultaneous transmission does not take place as nodes take turns in transmitting. While transmission in this setting is collision free, it leads to a higher data-collection latency.

Once a chain has been formed, data are propagated from both ends of the chain toward some designated sensor node called *leader*. The leader then transmits the aggregated data directly to the BS. Energy expense in each round of data collection thus consists of two parts. One is for inter-sensor communications and depends on the structure of the chain. The other is for leader-BS communications and mainly depends on the in-between distance.

This paper aims to minimize energy expense for chain-based data gathering schemes. For inter-sensor communications, finding an energy-optimal chain structure is similar to the travelling salesperson problem (TSP) on a complete graph, and thus NP-hard.[‡] Therefore, existing chain construction algorithms [5, 6] take heuristic approaches. These algorithms trade time complexity for power efficiency. For a better realization, we design a solution framework for the chain construction problem that accommodates existing solutions. Previously unseen solutions can also be systematically devised under the framework. Some of the new methods are highly power efficient yet have low time complexity. As a remark, we exploit the concept of virtual chain, where each edge of the chain can correspond to a multi-hop data propagation path rather then merely a direct radio link.

For leader-BS communications, we have pointed out that the previous leader scheduling approach [5], which selects the leader in a round-robin fashion, still results in non-uniform energy consumption among sensors as their distances to the BS vary. Section 3.4 formulates the problem of optimal leader scheduling as a linear programming problem and proposes a simple scheduling rule called maximum residual power first (MRPF). MRPF selects the node that has the maximum residual power to be the leader in each round of data collection. Simulation results show that MRPF performs only slightly worse than the optimal scheduling.

[‡] Not returning to the starting node (as in constructing a chain) dose not change the computational complexity of the problem.

DOI: 10.1002/dac

2. PROBLEM DEFINITION AND RELATED WORK

We consider n sensor nodes that are assumed to be almost stationary. A BS distant from these sensors collects sensory data from them for further processing. The BS is aware of all sensor's locations so that it can run a chain construction algorithm as well as a leader scheduling algorithm and broadcast results to all sensors. Each sensor node is assumed to have power control capability so that minimum energy is expended to reach intended recipients. The data-collection process is periodic and a round of data collection is completed when all sensed data are collected by the BS. The leader in each round of data collection is selected by the BS. A sensor may not have sufficient transmission power to reach the BS. Such sensors are ruled out by the BS in choosing the leader.

As mentioned, finding an energy-optimal chain is NP-hard. PEGASIS [5] uses a greedy algorithm for chain construction. The furthest node from the BS is first added into the chain as a head. Then the node not in the chain but closest to the head is appended to the chain and becomes the new head. The process repeats until all nodes are included in the chain. This method has $O(n^2)$ time complexity, but resulting chains are typically not power optimal. Du *et al*. [6] proposed an improvement on the chain construction algorithm. Unlike PEGASIS, where a non-chain node can only be *appended* to the end of the chain, the node can be *inserted* into any position within the chain to minimize the increase of energy use due to adding the node. In each round of the chain construction process, the node that increases energy to the least extent will be added into the chain. The constructed chains are generally power efficient, but the time complexity of this method is $O(n^3)$.

In these two methods, every edge of the chain represents a direct radio link between two nodes. In this paper, we exploit the concept of virtual chain, where each edge of the chain corresponds to a multi-hop data propagation path. In this way, the chain structure is independent of actual data propagation paths among nodes: the topology superimposed by all data propagation paths is generally a graph rather than a chain. A virtual chain can be formally defined as follows. Consider two arbitrary nodes X and Y. Let $P_{X,Y}$ be a data propagation path starting at X and terminating at Y, which is a sequence of nodes $X = x_i$, $x_{i+1}, \ldots, x_j = Y$, where $j \geqslant i+1$. The length of $P_{X,Y}$, $|P_{X,Y}|$, denotes the number of elements in $P_{X,Y}$ minus one. A sequence of n nodes $x_1, x_2, \ldots, x_n$ with $VP = \{P_{x_i,x_{i+1}} | 1 \leqslant i < n\}$ is a virtual chain if there exists some $P_{x_i,x_{i+1}} \in VP$ such that $|P_{x_i,x_{i+1}}| > 1$. The sequence is a conventional chain otherwise.

Sensor node's radio transmission range is typically limited due to technical limitation or for practical concern, which implies that not every node has a direct link with every others. This could be a problem of PEGASIS in constructing a chain. Take Figure 1 as an example, where a chain is under construction and the current head is d. Suppose that node e is reachable only from nodes already in the chain: a, b, and c. Then the chain construction process will fail as it is no longer possible to include e in this chain.

In Reference [6], the chain construction process will fail if there exists some node that is on neither end of the chain and has only one neighbour. Actually, two bidirectional links are essential for being a non-end member of a chain in both methods. With the concept of virtual chain, a chain structure can always be formed provided that the underlying network topology is connected. Therefore, virtual chains are more flexible than conventional chains.

We use the model described in Reference [1] to express energy dissipation caused by radio transmissions. This model has been adopted in References [2, 4–6]. The radio dissipates

DOI: 10.1002/dac

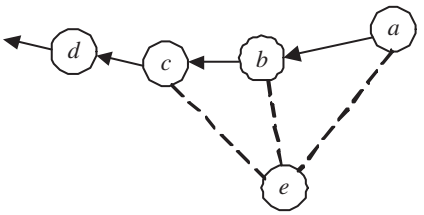

Figure 1. A chain under construction. Node e cannot be included in the chain.

$E_{\text{elec}} = 50$ nJ/bit to run the transmitter or receiver circuitry and the transmitter amplifier spends $\varepsilon_{\text{amp}} = 100$ pJ/bit/m$^{\alpha}$ to achieve an acceptable signal-to-noise ratio, where α is the path exponent that indicates the rate at which the pass loss increases with distance. The value of α typically ranges from 2 to 4, depending on characteristics of the communication environment [8]. Aforementioned studies assume that $\alpha = 2$, which is the case of free space. We assume that $\alpha = 3$, which is typical in noisy urban area [8], and thus is more realistic.

We assume that in-node processing is used so that every data message has k bits. It follows that if node x transmits a message to node y, x consumes energy $kE_{\text{elec}} + k\varepsilon_{\text{amp}}d(x, y)^{\alpha}$, where $d(x, y)$ denotes the distance between x and y, while y expends kE_{elec}. The energy dissipation per transmission therefore consists of two parts. One part is of fixed quantity denoted by $\delta_k = 2kE_{\text{elec}}$. The other depends on α and on the distance from transmitter to receiver.

Given a data propagation path $X = x_i, x_{i+1}, \ldots, x_j = Y$, the cost of $P_{X,Y}$ is defined to be the total energy expense for propagating a k-bit message from X to Y, i.e.

$$c(P_{X,Y}) = (j - i + 1)\delta_k + k\varepsilon_{\text{amp}} \sum_{t=i}^{j-1} d(x_t, x_{t+1})^{\alpha}$$

Let $\Phi(X, Y) = \{P_{X,Y}\}$ be the set of all possible data propagation paths from X to Y. Define $\text{mcp}(X, Y) = \{p | p \in \Phi(X, Y) \wedge \forall p' \in \Phi(X, Y) : c(p) \leqslant c(p')\}$ be the set of minimum-cost data propagation paths from X to Y. Given a virtual chain $\{N_i\}_{i=1}^{n}$ and its associated set of data propagation paths $\{P_{N_i,N_{i+1}}\}_{i=1}^{n-1}$, the cost of the virtual chain is defined as

$$\sum_{i=1}^{n-1} c(P_{N_i,N_{i+1}})$$

The chain has the lowest cost if $P_{N_i,N_{i+1}} \in \text{mcp}(N_i, N_{i+1})$ for all i. The optimal virtual chain problem is to find a virtual chain whose lowest cost is the minimum among all possible ones. This is an NP-hard problem.

3. THE PROPOSED SCHEME

Under our chain construction framework, a chain construction algorithm consists of two parts (Figure 2). The first is to compute and store the costs of every possible pair of nodes. Provided the cost information, the second part constructs a logical chain among all sensor nodes. The issue of leader scheduling is discussed in Section 3.4.

DOI: 10.1002/dac

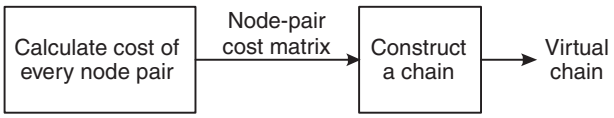

Figure 2. Framework for chain constructions.

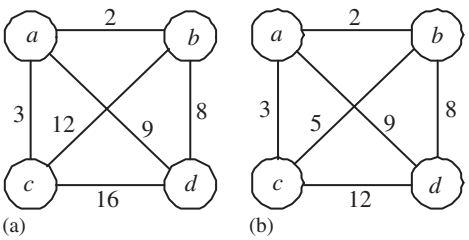

Figure 3. (a) M_d; and (b) the corresponding M_p.

3.1. Costs of node pairs

Conventionally, the cost of every pair of nodes is simply the energy expense of a direct transmission between them [5, 6]. Let M_d be a matrix whose element indexed by i, j, $M_d(i,j)$, is the energy expense of a direct transmission between nodes i and j. To allow a virtual chain, the costs should be associated with data propagation paths rather than direct links. Let M_p be the minimum cost matrix such that $M_p(i,j) = c(P_{i,j})$ for some $P_{i,j} \in \text{mcp}(i,j)$. Such a $P_{i,j}$ for every i and j can be found by running an all-pair shortest-path algorithm (e.g. Floyd-Warshall algorithm [9, pp. 558–562]) on the input M_d. As an example, Figure 3(a) represents M_d graphically for a four-sensor network, where each edge is labelled with the direct transmission cost between two terminal nodes. Figure 3(b) shows M_p that corresponds to all-pair shortest paths for M_d.

All-pair shortest-path algorithms are time expensive ($O(n^3)$ in case of Floyd-Warshall algorithm). Alternatively, we may find first a minimum-cost spanning tree (MST) on the weighted complete graph corresponding to M_d. Then $P_{i,j}$ is designated to be the shortest path (actually the only path) traversing the tree from i to j. We denote the matrix that keeps such costs by M_t. With this approach, the data propagation paths found may not be optimal. However, the time complexity of constructing an MST and traversing it from every node is only $O(n^2)$.

Taking Figure 3(a) as an example, Figure 4(a) shows an MST of Figure 3(a). M_t corresponding to the MST is illustrated in Figure 4(b). Here $M_t(c,d) = 13$ because the data propagation path from c to d is confined to be that along the tree (i.e. c, a, b, d). Observe that this is not a minimum-cost path.

It is interesting and also important to note the property of the triangle inequality in these cost matrices. The triangle inequality refers to that the cost between any two nodes A and B must be at most the cost between A and any other node C plus the cost between C and B. The triangle inequality does not hold if M_d is used as the cost matrix in our problem setting (due to the non-linear attenuation property of radio signals). That is, $M_d(i,j)$ can be larger than $M_d(i,k) + M_d(k,j)$ for some i, j, and k. Nevertheless, the triangle inequality does hold in case

DOI: 10.1002/dac

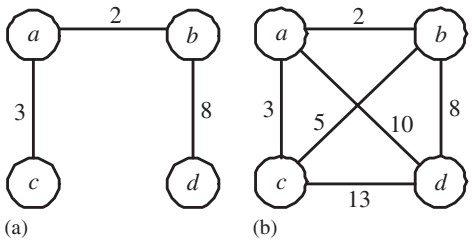

Figure 4. (a) MST of Figure 3(a); and (b) the corresponding M_t.

of M_p, as it is a property of shortest paths [9, p. 520]. For M_t computed based on an MST, the triangle inequality still hold by the following theorem.

Theorem 1
Let T_d be an MST built on the graph corresponding to M_d. If M_t is computed based on T_d, we have $M_t(i,j) \leqslant M_t(i,k) + M_t(k,j)$ for any i, j, and k.

Proof
For any two nodes i and j in a tree, there exists exactly a unique simple path[§] from i to j. The path from i to k and then to j is either the same path from i to j, for which the equality of cost holds, or a non-simple path. In the latter case, an edge incident with k must be included in the path twice, one immediately followed by the other (one joining at k and the other leaving k). If the occurrences of this edge are removed from the path, the path becomes either the exact simple path from i to j or a non-simple path with lower cost which can be further shrank by above arguments. The conclusion thus follows. □

3.2. Chain construction

Once M_p (or M_t) and every $P_{i,j}$ have been obtained, a virtual chain can be formed using any conventional chain construction algorithm such as those proposed in References [5, 6]. The only difference is that the algorithm may run on M_p or M_t instead of M_d. Figure 5 shows different chains obtained by running the appending-based chain construction algorithm of PEGASIS [5] on different cost matrices.

Although the insertion-based chain construction algorithm [6] generally performs well, here we consider an MST-based chain construction heuristic which is more time efficient. The basic idea is to find an MST first (on the weighted complete graph representing M_d, M_t, or M_p) and then convert it to a chain. A tree can be converted to a chain by traversing the tree from the root in prefix order. The visiting sequence then corresponds to a chain. Figure 6 shows an example. Time complexity of this approach is $O(n^2)$.

This heuristic has been devised for the TSP, and is often accompanied with the assumption of the triangle inequality. It can be shown that, thanks to the triangle inequality, the heuristic creates a TSP tour whose cost is at most twice the cost of the MST [9, pp. 969–972]. The cost can

[§] A path is simple if it does not include the same edge twice [10].

DOI: 10.1002/dac

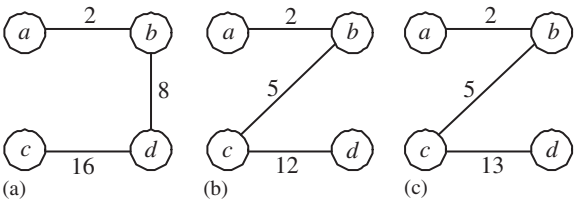

Figure 5. Different chains found by running PEGASIS on: (a) M_d of Figure 3(a); (b) M_p of Figure 3(b); and (c) M_t of Figure 4(b).

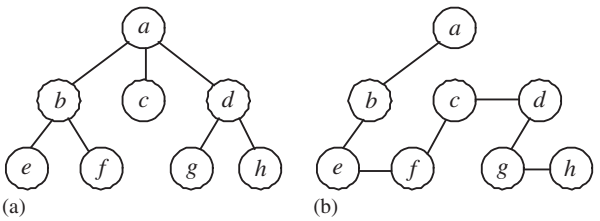

Figure 6. (a) A tree rooted at a; and (b) the chain corresponds to the prefix traversal of (a).

Table I. All possible cost-metric/chain construction combinations.

	Chain construction		
Cost matrix	Greedy appending	Greedy insertion	MST traverse
M_d (direct transmission)	PEGASIS [5]	Direct-insertion [6]	Direct-MST
M_p (all-pair shortest paths)	Shortest-appending	Shortest-insertion	Shortest-MST
M_t (paths confined to MST)	MST-appending	MST-insertion	MST-MST

be further reduced to at most 1.5 times as the minimum cost [11]. However, a constant performance ratio is impossible without the triangle inequality.

In summary, we have one design choice among three cost metrics and another design choice among three chain construction algorithms. Table I lists all possible combinations. Among them, the operations of MST-based chain constructions are detailed in Figure 7. The procedure MST-MST can be further simplified by the following theorem.

Theorem 2

Let T_d be an MST built on the graph corresponding to M_d. Assume that M_t is the cost matrix computed on T_d. Let T_t be an MST on the graph corresponding to M_t. The cost of T_t is equal to that of T_d.

Proof

For every edge $(i,j) \in T_t$, let $P_{i,j}$ denote the data propagation path from i to j that traverses T_d. If $|P_{i,j}| = 1$, edge (i,j) must be an edge of T_d as well. So if we can prove that $|P_{i,j}| = 1$ for every edge $(i,j) \in T_t$, the cost of T_t will be equal to that of T_d. Suppose, by contradiction, that there exists

DOI: 10.1002/dac

Direct-MST

1. Compute and store in M_d direct communication costs of all node pairs.
2. Find an MST T_d on M_d.
3. Convert T_d to a chain.

Shortest-MST

1. Compute and store in M_d direct communication costs of all node pairs.
2. Compute cost matrix M_p by running an all-pair shortest-path algorithm on M_d.
3. Find an MST T_p on M_p.
4. Convert T_p to a chain.

MST-MST

1. Compute and store in M_d direct communication costs of all node pairs.
2. Find an MST T_d on M_d.
3. Compute cost matrix M_t based on T_d.
4. Find an MST T_t on M_t.
5. Convert T_t to a chain.

Figure 7. Operations of MST-based chain constructions.

an edge $(i,j) \in T_t$ with $|P_{i,j}| > 1$. It follows that there is at least one intermediate node k on $P_{i,j}$. Since $P_{i,j}$ corresponds to the shortest path traversing T_d from i to j, it must be a simple path. Therefore, for any k we have $M_t(i,k) + M_t(k,j) = M_t(i,j)$.[¶] There are four possible cases depending on the relation among i, j, and k.

- Both edges (i,k) and (k,j) are included in T_t. This is impossible since the inclusion of these edges plus (i,j) creates a cycle in T_t.
- Edge (i,k) but not (k,j) is included in T_t. We can form T'_t by first removing (i,j) from T_t and then adding (k,j) into T_t. Note that T'_t does not contain cycle and the cost of T'_t is lower than that of T_t since we swap (i,j) for a lower-cost edge (k,j). It follows that T'_t is a tree with cost lower than that of T_t.
- Edge (k,j) but not (i,k) is included in T_t. Similarly, this leads to another tree whose cost is lower than that of T_t.
- Neither (i,k) nor (k,j) is included in T_t. T_t must contain a path from i to k and another from k to j as T_t is connected. The lengths of these paths must be greater than one. Now consider replacing (i,j) with the combination of (i,k) and (k,j) in T_t. Let the result be T'_t. Note that T'_t has the same cost as T_t but contains two cycles, one involving the path from i to k and the other j to k. We can remove any edge from the first path and any other from the second, resulting in a tree with cost lower than that of T_t.

All these cases lead to impossibility or contradiction, so we conclude that there exists no edge $(i,j) \in T_t$ with $|P_{i,j}| > 1$. □

Theorem 2 indicates that, in case of MST-MST, we may directly convert T_d instead of T_t to a chain. Procedure MST-reduced in Figure 8 thus replaces MST-MST.

Table II lists the time complexities of all mentioned methods. Among them, PEGASIS, Direct-MST, MST-appending, and MST-reduced are more time efficient than others.

[¶] Recall that the equality in Theorem 1 holds when k lies on the path from i to j.

DOI: 10.1002/dac

MST-reduced

1. Compute and store in M_d direct communication costs of all node pairs.
2. Find an MST T_d on M_d.
3. Convert T_d to a chain.
4. For every edge (i, j) of the chain, set $P_{i,j}$ to be that specified by T_d.

Figure 8. Operations of MST-reduced.

Table II. Time complexities of all methods.

Method	Cost matrix computation	Chain construction	Overall
PEGASIS [5]	$O(n^2)$	$O(n^2)$	$O(n^2)$
Direct-insertion [6]	$O(n^2)$	$O(n^3)$	$O(n^3)$
Direct-MST	$O(n^2)$	$O(n^2)$	$O(n^2)$
Shortest-appending	$O(n^3)$	$O(n^2)$	$O(n^3)$
Shortest-insertion	$O(n^3)$	$O(n^3)$	$O(n^3)$
Shortest-MST	$O(n^3)$	$O(n^2)$	$O(n^3)$
MST-appending	$O(n^2)$	$O(n^2)$	$O(n^2)$
MST-insertion	$O(n^2)$	$O(n^3)$	$O(n^3)$
MST-reduced	$O(n^2)$	$O(n^2)$	$O(n^2)$

3.3. Energy-latency trade-off

As mentioned, one drawback of using chains instead of trees or clusters is the increase of data latency. The situation may be aggravated when using virtual chains, as a virtual chain increases the number of hops to collect sensed data. Therefore, one may want to constrain data latency and meanwhile still make some gains in energy saving.

Given a conventional chain $\{N_i\}_{i=1}^{n}$, if we replace $L_{N_i,N_{i+1}}$, the link between N_i and N_{i+1} $(1 \leqslant i \leqslant n-1)$, with the best data propagation path from N_i to N_{i+1}, $P_{N_i,N_{i+1}}$, the number of hops will be increased by $|P_{N_i,N_{i+1}}| - 1$ while the energy gain is $c(L_{N_i,N_{i+1}}) - c(P_{N_i,N_{i+1}})$. Therefore, the maximal energy gain with latency constraint (MEGLC) problem can be defined as to find $E \subseteq \{1, 2, \ldots, n-1\}$ that maximizes

$$\sum_{i \in E} [c(L_{N_i,N_{i+1}}) - c(P_{N_i,N_{i+1}})]$$

subject to

$$\sum_{i \in E} (|P_{N_i,N_{i+1}}| - 1) \leqslant T$$

where T is the maximal number of additional hops allowed to be added. This problem is also NP-hard as it can be shown that the 0/1 Knapsack problem reduces to MEGLC. The 0/1 Knapsack problem is to choose a set of items to put into a limited-capacity Knapsack, where the ith item has a profit p_i and weighs w_i. The Knapsack capacity is essentially T; w_i can be transformed to $|P_{N_i,N_{i+1}}| - 1$; and p_i is $c(L_{N_i,N_{i+1}}) - c(P_{N_i,N_{i+1}})$.

It also can be shown that MEGLC reduces to the 0/1 Knapsack problem. As the 0/1 Knapsack problem can be solved by a dynamic programming algorithm, so can MEGLC. Nevertheless, we found through experiments that a greedy method performs well. Given

DOI: 10.1002/dac

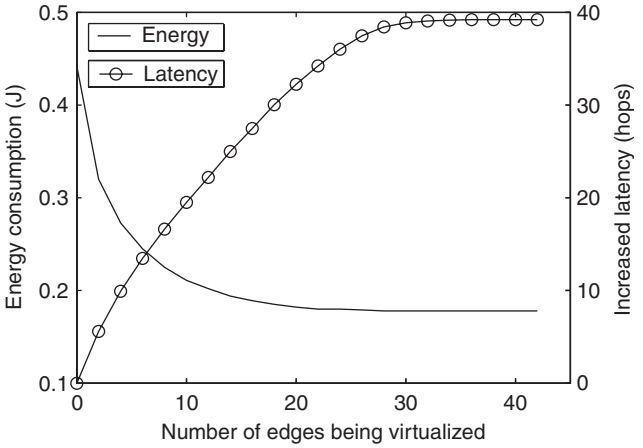

Figure 9. Trade-off between energy and latency with the greedy method. The results were obtained with 80 sensors under a 200×200 network.

a conventional chain, the greedy method 'virtualizes' the edge that maximizes the ratio of energy gain to the latency raised.

Figure 9 shows how the greedy method trades latency for energy. The energy consumed by a conventional chain (without any edge being virtualized) is 0.44 J. In contrast, the energy expense with a virtual chain can be as low as 0.18 J (with over 20 virtualized edges), a 60% reduction. On the other hand, the conventional chain incurs no additional latency while a virtual chain increases the number of hops to a maximum of 40, a 50% increase (a conventional chain consisting of 80 sensors has a fixed length of 79 hops.) As a remark, the energy gain is trivial after 20 edges have been virtualized. Further edge virtualization does not improve energy efficiency significantly.

3.4. Leader scheduling

Given a chain structure, leader scheduling determines which node acts as a leader in each round of the data-collection processes. The goal is to prolong network lifetime, i.e. to maximize the number of data-collection rounds. In the following, we analyse the maximum number of data collection rounds that can be achieved before any node exhausts its power. To simplify the analysis, we focus on leader scheduling in a conventional chain. Without loss of generality, we assume that nodes in the chain are numbered sequentially as $1, 2, \ldots, n$. We also use the following notations.

- e_i: the energy consumed by node i in transmitting a data message to the BS.
- $\rho_{i,j}$: the energy consumed by i in transmitting a k-bit message to node j, where $\rho_{i,j} = kE_{\text{elec}} + k\varepsilon_{\text{amp}}d(i,j)^{\alpha}$.
- $e_r = kE_{\text{elec}}$: energy consumed in receiving a k-bit message.
- E_i: the amount of energy that node i initially has.

When some node i is selected to be the leader, every node numbered $j < i$ (if any) expends energy $\rho_{j,j+1}$ in sending data to node $j+1$, at which energy e_r is consumed to receive the data. Likewise, every node numbered $k > i$ (if any) expends $\rho_{k,k-1}$ to send data to node $k-1$, where energy e_r is expended in receiving the data. The leader transmits the collected data to the BS, consuming energy e_i. Supposing that every node i is scheduled to be the leader x_i times,

DOI: 10.1002/dac

Table III shows the energy expense of every sensor node. Optimal leader scheduling problem is to find positive integer values of x_i's as to maximize $\sum_i x_i$ subject to the following constraints:

$$\begin{aligned}
E_1 &\geqslant (e_1 + e_r)x_1 + \rho_{1,2}x_2 + \rho_{1,2}x_3 + \cdots + \rho_{1,2}x_n \\
&\vdots \\
E_i &\geqslant (\rho_{i,i-1} + e_r)x_1 + \cdots + (\rho_{i,i-1} + e_r)x_{i-1} \\
&\quad + (e_i + 2e_r)x_i + (\rho_{i,i+1} + e_r)x_{i+1} + \cdots + (\rho_{i,i+1} + e_r)x_n \\
&\vdots \\
E_n &\geqslant \rho_{n,n-1}x_1 + \rho_{n,n-1}x_2 + \cdots + (e_n + e_r)x_n
\end{aligned}$$

These constraints can be reformulated as

$$\mathbf{A}\begin{pmatrix} x_1 \\ x_2 \\ x_3 \\ \vdots \\ x_n \end{pmatrix} \leqslant \begin{pmatrix} E_1 \\ E_2 \\ E_3 \\ \vdots \\ E_n \end{pmatrix} \tag{1}$$

where

$$\mathbf{A} = \begin{pmatrix} e_1 + e_r & \rho_{1,2} & \rho_{1,2} & \cdots & \rho_{1,2} \\ \rho_{2,1} + e_r & e_2 + 2e_r & \rho_{2,3} + e_r & \cdots & \rho_{2,3} + e_r \\ \rho_{3,2} + e_r & \rho_{3,2} + e_r & e_3 + 2e_r & \cdots & \rho_{3,4} + e_r \\ \vdots & \vdots & \vdots & \cdots & \vdots \\ \rho_{n,n-1} & \rho_{n,n-1} & \rho_{n,n-1} & \cdots & e_n + e_r \end{pmatrix}$$

The problem turns out to be a linear programming problem. Some sensors may be ruled out by the BS in the leader scheduling process. If sensor i cannot be selected as a leader for some reason

Table III. Energy expense of every sensor.

Node id.	In sending messages to the BS	In sending messages to neighbours	In receiving neighbour's messages
1	e_1x_1	$\rho_{1,2}\sum_{j=2}^{n} x_j$	e_rx_1
i, $2 \leqslant i \leqslant n-1$	e_ix_i	$\rho_{i,i-1}\sum_{j=1}^{i-1} x_j + \rho_{i,i+1} \times \sum_{j=i+1}^{n} x_j$	$e_r(\sum_{j=1}^{i-1} x_j + \sum_{j=i+1}^{n} x_j + 2x_i)$
n	e_nx_n	$\rho_{n,n-1}\sum_{j=1}^{n-1} x_j$	e_rx_n

x_i: the number of times node i is selected to be the leader; e_i: the amount of energy consumed in transmitting a message from node i to the BS; $\rho_{i,j}$: the energy consumed by i in transmitting a message to j; e_r: the energy consumed by any node in receiving a message.

DOI: 10.1002/dac

(for example, it has no direct link with the BS), variable x_i in (1) is bound to zero. Therefore, the existence of leader-ineligible sensors eases the scheduling work by reducing the population of leader candidates.

Round-robin leader scheduling (RR) equalizes the values of x_i's, which is generally far from optimal. In Reference [5], an improvement on RR is proposed. This approach sets up a threshold of distance, and nodes are not allowed to be leaders if their distances to their neighbours along the chain are beyond the threshold.

Instead of finding an optimal solution, we propose a simple rule called maximum residual power first (MRPF) for leader scheduling. As the name suggests, MRPF selects the node that has the maximum residual power to be the leader in each round of data collection. Residual power information can be piggybacked with data messages as part of the aggregated data. If every node attaches its own power level to data message and let the BS find the maximum value, it will incur an additional $O(n)$ overhead on every message. A better approach is to let every node compare its power level with the one attached with the incoming data message (if any) and send only the larger. This is similar to existing distributed maximum-finding algorithms on rings [12–15] and the message overhead is only $O(1)$.

Recall that the BS broadcasts the result of leader scheduling to all sensors before each data-collection round. The energy consumed in receiving broadcasts is not taken into account in the above model. If it is to be considered, a slight modification on the modelling is required. Suppose that receiving one broadcast consumes b unit of energy. As there are $\sum_i x_i$ data-collection rounds in total, all sensors uniformly spend $b\sum_i x_i$ unit of energy on receiving broadcasts. Taking account of this quantity, (1) becomes

$$\mathbf{A}\begin{pmatrix} x_1 \\ x_2 \\ x_3 \\ \vdots \\ x_n \end{pmatrix} \leqslant \begin{pmatrix} E_1/b \\ E_2/b \\ E_3/b \\ \vdots \\ E_n/b \end{pmatrix} \tag{2}$$

This formula is essentially the same as (1) with the only exception that the initial energy of each sensor E_i is uniformly divided by b. Therefore, if $\langle \chi_1, \chi_2, \ldots, \chi_n \rangle$ is the optimal value for $\langle x_1, x_2, \ldots, x_n \rangle$ that maximizes $\sum x_i$ subject to (1), $\langle \chi_1/b, \chi_2/b, \ldots, \chi_n/b \rangle$ will be the solution that maximizes $\sum x_i$ subject to (2). In other words, the consideration of energy expense on broadcasting only scales down the optimal value by a constant. It does not make the problem harder or easier to deal with.

The same conclusion also applies to other energy dissipation sources that have an equal effect on all sensor nodes. An example is the energy expense in idle mode.

4. SIMULATIONS AND IMPLEMENTATION ISSUES

We conducted simulations to analyse the performance of energy conservation techniques. In all experiments, message size was set to 2000 bits. The positions of sensor nodes were randomly determined by a uniform distribution over a square region.

DOI: 10.1002/dac

4.1. Performance of chain structure

We measured network lifetime, the number of data collection rounds that can be achieved by all chain construction approaches. Sensor networks of sizes 50×50 and 100×100 were considered, with a BS located at $(50, 150)$, $(50, 200)$, or $(50, 300)$. The number of nodes was set to 50, 100, and 200, respectively, with initial power of each sensor set to 50J. Round-robin leader scheduling was used in the experiments.

Figures 10–12 show the results averaged over 100 experiments. The results of direct-insertion, shortest-appending, shortest-MST, MST-insertion, and MST-reduced are nearly identical (they are 'good' methods) and are collectively denoted as 'Others' in these figures. Direct-MST generally performs better than PEGASIS does but worse than others (these two are 'naive' methods). These results provide insights on how well chain construction algorithms improve overall energy performance:

- Adding more sensor nodes into a bounded network increases network density, and thus decreases average distance between nodes. As a consequence, network lifetime increases as inter-sensor communication costs less power. Observe that the performance gain with good methods is nearly proportional to the number of sensor nodes. In contrast, the results of naive methods are not attractive.
- Fixing the number of sensors but increasing network size increases average distance between nodes. This is why the performance of naive methods degrades as network size increases. In contrast, good methods nearly perform the same even when network size increases.
- When the BS is further away from the network, the performance difference between good and naive schemes becomes insignificant (Figure 12). The reason is that under such condition, leader-BS communications dominate overall energy consumption. So a better chain structure does not improve network lifetime significantly in this scenario.

4.2. Performance of leader scheduling

We measured and compared the performance gains brought by several leader scheduling schemes including MRPF, RR, and RR with distance-based leader eligibility rule. A network of

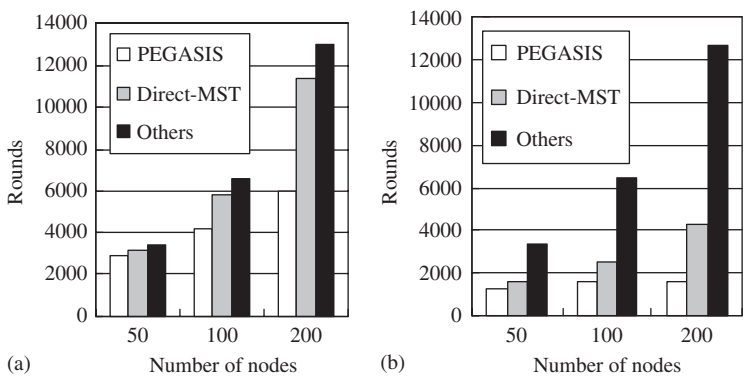

Figure 10. Number of rounds before any node exhausts its power in: (a) 50×50 network; and (b) 100×100 network. The BS was located at $(50, 150)$.

DOI: 10.1002/dac

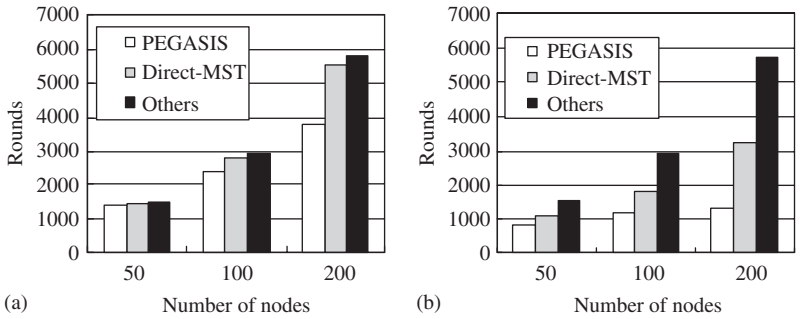

Figure 11. Number of rounds before any node exhausts its power in: (a) 50×50 network; and (b) 100×100 network. The BS was located at $(50, 200)$.

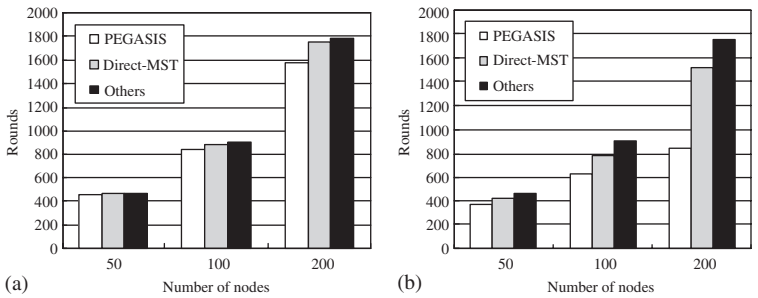

Figure 12. Number of rounds before any node exhausts its power in: (a) 50×50 network; and (b) 100×100 network. The BS was located at $(50, 300)$.

size 50×50 was considered, with a BS located at $(25, 150)$ or $(25, 250)$. All nodes were assumed to have power 50J initially. The chains to be tested with leader scheduling schemes were produced by PEGASIS. Figure 13 shows the results, where each result is obtained by averaging 10 experiments.

It can be seen that MRPF performs slightly worse than the optimal result obtained by a linear-programming problem solver. MRPF significantly outperforms RR. When the sensor population is low, RR with distance-based leader eligibility rule (RR with threshold) results in fewer data-collection rounds than RR does, and the gap increases as the threshold value of distance decreases. The reason is that the loads on leader nodes cannot be fairly shared if only few nodes are eligible for leaders. When the sensor population is sufficiently high, RR with threshold outperforms RR. Therefore, a critical issue of using RR with threshold is to determine an appropriate threshold so that leader-eligible nodes and others fairly share the communication load, which was untold in the original paper [6].

Figure 14 shows variances of all node's residual power when the first node dies. Observe that MRPF yields the minimal variance, meaning that it successfully equalizes power consumption among all nodes. The optimal leader scheduling does not minimize the variance of residual power but still performs good. This suggests the existence of another scheduling rule other than MRPF, which is left as our future work. The RR family does not perform well, but the results tend to be acceptable when the sensor population is getting high.

DOI: 10.1002/dac

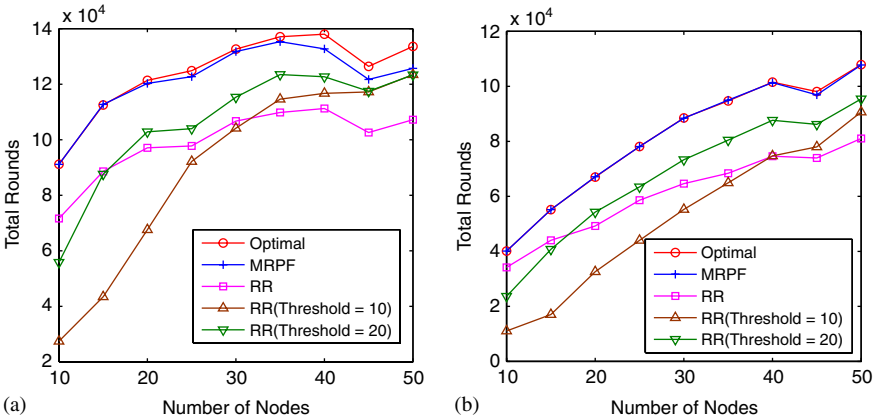

Figure 13. Number of rounds before any node exhausts its power: (a) the BS was located at (25, 150); and (b) the BS was located at (25, 250).

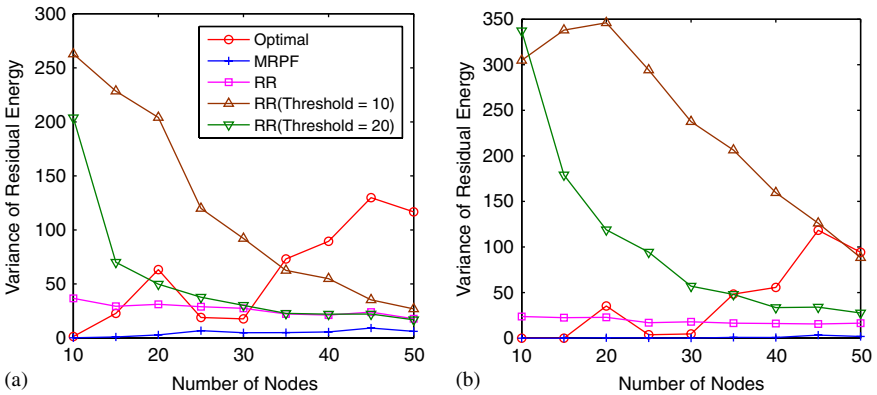

Figure 14. Variances of residual power when the 1st node dies: (a) the BS was located at (25, 150); and (b) the BS was located at (25, 250).

4.3. Implementation issues

The implementation of the proposed method demands some capability from sensor nodes. Each sensor should be equipped with a complementary device that enables the sensor to detect its own location. The location information is reported back to the BS before any data-collection activities. After that, the locating device can be shut down to save power. Each sensor should also have the capability to measure its residual power level. As mentioned, each sensor node should have power control capability so that minimum energy is expended to reach intended recipients.

It is a challenge to apply the proposed approach in harsh communication environments. Signal propagation problems such as interference and multi-path fading cause sensor nodes to spend more transmission power then expected for a desired signal-to-noise ratio, introducing estimation errors to our power consumption model. However, the effects of imperfect

DOI: 10.1002/dac

communications are environment dependent and the estimation errors are not easy to formulate. It is therefore a future work to include environmental factors in constructing an energy-efficient data-collection chain.

5. CONCLUSIONS

We have considered several energy-conserving techniques for chain-based data gathering. For inter-sensor communication, we have developed a framework for chain-formation algorithms that accommodates previous methods as well as new ones exploiting multi-hop data propagation paths. Among all methods, PEGASIS, Direct-MST, MST-appending, and MST-reduced all have $O(n^2)$ computation time while others have $O(n^3)$. On the other hand, direct-insertion, shortest-appending, shortest-MST, MST-insertion, and MST-reduced perform nearly the same and outperform others in terms of network lifetime. MST-appending and MST-reduced both have the merits of lower time cost and, in the same time, better results and are therefore recommended.

For leader-BS communication, we have shown that optimal leader scheduling is a linear programming problem. We have investigated the performance of MRPF scheduling rule, which selects leaders according to node's residual power. Simulation results show that MRPF equalizes energy expense among all sensors. Its performance is near-optimal and significantly better than that of simple round-robin leader scheduling.

In the future, we plan to convert the proposed methods into distributed protocols. Environmental factors such as interference and multi-path fading shall be considered in the future energy consumption model for a more realistic work. We also believe that the finding in this work could be extended to apply to other sensor structures such as trees and clusters.

ACKNOWLEDGEMENTS

This work has been jointly supported by National Science Council, Taiwan, under contract NSC-93-2213-E-216-024 and by Chung Hua University under grant CHU-93-TR-004.

REFERENCES

1. Heinzelman WR, Chandrakasan A, Balakrishnan H. Energy-efficient communication protocol for wireless microsensor networks. *Proceedings of the 33rd Annual Hawaii International Conference on System Sciences*, Hawaii, U.S.A., January 2000.
2. Handy M, Haase M, Timmermann D. Low energy adaptive clustering hierarchy with deterministic cluster-head selection. *Proceedings of the 4th International Workshop on Mobile and Wireless Communications Network*, Stockholm, Sweden, September 2002; 368–372.
3. Annamalai V, Gupta SKS, Schwiebert L. On tree-based convergecasting in wireless sensor networks. *IEEE Wireless Communications and Networking Conference*, New Orleans, U.S.A., March 2003.
4. Upadhyayula S, Annamalai V, Gupta SKS. A low-latency and energy-efficient algorithm for convergecast in wireless sensor networks. *Proceedings of the Globecom*, San Fransisco, December 2003.
5. Lindsey S, Raghavendra C, Sivalingam KM. Data gathering algorithms in sensor networks using energy metrics. *IEEE Transactions on Parallel and Distributed Systems* 2002; **13**(9):924–935.
6. Du K, Wu J, Zhou D. Chain-based protocols for data broadcasting and gathering in the sensor networks. *Proceedings of the International Parallel and Distributed Processing Symposium*, Nice, France, April 2003.
7. Lindsey S, Raghavendra CS. PEGASIS: Power efficient gathering in sensor information systems. *Proceedings of the 2002 IEEE Aerospace Conference*, Big Sky, MT, March 2002.

DOI: 10.1002/dac

8. Rappaport TS. *Wireless Communications*: *Principles and Practice* (2nd edn). Prentice-Hall: Englewood Cliffs, NJ, 2002.
9. Cormen TH, Leiserson CE, Rivest RL. *Introduction to Algorithms*. MIT Press: Cambridge, MA, 1990.
10. Liu CL. *Elements of Discrete Mathematics* (2nd edn). McGraw-Hill: New York, 1985; 145–435.
11. Christodes N. Worst-case analysis of a new heuristic for the travelling salesman problem. *Technical Report 388*, Graduate School of Industrial Administration, Carnegie Mellon University, Pittsburgh, PA, 1976.
12. Chang E, Roberts R. An improved algorithm for decentralized extrema-finding in circular configurations of processes. *Communications of the ACM* 1979; **22**(5):281–283.
13. Higham L, Przytycka T. A simple, efficient algorithm for maximum finding on rings. In *Distributed Algorithms 7th International Workshop*, *WDAG '93*, Schiper A (ed.). Springer: Berlin, Lausanne, Switzerland, September 1993; 249–263 (also published in Lecture Notes in Computer Science, vol. 725).
14. Hirschberg DS, Sinclair JB. Decentralized extrema-finding in circular configurations of processes. *Communications of the ACM* 1980; **23**(11):627–628.
15. Perterson GL. An $O(n \log n)$ unidirectional distributed algorithm for the circular extrema problem. *ACM Transactions on Programming Languages and Systems* 1982; **4**(4):758–762.

AUTHORS' BIOGRAPHIES

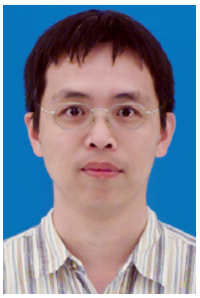

Li-Hsing Yen received his BS (1989), MS (1991), and PhD (1997) degrees in Computer Science, all from National Chiao Tung University, Taiwan. He was an Assistant Professor (1998–2003) and then an Associate Professor (2003–2006) at the Department of Computer Science and Information Engineering, Chung Hua University, Taiwan. He is currently an Associate Professor at the Department of Computer Science and Information Engineering, National University of Kaohsiung, Taiwan. His current research interests include mobile computing, wireless networking, and distributed algorithms. Dr Yen is a member of IEEE.

Ming-Zhou Cai received his MS degree in Computer Science from Chung Hua University, Taiwan, in 2004. He has worked for a wireless LAN chip vendor since 2004. His professional interests are wireless networks and Linux system.

Yang-Min Cheng was born in Taoyuan, Taiwan, ROC in 1981. He received his BS and MS degrees in Computer Science from Chung Hua University, Hsinchu, Taiwan, ROC in 2003 and 2005, respectively. He is currently an engineer at Inventec Enterprise System Corp. His research interests include wireless networks and network analysis.

DOI: 10.1002/dac

Ping-Yuan Yang was born in 1977. He received his MS degree in Computer Science from Chung Hua University, Taiwan. Mr Yang's research interests include WLAN, wireless sensor network, and GSM network. He is a software engineer at FiWin Co. in Hsinchu Science Park.

DOI: 10.1002/dac

Range-Based Density Control for Wireless Sensor Networks

Yang-Min Cheng Li-Hsing Yen
Dept. Computer Science & Information Engineering
Chung Hua University
Hsinchu, Taiwan 300, R.O.C.
{cs88625, lhyen}@chu.edu.tw

Abstract

Density control in a wireless sensor network refers to the process of deciding which node is eligible to sleep (enter power-saving mode) after random deployment to conserve energy while retaining network coverage. Most existing approaches toward this problem require sensor's location information, which may be impractical considering costly locating overheads. This paper proposes a new density control protocol that needs sensor-to-sensor distance but no location information. It attempts to approach an optimal sensor selection pattern that demands the least number of working (awake) sensors. Simulation results indicate that the proposed protocol is comparable to its location-based counterpart in terms of coverage quality and the reduction of working sensors.

1. Introduction

Rapid progress in wireless communications and microsensing MEMS technology has enabled the deployment of wireless sensor networks. A wireless sensor network consists of a large number of sensor nodes deployed in a region of interest. Each sensor node is capable of collecting, storing, and processing environmental information, and communicating with other sensors.

The positions of sensor nodes need not be engineered or predetermined [1] for the reason of the enormous number of sensors involved [3] or the need to deploy sensors in inaccessible terrains [1]. Due to technical limitations, each sensor node can detect only events that occur within some range from it. A piece of area in the deployment region is said to be covered if every point in this area is within the sensory range of some sensor. The area that are collectively covered by the set of all sensors is referred to as network coverage.

As sensor nodes are usually powered by batteries, power-conserving techniques are essential to prolong their operation lifetimes. In this paper, we are considering powering off redundant sensors temporarily after random deployment to conserve energy while retaining network coverage. *Density control* is a process deciding which node is eligible to sleep (entering power-saving mode), while node scheduling arranges the sleep time.

Existing approaches toward density control are mostly location-based [8, 7, 6, 12, 4, 9], meaning that these approaches require location information of sensors. Location-based density control algorithms can ensure 100% network coverage. However, the requirement of location information may not be practical if energy-hungry GPS (Global Positioning System) device is assumed for this purpose. There are other approaches that control density based on the count of working neighbors [10], the current node density [6], or the network coverage expected [11]. These approaches demand no locating devices and are thus more suitable for small-size sensors. However, it is intrinsic that 100% network coverage cannot be guaranteed.

This paper proposes a new density control protocol that needs no location information. It attempts to approach an optimal sensor selection pattern that demands the least number of working (awake) sensors. Our approach needs sensor-to-sensor distance information, which can be acquired by some range measurement technique. We conducted extended simulations for performance comparisons among our protocol and other counterparts. The results indicate that our protocol performs nearly well as a location-based scheme can do in terms of coverage quality and the reduction of working sensors.

The rest of this paper is organized as follows. The next section reviews existing density control protocols and Section 3 details our work. Experimental results are presented in Section 4. The last section concludes this paper.

2. Related Work and Motivation

PEAS [10] is a node density control protocol that demands no location information. In PEAS, all nodes are

Proceedings of the 4th Annual Communication Networks and Services Research Conference (CNSR'06)
0-7695-2578-4/06 $20.00 © 2006 IEEE

initially sleeping. These nodes awake asynchronously and broadcast a probe message. Any working node receiving the message should reply. If an awakening node receives a reply to the probe message, it enters sleep mode again. Otherwise, it becomes a working node for the rest of its operation life. The performance of PEAS heavily depends on *probing range*, the transmission range of the probe message. A small probe range usually leads to high coverage ratio but also a large population of working node.

There are also stochastic approaches that alter node density without location information. In the scheme proposed in [6], all nodes randomly and independently alternate between working and sleep modes on a time-slot basis. Given the probability that a sensor is in working mode, the authors have analyzed the probability of a point being uncovered. In [11], the time periods of working and sleep modes are exponentially distributed random variables. Though the method is stochastic in nature, it is deterministic to set the means of these two distributions for a specific expected network coverage.

Most existing density control protocols require location information. Cărbunar et al. [4] transform the problem of detecting redundant sensors to that of computing Voronoi diagrams. Node location information is required in their scheme to compute the Voronoi diagram corresponding to the current node deployment. Xing et al. [9] also exploit Voronoi diagram to ensure k-coverage, which refers to the condition that every point in the deployment region is covered by at least k sensor nodes. They have shown that k-coverage is ensured if every critical point (where two sensor's coverage areas intersect or a sensor's coverage area and border line intersect) is covered by at least k sensors. The protocol they proposed needs location information of every sensor as well.

A coverage-preserving density control scheme presented in [8] demands that each sensor advertises its location information and listens to advertisements from neighbors. After calculating its coverage and its neighbors', a node can determine if it is eligible to turn off its sensory circuitry without reducing overall network coverage. To avoid potential "coverage hole" due to simultaneous turning off, a back-off protocol is proposed that requires each off-duty eligible sensor to listen to other sensor's status advertisement and, if necessary, announce its own after a random back-off time period expires. The behaviors of some other schemes [7, 6, 12] are similar to [8] in that they all require the exchanges of location information and eligibility status. Among them, OGDC [12] aims to arrange a particular deployment pattern of working sensors. It has been shown [12] that, to minimize the population of working sensors while preserving network coverage, the locations of any three neighbor sensors should form an equilateral triangle with side length $\sqrt{3}r_s$, where r_s is the sensory range. Extending this argument, the optimal deployment pattern that requires the least number of working sensors should be that shown in Fig. 1. Each working sensor S is surrounded by six working neighbors (co-workers) that from a regular hexagon centered at S with side length $\sqrt{3}r_s$. Provided that the node density is sufficiently high, it is feasible to seek such a pattern among all deployed sensors.

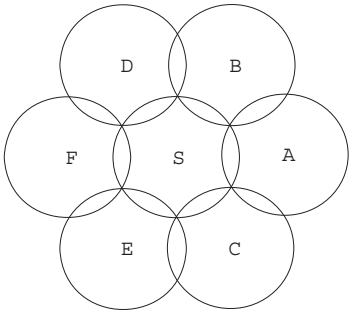

Figure 1. Optimal deployment pattern that demands the least number of working sensors to cover entire region

Network connectedness is another issue that should be addressed in density control. It has been proven [12, 9] that given 100% coverage ratio, $r_t \geq 2r_s$ suffices to ensure network connectedness, where r_t is the transmission range of every sensor. Many protocols [12, 9] therefore focus on maintaining full coverage and simply set $r_t = 2r_s$ to ensure network connectedness at the same time.

Our approach assumes the availability of a ranging technology that estimates the distance between pair-wise neighbors. Several ranging techniques have been proposed for wireless sensor networks. One possible way is to establish a mathematical or empirical model that describes radio signal's path loss attenuation with distance [2]. A received signal strength indication (RSSI) can thereby be translated into a distance estimate. Another trend of ranging technologies turns signal propagation time into distance information. If the sender and the receiver of a radio signal are precisely time-synchronized, the distance in-between can be derived from the time of arrival (ToA). If two signals (one is RF and the other is acoustic signal, for example) are transmitted simultaneously, the time difference of the arrivals (TDoA) can be used for ranging [5].

Signal propagation problems such as environmental interference and multi-path fading introduce estimation errors to almost all existing ranging technologies. The degree of errors is environment-dependent. In harsh networking environments, the errors can be so high that makes ranging techniques ineffective. Nevertheless, we assume a perfect ranging scheme behind our work. The motivation of this research is merely to see how well density control can be done

Table 1. Parameter/Timer setting

Parameter/Timer	Value
p_0	$1/n$
r_t	$\sqrt{3}r_s$
T_s	$[0, 0.01]$
T_p	$[0, 0.1]$
T_o	2
T_e	0.05
T_d	0.25
T_c	5
D_1	$r_t/2$
D_2	r_s

Note: An interval value means a value randomly generated within the interval.

with range but location information. The results therefore only stand for those of a best-case study.

3. Proposed Scheme

The basic idea behind our approach is that the deployment pattern shown in Fig. 1 can be approached without exact location information. If the transmission range of each sensor in Fig. 1 is uniformly $\sqrt{3}r_s$, S's co-workers are exactly S's neighbors that have the maximum transmission distance to S. S can first search for one such co-worker, say, A, then repeatedly looks for nodes that are both the co-workers of S and an already-found co-worker. If the second co-worker found is B (C), the third co-worker will be C or D (B or E). If the third co-worker is B or C, the fourth co-worker will be D or E. In this way, all six co-workers, if exist, can be found without knowing their exact locations.

3.1. Protocol Description

Our protocol uses three control messages: CO-WORKER REQUEST, CO-WORKER RESPONSE, and RECRUITMENT DONE. Table 1 lists settings of some parameters and timers used by our protocol. Every sensor locally maintains two lists: neighbor list and co-worker list. The former keeps the ID (identification) and distance of each neighbor. The latter records the IDs of known co-workers. Every CO-WORKER REQUEST sent by a sensor is attached with the sender's ID and its co-worker list.

Figure 2 shows the state transition diagram of the proposed protocol. All nodes are initially in Role-deciding state, where each node tests if it can become a starting node, a node that initiates co-worker recruitment. The test is pure stochastic; a node can be a starting node with initial probability p_0, where p_0 is a variable inversely proportional to

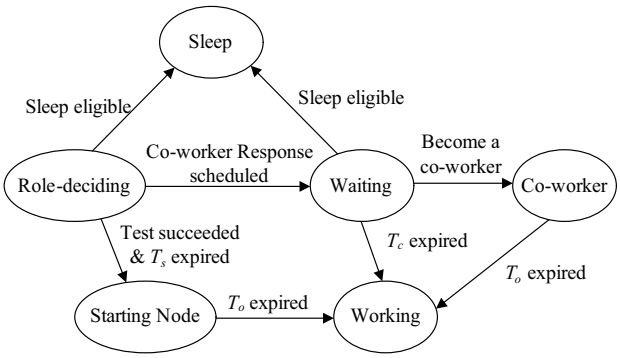

Figure 2. State transition diagram of the proposed protocol

the node density of the network. If the test fails, the node conducts the test again in the following second. The probability of success exponentially increases with time: it is $\min\{2^{i-1}p_0, 1\}$ in the ith second. The process repeats until the test succeeds or the node hears CO-WORKER REQUEST from one of its neighbors. The latter case indicates that some neighbor has successfully become a starting node. The node ceasing the test process then executes the procedure shown in Fig. 3 to decide whether it is eligible to sleep or should be a co-worker of its neighbor.

---

if the distance between S and R is less than D_1 **then**
    enter sleep mode directly; skip all the following steps
if R is listed in the attached co-worker list **then**
    wait T_p seconds
    broadcast Co-worker Request and set timer T_o
    go to Co-Worker state
else // R has not yet replied to S
    determine if R should reply by the rule shown in Table 2
    if R need not reply **then**
        enter sleep mode directly
    if S is not in R's neighbor list **then**
        add S into R's neighbor list
    for each node i that is in the attached co-worker list **do**
        add i to R's co-worker list if i is R's neighbor
    set T_r according to Table 2
    go to Waiting state
end if

Figure 3. The procedure for node R to process Co-worker Request received from S

When the test succeeds, the node waits T_s seconds before broadcasting CO-WORKER REQUEST. The value of T_s is randomly chosen to avoid possible transmission colli-

Table 2. The rule of replying Co-worker Response

Condition			
$\|L\|$	$\|L \cap N\|$	Reply?	T_r
0	0	Yes	*dtime*
≥ 1	0	Yes	*dtime*+T_d
	1 or 2	Yes	*dtime*
	> 2	No	–

Note: L and N are the sets of S's co-workers and R's neighbors, respectively.

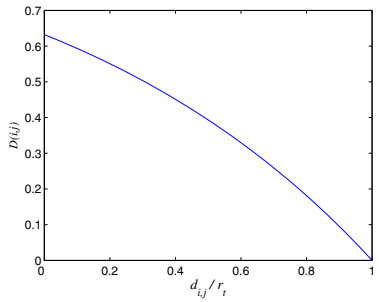

Figure 4. The value of $D(i, j)$ versus the ratio of $d_{i,j}$ to r_t

sions that may occur when multiple nearby sensors decide to send CO-WORKER REQUEST at the same time. If no CO-WORKER REQUEST is heard during that interval, the node broadcasts CO-WORKER REQUEST, sets timer T_o, and then enters Starting Node state. If the node hears another CO-WORKER REQUEST before it issues its own, the procedure in Fig. 3 is executed.

The procedure in Fig. 3 decides whether a node receiving CO-WORKER REQUEST is eligible to sleep or should be a co-worker. Suppose that R receives CO-WORKER REQUEST from S. If R is close to S (i.e., R's distance to S is less than D_1), R will enter sleep mode directly as it does not contribute substantial coverage to S. Otherwise, the "else" part of the outer if-statement will be executed, as R has not yet responded to any CO-WORKER REQUEST and thus cannot be a co-worker of anyone. The code segment there determines whether R need reply to S's request and, if it need, how long it should wait before sending the reply. Table 2 details the decision rule. If more than two of R's neighbors are already S's co-workers, R can sleep for its expected-low coverage contribution. Otherwise, the value of the reply delay timer T_r is chosen to let the most appropriate node (the one that is closest to the intended location) reply first.

The setup of T_r involves calculating the value of *dtime*. For any CO-WORKER REQUEST sent from S to R, let L and N be the sets of nodes that are the listed co-workers of S and the neighbors of R, respectively. *dtime* in Table 2 is defined as

$$dtime = D(S, R) + \sum_{j \in L \cap N} D(R, j). \quad (1)$$

Function $D(i, j)$ is defined as

$$D(i, j) = \left(1 - \exp\left(\frac{d_{i,j}}{r_t} - 1\right)\right),$$

where $d_{i,j}$ is the distance between nodes i and j. See Fig. 4.

After T_r is set, R enters Waiting state, in which the CO-WORKER RESPONSE is scheduled to be sent to S when T_r expires. R cancels the scheduled sending (by resetting T_r), however, if it overhears a CO-WORKER RESPONSE addressed to S at any time before T_r expires. R does this because the sender of the CO-WORKER RESPONSE is more qualified to be S's co-worker than R. The overheard CO-WORKER RESPONSE updates R's neighbor list to include the sender's ID. If a new CO-WORKER REQUEST is received before T_r expires, the scheduled sending is canceled as well and the incoming message is processed by the same procedure shown in Fig. 3.

The action of aborting the scheduled response on the receipt of a new request deserves a further note. The sender of the new request can be an independent starting node or a co-worker of the one that initiates the first request. We may devise a thoughtful yet complicated scheme to resolve the race condition between the old and the new requests. However, we found through simulations that doing so does not improve the results significantly. Therefore, we choose to ignore the old request for the sake of simplicity and the likelihood of saving power. This approach can save power as the early sender, expected to be a co-worker firstly, may be proved sleep-eligible later by the second or subsequent requests.

After sending CO-WORKER RESPONSE, R sets timer T_c and stays in Waiting state. Subsequent CO-WORKER REQUEST received before T_c expires, if any, is processed by the same procedure (Fig. 3), where the "if" part of the second if-statement is executed if the co-worker list attached with the received request contains this node's ID. In that case, this node has been recruited by some starting node. The node then broadcasts its own CO-WORKER REQUEST and enters Co-Worker state. If no further message is received before T_c expires, the node enters working mode directly. If a RECRUITMENT DONE is received and its distance to the sender is less than D_2, the node enters sleep mode directly.

Before node S enters Starting Node or Co-worker state, it must have broadcasted a CO-WORKER REQUEST mes-

On receiving Co-worker Response from node R
  add R's ID and distance to S into S's neighbor list
  if the message is addressed to S and R is not S's co-worker **then**
    add R's ID to S's co-worker list
    if *first_received* **then**
      reset timer T_o
      set timer T_e
      first_received = false
    end if
  end if

expired T_e **then**
  broadcast Co-worker Request with the updated co-worker list
  set timer T_o
  first_received = true
end expired

expired T_o **then**
  broadcast RECRUITMENT DONE
end expired

Figure 5. The procedure for node S to process Co-worker Response replied by R. *first_received* is initially true.

sage and set timer T_o. In either state, if the corresponding CO-WORKER RESPONSE is not received before T_o expires, S simply broadcasts RECRUITMENT DONE and then enters working mode. If a CO-WORKER RESPONSE from node R is received or overheard, S puts R into its neighbor list. If R is not yet S's co-worker and this message is addressed to S (i.e., not a overheard message), S adds R into its co-worker list, resets T_o, waits some time for additional responses (if any), and then broadcasts a new CO-WORKER REQUEST with the updated co-worker list. This gives S another call for additional co-workers and also instructs all its new co-workers to start their own recruitment. The detailed procedure for handling CO-WORKER RESPONSE is shown in Fig. 5.

3.2. Discussion

We shall now analyze the range of *dtime* and then clarify the design philosophy behind the decision rule shown in Table 2. Let $d_{i,j}$ be the distance between nodes i and j. For a node R receiving CO-WORKER REQUEST from node S, we have $d_{S,R} \geq 0.5r_t$ since otherwise R will enter sleep mode directly. It follows that $0 \leq D(S,R) \leq 1 - e^{-0.5}$. For all other nodes $j \in L \cap N$, where L and N are the sets of S's co-workers and R's neighbors, respectively, we have $0 \leq D(R,j) \leq 1 - e^{-1}$ since $0 \leq d_{R,j} \leq r_t$. Accordingly,

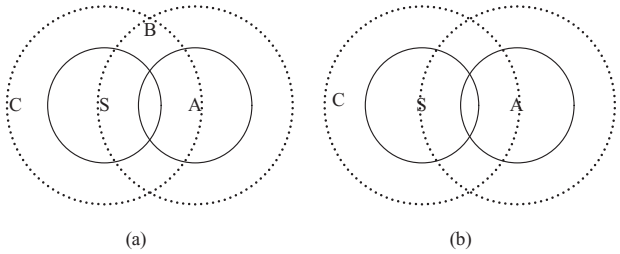

Figure 6. S is a staring node and A is a recruited co-worker. Solid and dotted lines correspond to sensory and communication ranges, respectively.

the range of *dtime* is

$$\begin{cases} [0, 1 - e^{-0.5}] & \text{if } |L| = 0, \\ [T_d, 1 - e^{-0.5} + T_d] & \text{if } |L| > 0 \text{ and } |L \cap N| = 0, \\ [0, 2 - e^{-0.5} - e^{-1}] & \text{if } |L| > 0 \text{ and } |L \cap N| = 1, \\ [0, 3 - e^{-0.5} - 2e^{-1}] & \text{if } |L| > 0 \text{ and } |L \cap N| = 2. \end{cases}$$

The objective of the decision rule in Table 2 is to pick up sensors that nearly form an equilateral triangle to be working nodes. First consider the scenario in Fig. 6(a), where S is a staring node and A is a co-worker that has responded to S's request. Suppose now S broadcasts the second CO-WORKER REQUEST. Though it appears that C contributes a larger coverage area than B does, S should recruit B rather than C in this case as nodes S, A, and B nearly form an equilateral triangle. C should be recruited later.

By Table 2 and (1), B will respond to S after $D(S,B) + D(B,A)$ seconds (as $|L| = 1$ and $|L \cap N| = 1$) while C will do so after $D(S,C) + T_d$ seconds (as $|L| = 1$ and $|L \cap N| = 0$). Observe that $D(S,B) \simeq D(S,C)$, so B's response will be sent earlier than C's if

$$\frac{d_{B,A}}{r_t} > 1 + \ln(1 - T_d). \quad (2)$$

With the default value of T_d (0.25 in Table 1), (2) implies that B will respond earlier than C (and hence causes a cancellation of C's response) if $d_{B,A} > 0.71r_t$. Therefore, B rather than C will be the next recruited co-worker. Nevertheless, C still has the chance to respond to the second CO-WORKER REQUEST. But this happens only when B's response message is garbled due to transmission errors, similar to the case of C in Fig. 6(b).

Next consider the scenario in Fig. 7, where S is a staring node and A and B are recruited co-workers. Suppose now S broadcasts the third CO-WORKER REQUEST. In Fig. 7(a), C should respond earlier than D because S, B, and C nearly form an equilateral triangle. (C also contributes a larger coverage area than D does.)

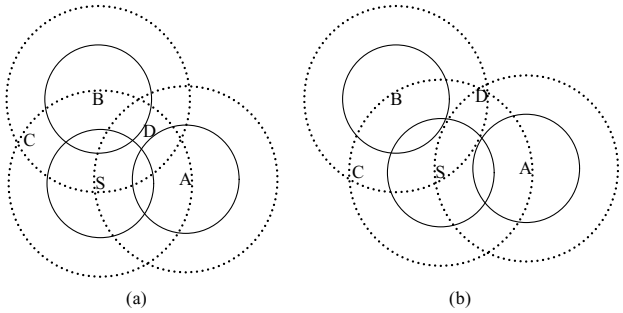

Figure 7. S is a staring node and A and B are recruited co-workers. Solid and dotted lines correspond to sensory and communication ranges, respectively.

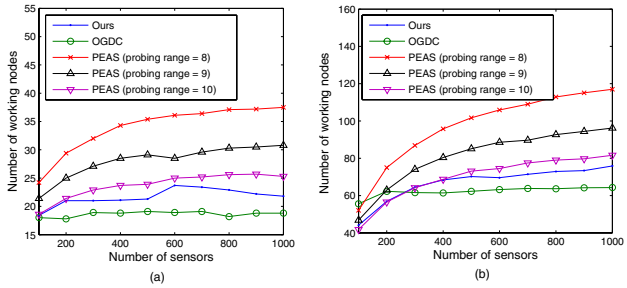

Figure 8. Number of working nodes in a (a) 50×50 and (b) 100×100 network

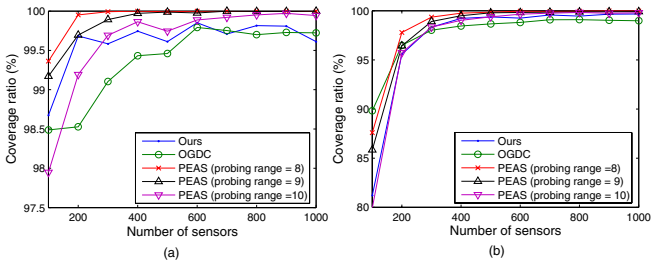

Figure 9. Coverage ratio in a (a) 50×50 and (b) 100×100 network

Table 3. Simulation setup

Parameter	Setting
Network size	50×50 and 100×100
Sensor deployment	Random (uniform distribution)
MAC	IEEE 802.11 CSMA/CA
Sensor population	100 – 1000
Sensory range (r_s)	10
Communication range (r_t)	$2 \times r_s$ (PEAS and OGDC) or $\sqrt{3} \times r_s$ (Ours)
Probing range (for PEAS)	8, 9, or 10
Data transmission rate	60 Kbps

By our design, C will respond to S after $D(S,C) + D(C,B) \simeq 0$ seconds while D will do so after $D(S,D) + D(D,A) + D(D,B)$ seconds. So normally C responds earlier than D, unless S does not receive C's response. In contrast, both C and D in Fig. 7(b) can be the next recruited coworker, as $D(S,C) + D(C,B) \simeq D(S,D) + D(D,A) + D(D,B) \simeq 0$.

4 Experiments and Results

We conducted simulations with ns-2 network simulator[1] for performance comparisons among three representative node-density control methods: PEAS, OGDC, and the proposed scheme. Table 3 details the simulation setting.

4.1 Population of Working Nodes

We first measured the number of working nodes. We assumed that all sensors are initially awake and counted the number of working sensors after running each density control protocol. Fig. 8 shows the obtained results. All values are averaged over ten experiments.

As can be seen from the figure, OGDC yields the least number of working sensors, followed by our protocol and then PEAS. OGDC's results also have a desirable property: the number of working sensors does not increase with the overall sensor population. In contrast, the population of working sensors picked by PEAS family increases with the probing range as well as the overall sensor population.

4.2 Coverage Ratio

To calculate network coverage, we divided the whole deployment area into 1×1 grids, where a gird is said to be covered if the center of the grid is covered by some sensor. Coverage ratio is defined to be the ratio of the number of covered grids to the whole. When the network is partitioned, only the largest connected component (the one that covers the largest area) will be considered in the coverage ratio calculation. Therefore, even though network connectedness was not explicitly gauged, it is reflected by the degree of network coverage. Fig. 9 shows the results averaged over ten experiments.

In Fig. 9(a), PEAS with probing range 8 has the highest

[1] http://www.isi.edu/nsnam/ns/

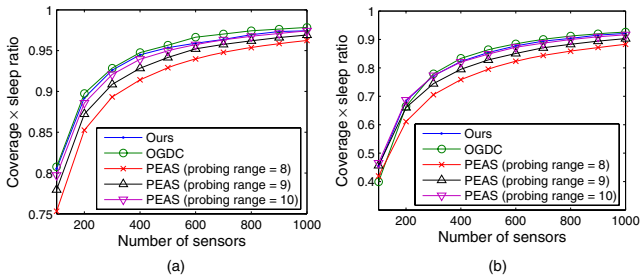

Figure 10. Sleep $\times$ coverage ratio in a (a) 50×50 and (b) 100×100 network

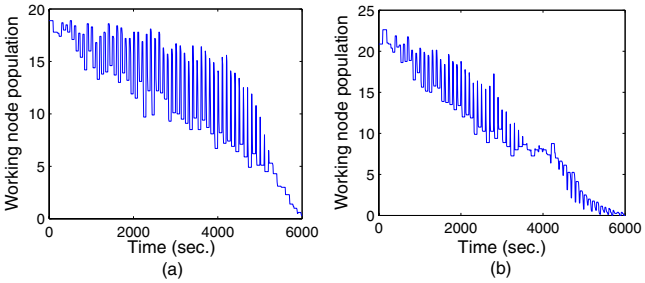

Figure 11. Number of working nodes versus time in a 50×50 network with (a) OGDC and (b) our protocol

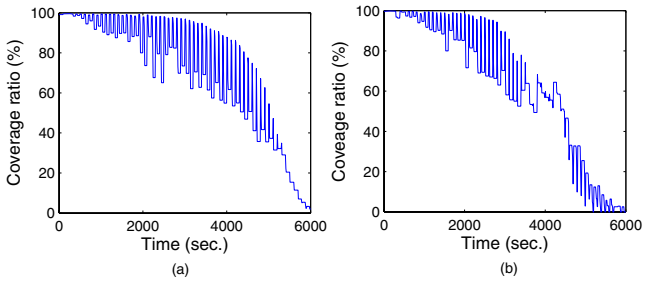

Figure 12. Coverage ratio versus time in a 50×50 network with (a) OGDC and (b) our protocol

coverage ratio. PEAS with probing range 9 or 10 did not perform well if less than 300 sensors were deployed. The performance of our method is next to PEAS but generally better than OGDC. We observed the same trend in Fig. 9(b) when the number of sensors is larger than 500. When only 100 sensors were deployed, OGDC has the best coverage. However, it is overtaken by PEAS and our protocol as the number of sensors increases.

4.3 Overall Performance Index

The above results reveal that a density control scheme may trade the ratio of sleep sensors for coverage ratio. We therefore propose sleep ratio multiplying coverage ratio as an overall performance index. This index emphasizes the balance between sleep and coverage ratios, as favoring sleep or coverage ratio alone usually does not lead to a high index value.

Figure 10 shows the results for this index. Clearly, OGDC has the highest value, followed by our protocol. PEAS family performs the worst, especially with probing range 8. The reason for the poor performance of PEAS with probing range 8 despite its highest coverage ratio is due to the fact that it selects more working sensors than actually needed.

4.4 Time Domain Comparison

The above comparisons focus on space domain, meaning that all values were measured by running a density control protocol right after sensors were deployed. These values actually may change over time, as some sensors may die for power exhaustion. In light of this, we also made performance comparisons in time domain.

We applied an energy model similar to that used by PEAS [10]. The power consumptions in reception, idle, and sleep modes are 4 mW, 4 mW, and 0.01 mW, respectively. The power consumption in transmission mode is 20 mW if $r_t = 20$ m and 16 mW if $r_t = 10 \times \sqrt{3}$ m. For OGDC, the energy consumed in node locating was ignored in our energy model. Total 300 sensors are deployed, each has initial power of 1 W.

We assumed that all sensors are time synchronized, waking up and making powering-off decisions every 100 seconds. We excluded PEAS in our time-domain comparisons for its work-to-death behavior not fitting our alternating work-sleep model.

Figure 11 shows how the number of working nodes changed in every ten seconds. The observed periodic fluctuations deserve an explanation. The population of working nodes raises every 100 seconds due to scheduled executions of the density control protocol. However, working sensors rapidly exhausted their energy, as a working sensor in idle mode dissipates at least 0.4 W per 100 seconds. So the working sensor population drops before the next scheduled execution.

After nearly 3000 seconds of executions, both methods cannot find out sufficient number of working sensors to maintain coverage. Fig. 12 shows the change of coverage ratio over time. It was observed that our superiority over OGDC in terms of coverage (Fig. 9) disappears. The reason is that our approach uses more working nodes than OGDC initially, resulting in fewer available sensors later.

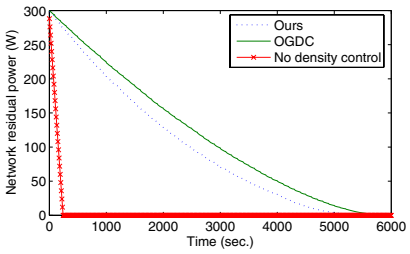

Figure 13. Network residual power versus time in a 50×50 network.

Finally, Fig. 13 demonstrates how the amount of residual power decreases with time. If no density control is conducted, all sensors die after 250 seconds. In contrast, both OGDC and the proposed protocol extend network life time to over 5000 seconds. OGDC consumes less energy than our protocol, as it usually finds fewer working nodes.

5 Conclusions

We have reviewed existing density control protocols and presented a distance-based approach. Extended simulations have been conducted for performance comparisons between the proposed protocol and its counterparts. When compared with PEAS, an elegant counter-based approach, the proposed method can find fewer working sensors while maintaining a similar coverage level. Our approach performs nearly the same as OGDC, a state-of-the-art location-based protocol, when considering both the reduction of working nodes and coverage ratio. Time-domain simulation results show that the proposed protocol consumes a little more energy than OGDC does. But this was obtained when the cost of locating incurred by OGDC is not taken into account.

In the future, we shall refine our protocol design for further reduction of working sensors. The number of control messages should be decreased to save power. Timer values and other parameters should be fine tuned to shorten protocol execution time, as more energy can be saved if nodes can enter sleep more earlier. Finally, it is interesting to see any efforts at integrating our protocol with a node locating scheme, as they all require range information.

Acknowledgement

We would like to thank the authors of [12] for kindly providing us the ns-2 source codes of OGDC. This work has been jointly supported by the National Science Council, Taiwan, under contract NSC-94-2213-E-216-001 and by Chung Hua University under grant CHU-94-TR-02.

References

[1] I. F. Akyìldìz, W. Su, Y. Sankarasubramaniam, and E. Cayirci. A survey on sensor networks. *IEEE Commun. Magazine*, 40(8):102–114, Aug. 2002.

[2] P. Bahl and V. Padmanabhan. RADAR: an in-building RF-based user location and tracking system. In *Proc. IEEE INFOCOM 2000*, pages 775–784, Mar. 2000.

[3] N. Bulusu, D. Estrin, L. Girod, and J. Heidemann. Scalable coordination for wireless sensor networks: Self-configuring localization systems. In *Proc. 6th IEEE Int'l Symp. on Commun. Theory and Application*, Ambleside, U.K., July 2001.

[4] B. Cărbunar, A. Grama, J. Vitek, and O. Cărbunar. Coverage preserving redundancy elimination in sensor networks. In *1st IEEE Int'l Conf. on Sensor and Ad Hoc Communications and Networks*, pages 377–386, Oct. 2004.

[5] L. Girod and D. Estrin. Robust range estimation using acoustic and multimodal sensing. In *Proc. 2001 IEEE/RSJ Int'l Conf. on Intelligent Robots and Systems*, pages 1312–1320, Maui, USA, Oct.-Nov. 2001.

[6] C.-F. Hsin and M. Liu. Network coverage using low duty-cycled sensors: Random & coordinated sleep algorithms. In *Int'l Symp. on Information Processing in Sensor Networks*, pages 433–442, Apr. 2004.

[7] J. Lu and T. Suda. Coverage-aware self-scheduling in sensor networks. In *Proc. IEEE 18th Annual Workshop on Computer Communications*, pages 117–123, Oct. 2003.

[8] D. Tian and N. D. Georganas. A coverage-preserving node scheduling scheme for large wireless sensor networks. In *First ACM International Workshop on Wireless Sensor Networks and Applications*, pages 32–41, 2002.

[9] G. Xing, X. Wang, Y. Zhang, C. Lu, R. Pless, and C. Gill. Integrated coverage and connectivity configuration for energy conservation in sensor networks. *ACM Trans. on Sensor Networks*, 1(1):36–72, Aug. 2005.

[10] F. Ye, G. Zhong, J. Cheng, S. Lu, and L. Zhang. PEAS: A robust energy conserving protocol for long-lived sensor networks. In *Proc. 23rd Int'l Conf. on Distributed Computing Systems*, pages 28–37, May 2003.

[11] L.-H. Yen, C. W. Yu, and Y.-M. Cheng. Expected k-coverage in wireless sensor networks. *Ad Hoc Networks*. in press.

[12] H. Zhang and J. C. Hou. Maintaining sensing coverage and connectivity in large sensor networks. *Wireless Ad Hoc and Sensor Networks: An International Journal*, 1(1-2):89–123, Jan. 2005.